

# ENFI 2024

## Book of Abstracts

**15<sup>th</sup> International Workshop on Engineering of  
Functional Interfaces**

**Linz, 29<sup>th</sup> – 30<sup>th</sup> August 2024**



**Institute of  
Chemical Technology  
of Inorganic Materials**

Sponsored by



# Welcome to EnFI

Dear Friends of EnFI, Dear colleagues,

It is my very pleasure to welcome you to Linz for the 15<sup>th</sup> edition of the international symposium on the “Engineering of Functional Interfaces”.

On behalf of the Organizing Committee and the Scientific Advisory Board I want to express my sincerest gratitude to all of you for taking the time and effort for your participation and contribution.

After 2011 it is the 2<sup>nd</sup> time that this symposium will be held at the Johannes Kepler University Linz (JKU) in Austria organized by the Institute for Chemical Technology of Inorganic Materials (TIM). Since then the JKU the university has left the list of young universities (< 50y) and has grown significantly as you will see also by the large number of new buildings. Moreover, this year we are celebrating the founding of the medical faculty 10 years ago which is located at the MedCampus in the city, directly connected to 3 hospitals. With its lovely campus the JKU stands out amongst Austrian universities. It was the first European university with a study track in *Mechatronics*. More recently *Artificial Intelligence*, *Natural Sciences* and *Medical Engineering* were established and are well accepted, as can be seen by the increasing number of students.

The specific structure of the EnFI will be retained also this year. Four internationally renowned speakers will introduce the four sessions A: *Electrochemical Methods and Sensors*, B: *Biological Systems and Sensors*, C. *Advanced Characterisation Methods* and D: *Medicine and Surface Function*. Short, three minute teasers will advertise the contributed posters and then all participants will have ample time for discussions, scientific networking and development of new ideas at the *Poster Market* which may be used as Coffee Break.

Lunch will be served in the JKU Mensa, which is conveniently located in the ground floor of the conference. On Thursday 29<sup>th</sup> a Bus will take us directly from the conference site to the private microbrewery *Eder Bräu* which is located snugly in a hop garden in the average mountain *Mühlviertel* some half an hour driving time from Linz.

At the end of the symposium on Friday 30<sup>th</sup> you will have the opportunity for a Lab-Tour to TIM. Please also keep the chance in mind to publish your results in a Topical Section on “Engineering of Functional Interfaces” in the journal *Physica Status Solidi A*.

I wish you a pleasant conference, inspiring discussions, lots of fun and a joyful time.

Achim Walter Hassel  
(Chairman of EnFI2024)

## **Organizing Committee**

Achim Walter HASSEL	(Chair)	Johannes Kepler University Linz
Andrei Ionut MARDARE	(Co-Chair)	Johannes Kepler University Linz
Hüseyin ZENGIN		Johannes Kepler University Linz
Andreas Elias GREUL		Johannes Kepler University Linz
Manuel HOFINGER		Johannes Kepler University Linz
Lisa LARNDORFER		Johannes Kepler University Linz
Martin KONRAD		Johannes Kepler University Linz
Lukas PÖTSCHER		Johannes Kepler University Linz

## **Scientific Advisory Board**

Wim DEFERME	Hasselt, Belgium
Theodor DOLL	Hannover, Germany
Kasper EERSELS	Maastricht, The Netherlands
Bart van GRINSVEN	Maastricht, The Netherlands
Achim Walter HASSEL	Linz, Austria
Sven INGEBRANDT	Aachen, Germany
Steffi KRAUSE	London, United Kingdom
Fred LISDAT	Wildau, Germany
Patricia LOSADA. PÉREZ	Brussels, Belgium
Michael MERTIG	Dresden, Germany
Marloes PEETERS	Manchester, United Kingdom
Michael Josef SCHÖNING	Jülich, Germany
Patrick WAGNER	Leuven, Belgium
Thorsten WAGNER	Jülich, Germany



# Practical Information

Once your registration is fully settled, you will be given a badge that you should wear at all times. Your registration fee will grant you access to the conference lunches, coffee breaks and dinner.

The certificate of attendance will be sent to registered participants by email upon request after the conference.

## Access to the conference venue

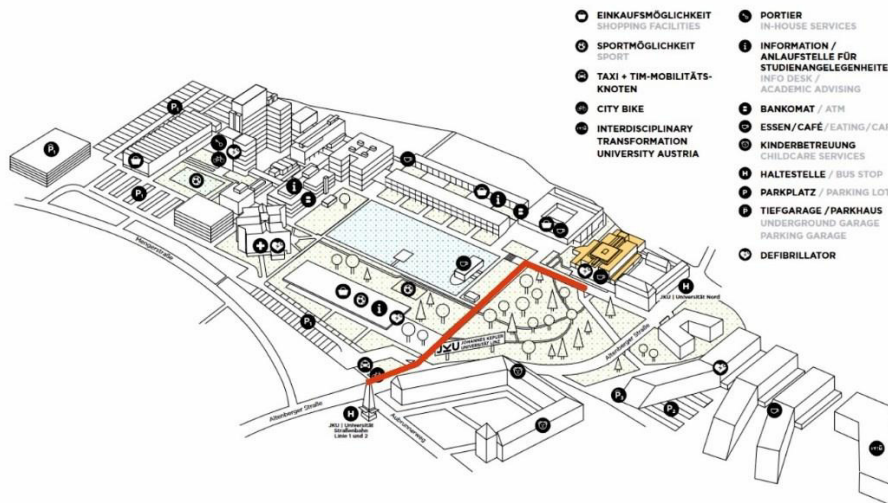
The conference will be held at the Festsaal of the Uni-Center, which is located above the Mensa of the Johannes Kepler University. If you come by tram, you can take either line number 1 or 2 towards “Universität” and exit at the final station. From there you can walk through the campus avenue. You will find the conference venue to your right just after the end of the avenue, as indicated on the campus plan below.

Venue address:

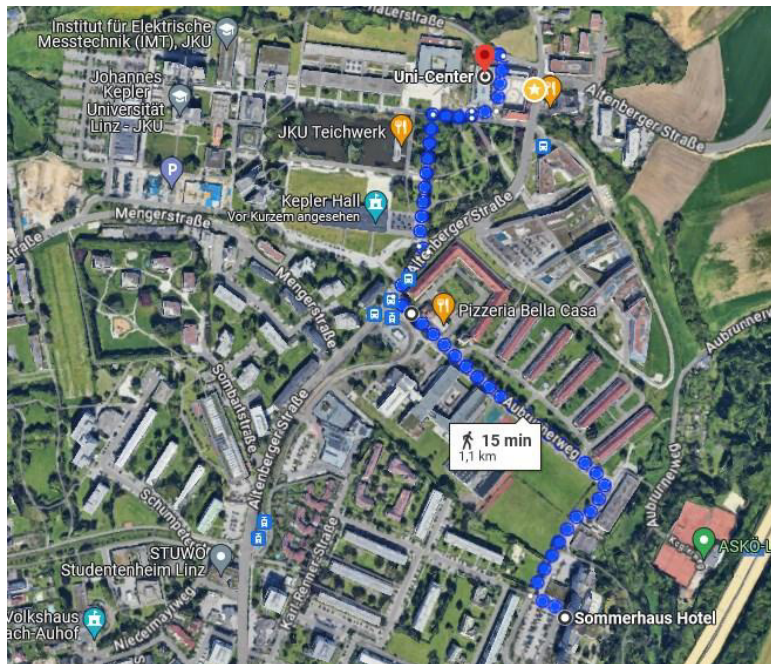
Uni Center Festsaal, Altenberger Straße 69, 4040 Linz

**JKU CAMPUS.**  
UNI-CENTER (MENSA)

**JKU**  
JOHANNES KEPLER  
UNIVERSITÄT LINZ



If you are staying at the “Sommerhaus”, you will pass the tram station on your way to the venue. There will be also a pick up on the first day, starting at 8:15 from right in front of the hotel. The way from the Sommerhaus is indicated in the map below.



## Tutorial Lectures

Tutorial lectures are scheduled to last 40 minutes plus 10 minutes of discussion.

## Short Oral Presentations

The short oral presentations have to be presented by means of a PowerPoint presentation that is **strictly limited to 3 minutes**.

Please double-check the overview of abstracts in each topical section in this booklet. If you have not sent your presentation by email before the deadline announced by the conference organization, there are EnFI organizing team members present in the conference hall that will help you to put your presentation on the computer used for presenting. Please check beforehand in which section you will present and bring your presentation on a Flash drive **1 hour** before the start of the topical section (so before the tutorial lecture). The PowerPoint file has to be named after the assigned poster number and with the last name (e.g. A10\_Doll).

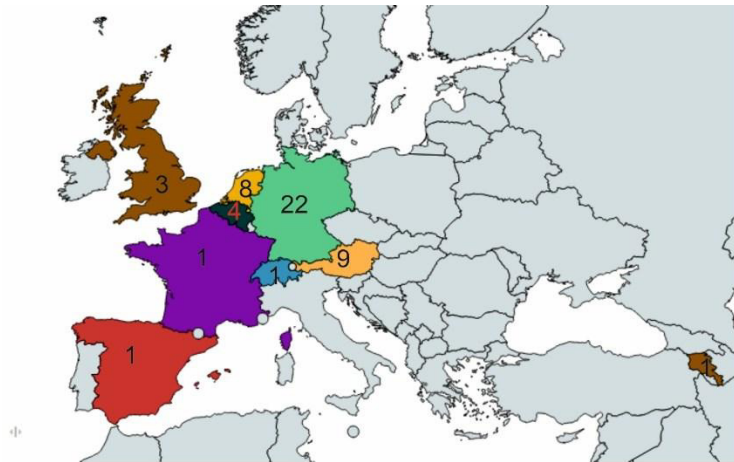
## Poster presentation

The poster market will take place in the Festsaal to the left and right of the podium. The location where posters need to be placed will be labelled with the session codes and poster numbers (i.e. A10). Please check the schedule of each topical session beforehand and remember your unique code.

## WIFI

Wi-Fi is provided at the location via the unique access key in your welcome bag.

## EnFI 2024 participants in a nutshell



<b>Armenia:</b>	National Academy of Sciences of the Republic of Armenia
<b>Austria:</b>	Johannes Kepler Universität Linz, Danube Private University Krems
<b>Belgium:</b>	Katholieke Universiteit Leuven
<b>France:</b>	University of Lille
<b>Germany:</b>	Hannover Medical School, Rheinland-Pfälzische Technische Universität Kaiserslautern, Rheinisch-Westfälische Technische Hochschule Aachen, University of Applied Science Aachen,
<b>Japan:</b>	Kyoto Institute of Technology, Tohoku University
<b>Spain:</b>	ALBA Synchrotron
<b>Switzerland:</b>	University of Geneva
<b>The Netherlands:</b>	Maastricht University
<b>United Kingdom:</b>	Queen Mary University of London

# Scientific Program

## Day 1 – Thursday 29<sup>th</sup> August 2024

- 08:30 Registration  
09:00 Opening by Univ. Prof. Hon. Prof. Dr. Achim Walter HASSEL

### Session A: Electrochemical Methods and Sensors

- 09:15 Tutorial Lecture A: Prof. Eric BAKKER, University of Geneva, Switzerland  
*“From Electrochemical Sensing to Imaging with Ionophores”*  
10:05 Poster Teaser A  
11:00 Poster Market A and Coffee  
12:00 Lunch (JKU Mensa)

### Session B: Biological Systems and Sensors

- 13:00 Tutorial Lecture B: Prof. Dr. Sabine SZUNERITS, University of Lille, France  
*“Multifunctional bandages as strategy for wound management”*  
13:50 Poster Teaser B  
14:50 Poster Market B and Coffee

### Session C: Advanced Characterisation Methods

- 15:50 Tutorial Lecture C: Dr. Juan Jesús VELASCO VÉLEZ, ALBA Synchrotron, Spain  
*“Characterization of working electrochemical interfaces with X-ray spectroscopies and electron microscopy”*  
16:40 Poster Teaser C  
17:40 Poster Market Session C with Coffee  
18:30 Group Photo (in front of the conference site)  
18:45 Bus transfer to Dinner location (directly from conference site)  
19:15 Dinner at Micro Brewery Eder Bräu (Netzberg 32, 4292 Pregarten)  
22:00 Bus transfer back to Linz  
22:30 Arrival at Hotels (Sommerhaus, Harry’s Home and Tram Station “Universität”)

## **Day 2 – Friday 30<sup>th</sup> August 2024**

### **Session D: Medicine and Surface Function**

- 08:30 Tutorial Lecture D: Univ.-Prof. Dr. Christoph KLEBER, Danube Private University, Austria  
*„Surface modifications of implants for tailored osseointegration properties“*
- 09:20 Poster Teaser D
- 10:00 Poster Market D and Coffee

### **Closing Session**

- 11:30 Poster awards, closing ceremony and announcement of EnFI 2025
- 12:00 Lunch (JKU Mensa)
- 13:00 Adjour
- 13:00 Optional Lab Tour to TIM (Meeting Point in front of the Mensa)

## Topical Session A: Electrochemical Methods and Sensors

**Tutorial Lecture A:** *“From Electrochemical Sensing to Imaging with Ionophores”* -  
**Prof. Eric BAKKER** (University of Geneva, Switzerland) p.1

### **Short Oral Presentations:**

- A1 **Stefan SCHMIDT** (University of Applied Science Aachen, Germany) - *Electrokinetic studies about the impact of compressed nitrogen on the zeta potential of aluminum oxide surfaces* p. 2
- A2 **Hüseyin ZENGİN** (Johannes Kepler University Linz, Austria) - *Contrasting corrosion behaviour of pure Mg and Mg-1.8Ca (at.%) alloy: Insights from thin film and bulk structures* p.3
- A3 **Fatemeh AHMADI TABAR** (KU Leuven, Belgium), - *Electrochemical determination of PFOA with screen-printed electrodes modified with molecularly imprinted polymers* p.4
- A4 **Tobias KARSCHUCK** (University of Applied Science Aachen, Germany) - *Electrochemical characterization of capacitive field-effect sensors by means of a portable measurement device* p. 5
- A5 **Karl Frederik WERNER** (Kyoto Institute of Technology, Japan) - *Detection of alpha-synuclein with a lipid layer-immobilized light-addressable potentiometric sensor* p. 6
- A6 **Dua ÖZSOYLU** (University of Applied Science Aachen, Germany) - *Monitoring of saliva pH and buffer capacity using a miniaturized multiwell capacitive sensor* p. 7
- A7 **Minh-Hai NGUYEN** (Hannover Medical School, Germany) - *Electrochemical degradation of molecularly imprinted polymers for advanced inflammation sensors in cochlear implants* p. 8
- A8 **Manuel HOFINGER** (Johannes Kepler University Linz, Austria) - *Investigation on the influence of Ytterbium on potentiodynamic polarization of co-evaporated Magnesium thin-films* p. 9
- A9 **Kevin JANUS** (University of Applied Science Aachen, German) - *Fibroin as biocompatible and bioabsorbable immobilization matrix for amperometric biosensors?* p. 10
- A10 **Theodor DOLL** (Hannover Medical School, Germany) - *Work Function Tuning by Alloying: Silver – Ln Libraries* p. 11
- A11 **Stefan ACHTSNICHT** (University of Applied Science Aachen, Germany) - *Aluminium-doped manganese dioxide particles “boosting” hydrogen peroxide sensitivity?* p. 12
- A12 **Animesh Pratap SINGH** (RWTH Aachen, Germany) - *Exploring 2D material-substrate dielectric interface in MoS<sub>2</sub> liquid-gated transistors* p. 13
- A13 **Lukas PÖTSCHER** (Johannes Kepler University Linz, Austria) - *Combinatorial study of Aluminium-Dysprosium thin films* p. 14
- A14 **Maximillian KNOLL** (University of Applied Science Aachen, Germany) - *Characterization of an Al<sub>2</sub>O<sub>3</sub> extended-gate ion-sensitive field-effect transistor with Nernstian behavior* p. 15
- A15 **Martin KONRAD** (Johannes Kepler University Linz, Austria) - *Combinatorial analysis of silver-gold alloy thin films for possible application in AIMD* p. 16

## **Topical Session B: Biological Systems and Sensors**

**Tutorial Lecture B:** *“Multifunctional bandages as strategy for wound management”* -  
**Prof. Dr. Sabine SZUNERITS** (University of Lille, France) p. 17

### **Short Oral Presentations:**

- B1 **Nathalie PHILIPPAERTS** (Maastricht University, The Netherlands) - *Surface Imprinted Polymers for the Detection of Fungal Spores* p. 18
- B2 **Dua ÖZSOYLU** (University of Applied Science Aachen, Germany) - *New concept for surface-MIPs for bacteria detection: no need for template cell, well-ordered high cavity density* p. 19
- B3 **Clara ZOBLEY** (RPTU Kaiserslautern, Germany) - *Bottom-up Assembly of a 3D Structure of Icosahedral Viral Nanoparticles via Specific Binding* p. 20
- B4 **Flavia DI SCALA** (Maastricht University, The Netherlands) - *A real-time viscosity technique: from the monitoring of PDMS polymerization to the investigation of biological fluids* p. 21
- B5 **Andrei Ionut MARDARE** (Johannes Kepler University Linz, Austria) - *Anodic memristors as future of artificial synapses* p. 22
- B6 **Fereshteh ALIAZIZI** (KU Leuven, Belgium) - *Development and Calibration of a Sensor System for Assessing the Physical Properties of Water Samples in Aquaculture* p. 23
- B7 **Kevin JANUS** (University of Applied Science Aachen, Germany) - *Adjusting the working potential of a bioabsorbable screen-printed carbon-based glucose biosensor on silk-fibroin* p. 24
- B8 **Tao HE** (RPTU Kaiserslautern, Germany) - *Building a Virus Actuator* p. 25
- B9 **Melanie WELDEN** (University of Applied Science Aachen, Germany) - *Turnip vein-clearing virus particles as versatile nanotemplates for the binding of biomolecules on capacitive field-effect sensors* p. 26
- B10 **Valerii MYNDRUL** (Maastricht University, The Netherlands) - *PSi/SiP Photonic Composites for the Point-of-Care Diagnosis of Bacterial Urinary Tract Infections* p. 27
- B11 **Csongor Tibor URBAN** (KU Leuven, Belgium) - *A heat-transfer biosensor with variable geometry* p. 28
- B12 **Rocio ARREGUIN-CAMPOS** (Maastricht University, The Netherlands) - *Whole-Cell Thermal Sensor for the Detection of P. falciparum-infected Erythrocytes: Expanding the Boundaries of Imprinted Polymers for the Detection of Malaria* p. 29
- B13 **Tobias KARSCHUCK** (University of Applied Science Aachen, Germany) - *Detection of C-reactive protein with capacitive field-effect sensors using antibody-functionalized magnetic nanoparticles* p. 30
- B14 **Xuan Thang VU** (RTWH Aachen, Germany) - *Design and implementation of a wafer-scale process for SiC microwire aiming for biochemical sensing applications* p.31

## **Topical Section C: Advanced Characterisation Methods**

**Tutorial Speaker C:** “*Characterization of working electrochemical interfaces with X-ray spectroscopies and electron microscopy*” – **Dr. Juan Jesús VELASCO VÉLEZ**  
(ALBA Synchrotron, Spain) p. 32

### **Short Oral Presentations:**

- C1 **Ko-ichiro MIYAMOTO** (Tohoku University, Japan) - *In-situ measurement of the work function of steel surface by photoelectron yield spectroscopy under atmospheric condition* p. 33
- C2 **Heping CUI** (RWTH Aachen, Germany ) - *Ohmic contacts in tellurium nanowires semiconductor devices* p. 34
- C3 **Jiazhe ZHAO** (Queen Mary University of London, UK) - *3D Photoelectrochemical Imaging* p. 35
- C4 **Andreas GREUL** (Johannes Kepler University Linz, Austria) - *Combinatorial property mapping of a Al-Eu Compositional Thin Film Library* p. 36
- C5 **Gil van WISSEN** (Maastricht University, The Netherlands) - *Thermal Detection of Riboflavin in Almond Milk Using Molecularly Imprinted Polymers* p.37
- C6 **Dua ÖZSOYLU** (University of Applied Science Aachen, Germany) - *Exploring of a multi-sensor array system for on-site monitoring of groundwater quality* p.38
- C7 **Ruixiang LI** (Queen Mary University of London, UK) - *Live Cell Imaging with Photoelectrochemical Imaging and Scanning Ion Conductance Microscopy* p.39
- C8 **Ramiro MARROQUIN-GARCIA** (Maastricht University, The Netherlands) - *Colorimetric detection of veterinary tranquilizer in adulterated alcoholic beverages* p. 40
- C9 **Astghik TSOKOLAKYAN** (A.B. Nalbandyan Institute of Chemical Physics, Armenia) - *Detection of urea in artificial urine using capacitive field-effect biosensors modified with a stacked polyelectrolyte-enzyme bilayer* p. 41
- C10 **Huijie JIANG** (RWTH Aachen, Germany) - *Temperature and solvent effect on the electrical characteristics of two-dimensional metal-organic frameworks* p. 42
- C11 **Maximillian KNOLL** (University of Applied Science Aachen, Germany) - *Fluidic setup for automated electrochemical characterization of extended-gate ISFETs* p. 43
- C12 **Niels KNIPPENBERG** (Maastricht University, The Netherlands) - *Development towards a novel screening method for nipecotic acid bioisosteres using molecular imprinted polymers (MIPs) as alternative to in vitro cellular uptake assays* p. 44
- C13 **Stefan SCHMIDT** (University of Applied Science Aachen, Germany) - *A portable platform for the multiplexed characterization of 16 capacitive field-effect sensors* p.45
- C14 **Elena ATANASOVA** (Johannes Kepler University Linz, Austria) - *Sensing capabilities of anodic memristors in the Nb-Ti System* p. 46
- C15 **Torsten WAGNER** (University of Applied Science Aachen, Germany) - *A project introduction "PFAS-resolve": On-site monitoring of per- and polyfluoroalkyl substances (PFAS) in soil and wastewater* p.47



## **Topical Session D: Medicine and Surface Function**

**Tutorial Speaker D:** “*Surface modifications of implants for tailored osseointegration properties*” - **Univ.-Prof. Dr. Christoph KLEBER** (Danube Private University, Austria) p. 48

### **Short Oral Presentations:**

- D1 **Wiktor ŁUCZAK** (Danube Private University Krems, Austria) - *TM-AFM analysis of laser-treated surface compared to 3D-printed ceramic and titanium dental implants* p. 49
- D2 **Anastasija LINK** (RPTU Kaiserslautern, Germany) - *Interaction of Dextran with Dental Surfaces* p. 50
- D3 **Nils HEINE** (Hannover Medical School, Germany) - *Medical-grade liquid-infused titanium for biofilm reduction* p. 51
- D4 **Soroush BAKHSHI SICHANI** (KU Leuven, Belgium) - *Study of spontaneous cell detachment using a multiparametric biosensing platform based on HTM, EIS, and QCM-D* p. 52
- D5 **Muhammad Usman ANWAR** (RPTU Kaiserslautern, Germany) - *Cell adhesion and behaviour on micro-nano-structured glass surfaces produced by wet etching* p. 53
- D6 **Kevin BRUNKE** (Hannover Medical School, Germany) - *Design of a microfluidic channel system for real-time monitoring of the perilymphatic fluid of the inner ear using molecularly imprinted polymers* p. 54
- D7 **Margaux FRIGOLIA** (Maastricht University, The Netherlands) - *Gold screen-printed electrodes coupled with molecularly imprinted conjugated polymers for ultrasensitive detection of streptomycin in milk* p. 55
- D8 **Eashika GHOSH** (RWTH Aachen, Germany) - *Concept of foldable active intraocular implants for artificial vision with enhanced spatial resolution* p. 56
- D9 **Adrian ONKEN** (Hannover Medical School, Germany) - *Investigating Diffusion-Triggered Corrosion in AIMD* p. 57
- D10 **Andreas GREUL** (Johannes Kepler University Linz, Austria) - *Quantification of the Titanium Dissolution during a new Explantation Procedure* p. 58

## Call for Papers



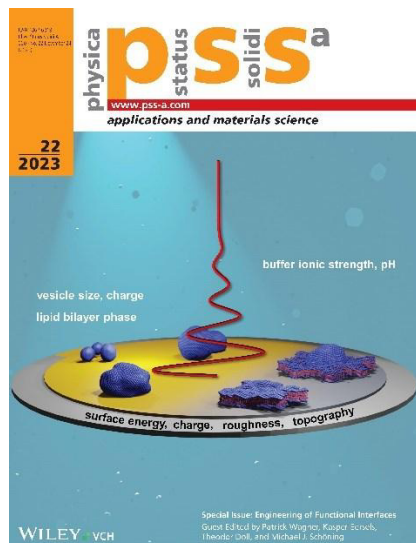
On behalf of our Guest Editors and organizing committee members of the EnFI series Achim Walter Hassel, Patrick Wagner, Michael Josef Schöning and Theodor Doll we sincerely invite you to contribute to this upcoming regular special issue (no conference proceedings)

### **Engineering of Functional Interfaces 2024**

that will be published in **Physica Status Solidi A: Applications and Materials Science**. You are welcome to submit a Review or a Research Article manuscript (with new unpublished results) based on, or related to your conference presentation.

pss (a) is a peer-reviewed, well-known journal that is indexed in Web of Science (Impact Factor 2023 is 1.9). Articles related to EnFI fit perfectly to the scope of the journal and are regularly highlighted as cover articles already since 2009.

pss (a) is a hybrid Open Access (OA)/subscription journal. The OA option is compliant with national or funder mandates, supported by an ever-increasing number of countries and institutions around the world. Wiley has OA agreements with many European and other countries as well as academic and research institutions, for details see Wiley Author Services (<https://bit.ly/3DZiqbd>) and contact us with questions.



Deadline for papers to be included in the Topical section is **1<sup>st</sup> December 2024**.

# Tutorial Lecture A

## From Electrochemical Sensing to Imaging with Ionophores

Eric Bakker<sup>1</sup>, Gabriel Mattos, Nikolai Tiuftiakov, Yupu Zhang, Yaotian Wu, Robin Nussbaum

[eric.bakker@unige.ch](mailto:eric.bakker@unige.ch)

<sup>1</sup> University of Geneva, Faculty of Science, Quai-E.-Ansermet 30, 1211 Geneva, Switzerland

**Abstract:** The selective recognition of ionic species with ion carriers, so-called ionophores, has been a success story in clinical diagnostics and is the basis for billions of yearly measurements in patient care. This talk focuses on recent innovations in materials sciences, methodologies and applications from our group to allow for new applications from sensing to novel chemical imaging principles.

**Keywords:** ionophores, ion transfer electrochemistry, click chemistry, constant potential coulometry, chemical microscopy.

### Introduction

Our conceptual understanding of polymeric membrane electrodes has evolved significantly over the years and this new knowledge has helped to open exciting novel applications. At the beginning stood ground-breaking work that demonstrated the usefulness of organic membranes doped with electrically neutral receptors (ionophores) for selectively detecting ionic species in complex samples such as whole blood. But it turned out to be very difficult to understand how these systems function, and a kinetic steady-state model based on electrical migration principles was required to rationalize the findings. Later, new experimental evidence helped to establish a simplified equilibrium theory to relate the characteristics of such polymeric membrane electrodes to extraction principles [1]. Still, diffusional mass transport at zero current was later shown to be important to understand deviations from ideality, especially for the determination of selectivity and the understanding and improvement of the lower detection limit. Further advances and a plethora of new applications were later made possible by using dynamic electrochemistry principles to impose and control transmembrane ion fluxes, departing from a zero current protocol [2].

### Results and Discussion

This talk will discuss recent advances of membrane electrodes by improving their materials and changing the way these sensors are interrogated. An important improvement of sensitivity is achieved by constant potential coulometry as a readout method, which offers many advantages compared to zero current potentiometry. Possible readout circuits and electronic control of the protocol will be presented, including unsurpassed precision for the detection of pH on the order of tens of  $\mu\text{pH}$  with pH glass electrodes [3], which is important for the assessment of ocean acidification.

If one may tolerate transient currents of limited amplitude, self-powered sensing systems with optical readout may be realized that otherwise still work like potentiometric sensing probes. The direct coupling of potentiometric probes to e-paper is shown to be particularly attractive [4].

The use of solid-contact electrodes with membranes of very limited thickness may be probed with dynamic electrochemistry, achieving an electrochemical equilibration step at each applied potential during a linear sweep. Such systems provide a rich tool to assess ion extraction and interaction processes in polymeric membranes. This principle also forms the basis for a novel chemical imaging method. A lipophilic dye is incorporated whose fluorescence is quenched by the radical form of the redox probe, lipophilic TEMPO. A local concentration change results in a potential shift of the ion transfer wave, which is now detectable an imaging camera. The analysis of the associated imaging stack within one voltammetric scan gives the point of largest fluorescence change for each pixel position. This information can then be used in a fully automated procedure to produce a concentration image.

### References

- [1] E. Bakker, P. Buhlmann, E. Pretsch, *Chem. Rev.* 97 (1997) 3083-3132, doi: [10.1021/cr940394a](https://doi.org/10.1021/cr940394a)
- [2] E. Bakker, *TRAC-Trends in Anal. Chem.*, 53 (2014) 98-105, doi: [10.1016/j.trac.2013.09.014](https://doi.org/10.1016/j.trac.2013.09.014)
- [3] R. Nussbaum, S. Jeanneret, E. Bakker, *Anal. Chem.*, 96 (2024) 6436-6443, doi: [10.1021/acs.analchem.4c00592](https://doi.org/10.1021/acs.analchem.4c00592)
- [4] Y. Wu, E. Bakker, *ACS Sens.*, 7 (2022) 3201-3207, doi: [10.1021/acssensors.2c01826](https://doi.org/10.1021/acssensors.2c01826)

### Acknowledgements

The authors acknowledge the Swiss National Science Foundation, Eaglenos Sciences and the China Scholarship Council for supporting their work.

# Electrokinetic studies about the impact of compressed nitrogen on the zeta potential of aluminum oxide surfaces

S. Schmidt<sup>1,2</sup>, H. Iken<sup>1</sup>, S. Meier<sup>3</sup>, E. Müllner<sup>3</sup>, A. Poghossian<sup>4</sup>, M. Keusgen<sup>2</sup>, M. J. Schöning<sup>1,5</sup>

[s.schmidt@fh-aachen.de](mailto:s.schmidt@fh-aachen.de)

<sup>1</sup>Institute of Nano- and Biotechnologies (INB), Aachen University of Applied Sciences, Campus Jülich, Heinrich-Mußmann-Str. 1, 52428 Jülich, Germany

<sup>2</sup>Institute of Pharmaceutical Chemistry, Philipps University of Marburg, Wilhelm-Roser-Str. 2, 35037 Marburg, Germany

<sup>3</sup>Texas Instruments Deutschland GmbH, Haggertystraße 1, 85356 Freising, Germany

<sup>4</sup>MicroNanoBio, Liebigstr. 4, 40479 Düsseldorf, Germany

<sup>5</sup>Institute of Biological Information Processing (IBI-3), Forschungszentrum Jülich GmbH, Wilhelm-Johnen-Str., 52425 Jülich, Germany

**Abstract:** The zeta ( $\zeta$ ) potential of an  $\text{Al}_2\text{O}_3$  surface was characterized while the measurement electrolyte was exposed to ambient air or gassed with  $\text{N}_2$ . Results gained in ambient air showed an elevated measurement variance as the  $\zeta$  potential fluctuated by ca. 5 mV between two distinct levels.

**Keywords:** zeta potential; aluminum oxide; pH sensing; nitrogen flushing; carbon dioxide

## Introduction

An important parameter in surface functionalization is the  $\zeta$  potential, as it is decisive for how well molecules bind to a surface or are repelled from it by electrostatic interaction [1]. The  $\zeta$  potential is an indirect measure of the charge difference between a stationary and a mobile phase. Precisely, it is the electric potential measured at the slipping plane under which ions remain bound to the stationary phase while the mobile phase moves across it [2]. In this study, the  $\zeta$  potential of field-effect sensor chips covered with an  $\text{Al}_2\text{O}_3$  layer (Texas Instruments GmbH, Freising, Germany) was characterized with the electrokinetic analyzer SurPASS 3 (Anton Paar GmbH, Ostfildern-Scharnhausen, Germany). The  $\text{Al}_2\text{O}_3$  surface was fabricated by atomic layer deposition with a thickness of ca. 25 nm, confirmed by ellipsometry. Regarding the  $\zeta$  potential, a comparison was made between measurements in which the electrolyte was either fumigated with  $\text{N}_2$  or exposed to ambient air.

## Results and Discussion

Two 10 mm  $\times$  20 mm sensor chips (stationary phase) from the same wafer were mounted into the adjustable gap cell of the SurPASS 3. The gap between the chip pair was set to 100  $\mu\text{m}$ . The measurement electrolyte (mobile phase) was prepared by adjusting 200 mL of ultrapure water with KCl to a conductivity of 14.7 mS/cm (ca. 1 mM KCl, ca. pH 5.7). Prior to measurements, the chips were conditioned by rinsing them with the electrolyte for 2 h. Afterwards, the  $\zeta$  potential was measured 30  $\times$  (ca. 60 min) with activated  $\text{N}_2$  purge at 1 bar. The purge was switched off and the measurement cycle repeated with the electrolyte now exposed to ambient air. The  $\zeta$  potential was almost stable at around  $-32$  mV during  $\text{N}_2$  flushing (see Figure 1). It gener-

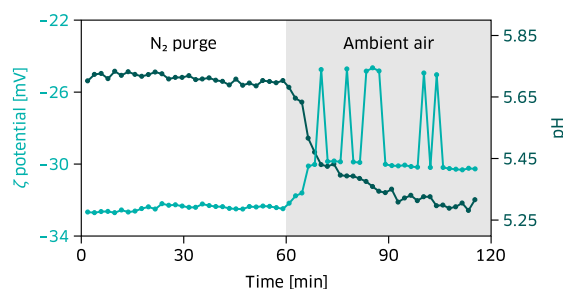


**Figure 1:** pH value of a 1 mM KCl electrolyte (dark mint) while flushed with an  $\text{N}_2$  purge (white) or exposed to ambient air (grey).  $\zeta$  potential of an  $\text{Al}_2\text{O}_3$  surface (bright mint) rinsed with the electrolyte.

ally became less negative after deactivating the  $\text{N}_2$  purge, which was caused by an acidification of the electrolyte (entry of  $\text{CO}_2$  as carbonate). Also, the measurement became instable, evident by random  $\zeta$  potential shifts of ca. 5 mV between two distinct levels. These kind of shifts were observed in other experiments with similar chips. A possible reason for this could be that the carbonate ions are a distorting factor or that the precisely controlled pressure stabilizes the measurement.

## Conclusions

Flushing the electrolyte with  $\text{N}_2$  under controlled pressure can have a positive effect on the constancy of  $\zeta$  potential measurements when characterizing sensor chip surfaces.

## References

- [1] N. Schulz, G. Metreveli, M. Franzreb, F. H. Frimmel, C. Syldatk, *Colloids Surf. B*, **66** (2008) 39-44
- [2] R. J. Hunter, *Zeta potential in colloid science: Principles and applications*, Academic Press, 1986

## Contrasting corrosion behaviour of pure Mg and Mg-1.8Ca (at.%) alloy: Insights from thin film and bulk structures

Hüseyin Zengin<sup>1</sup>, Andrei Ionut Mardare<sup>1</sup>, Andreas Greul<sup>1</sup>, Manuel Hofinger<sup>1</sup>, Gianina Popescu-Pelin<sup>2</sup>, Gabriel Socol<sup>2</sup>, Achim Walter Hassel<sup>1,3</sup>  
[hueseyin.zengin@jku.at](mailto:hueseyin.zengin@jku.at)

<sup>1</sup> Institute of Chemical Technology of Inorganic Materials (TIM), Johannes Kepler University Linz, Altenberger Str. 69, 4040, Linz, Austria

<sup>2</sup> Lasers Department, National Institute for Lasers, Plasma and Radiation Physics, 077125 Magurele, Romania

<sup>3</sup> Danube Private University, Steiner Landstraße 124, 3500 Krems an der Donau, Austria

**Abstract:** Pure Magnesium (Mg) and Mg-1.8Ca (at.%) alloy were produced in thin film and bulk forms and their corrosion behaviours were comparatively investigated. Thin films were produced by thermal evaporation technique whereas bulk samples were fabricated through permanent mould casting. Microstructural analyses showed that the bulk and thin film microstructures significantly differed from each other. Bulk samples mainly consisted of coarse Mg grains and intermetallics, while thin films comprised fine hexagonal facets with no intermetallic formation. Electrochemical characterisations revealed that the corrosion resistance of pure Mg was comparable in bulk and thin films, whereas in the Mg-1.8Ca (at.%) alloy, the bulk form exhibited drastically poor corrosion resistance compared to its thin film counterpart.

**Keywords:** magnesium alloy; thin film; calcium; corrosion resistance

### Introduction

The combinatorial analysis of alloys in thin film form is a novel strategy for the development of novel alloys, enabling the identification of alloy compositions with optimal properties without the need for time-consuming and expensive traditional manufacturing processes. However, the degree to which thin films accurately represent the properties of bulk materials remains uncertain. Therefore, this study investigates and compares the corrosion resistance of Mg-Ca alloys, specifically focusing on pure Mg and a single Ca composition (1.8 at%), in both bulk and thin film forms.

### Results and Discussion

Microstructural analyses demonstrated that bulk pure Mg consisted of large  $\alpha$ -Mg grains while Ca addition resulted in a formation of fine equiaxed grain structure with a substantial amount of  $Mg_2Ca$  intermetallic. The thin films were composed of fine hexagonal facets with no trace of  $Mg_2Ca$  formation.

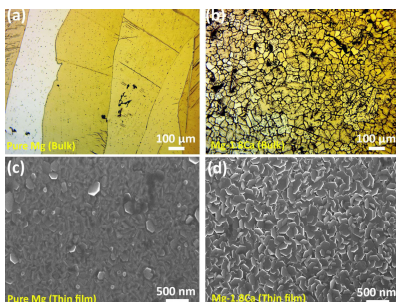


**Figure 1:** Optical and SEM images of pure Mg and Mg-1.8Ca alloy

Electrochemical analyses showed that the bulk samples exhibited higher open circuit potential and corrosion potential values than those for thin films. The corrosion rate calculated based on Tafel plots was comparable for thin film and bulk pure Mg. However, a significant difference was observed between the corrosion behaviours of the thin film and bulk forms of the Mg-Ca alloy.

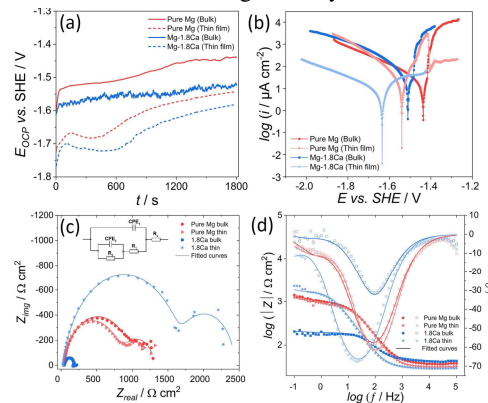


**Figure 2:** Corrosion test results: (a) Open circuit potential, (b) Tafel, (c) Nyquist and (d) Bode plots

### Conclusions

Pure Mg in thin film form can represent the corrosion properties of the bulk form while its corrosion behaviour in these two forms is completely altered when alloyed with Ca.

### References

[1] H. Zengin, A.I. Mardare, G. Popescu-Pelin, G. Socol, A.W. Hassel, *Materials Letters* 2024, 362, 136246.



# Electrochemical determination of PFOA with screen-printed electrodes modified with molecularly imprinted polymers

Fatemeh Ahmadi Tabar<sup>1</sup>, Joseph W. Lowdon<sup>2</sup>, Kasper Eersels<sup>2</sup>, Bart van Grinsven<sup>2</sup>, Patrick Wagner<sup>1</sup>

[Patrickhermann.Wagner@kuleuven.be](mailto:Patrickhermann.Wagner@kuleuven.be)

<sup>1</sup>Department of Physics and Astronomy, Laboratory for Soft Matter and Biophysics ZMB, KU Leuven, Celestijnenlaan 200 D, B-3001 Leuven, Belgium

<sup>2</sup>Sensor Engineering Department, Faculty of Science and Engineering, Maastricht University, P.O. Box 616, 6200 MD Maastricht, the Netherlands

**Abstract:** Current detection platforms for polyfluoroalkyl substances (PFAS) are lab-based, too costly and time-consuming. Electrochemical sensors offer a promising alternative for PFAS detection with the possibility of on-site screening. This study employs screen-printed electrodes (SPEs) modified with molecularly imprinted polymers (MIPs) to detect perfluorooctanoic acid (PFOA), one of the most common PFAS compounds. The sensor's performance was evaluated using electrochemical impedance spectroscopy (EIS), demonstrating its ability to detect PFOA at concentrations ranging from 1 nM to 10  $\mu$ M, with a detection limit (LoD) of 69 pM.

**Keywords:** polyfluoroalkyl substances; electrochemical impedance spectroscopy; molecularly imprinted polymers; on-site detection

## Introduction

PFAS are a class of materials that have been widely used in production of a wide range of consumer products. After decades of bioaccumulation in the environment, research has demonstrated that these compounds are toxic and potentially carcinogenic [1]. Hence, there is a strong need for a highly sensitive, rapid, and cost-effective PFAS monitoring tool [2,3]. Electrochemical sensors have shown great potential for PFAS monitoring by using proportional changes in electrochemical signals. Molecularly imprinted polymers (MIPs) can be employed for surface functionalization of electrochemical sensors, enhancing their selectivity. This study demonstrates how combining PFOA MIPs with EIS can produce a low-cost, robust sensor platform for real-sample analysis.

## Results and Discussion

In this study, previously synthesized MIPs were used to modify SPEs and their impedance values were recorded by performing EIS measurements. Thereafter, the time-dependent  $\Delta$  Abs Z values for MIP- and non-imprinted polymer (NIP)-modified electrodes were calculated. Subsequently, the average of  $\Delta$  Abs Z value for each concentration was used to draw the dose-response curves (Figure 1). The data shows that increasing the concentration of PFOA will result in the impedance decreasing. The LoD for MIP sample was 69 pM calculated by the  $3\sigma$  method. The impedance change for the NIP sample was much less than the MIP sample, which confirms the non-specific binding of the target to the polymeric matrix.

Furthermore, the sensor's real-world application was assessed through EIS measurements in tap water. The developed sensor, which integrates SPEs

with MIPs, has the potential to be produced in large-scale for on-site PFOA monitoring.

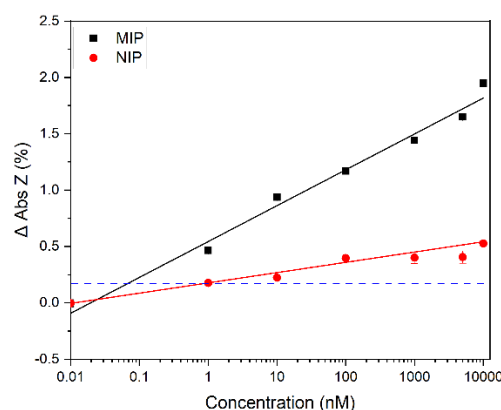


**Figure 1:** Dose-response curves for MIP- and NIP-modified SPEs.

## Conclusions

This research presents a MIP-based sensor capable of detecting PFOA in real-world samples, demonstrating its potential as a cost-effective tool for rapid on-site screening of PFAS compounds.

## References

- [1] F. Ahmadi Tabar et al., *Sensors*, **24.1** (2023) 130
- [2] C. S. Law et al., *Sens. Actuators. B Chem.*, **355** (2022) 131340
- [3] F. Ahmadi Tabar et al., *Environmental Technology & Innovation*, **29** (2023) 103021

## Acknowledgements

KU Leuven and Maastricht University through the Global PhD Partnership funded the work presented in this article.

# Electrochemical characterization of capacitive field-effect sensors by means of a portable measurement device

T. Karschuck<sup>1,2</sup>, S. Schmidt<sup>1</sup>, S. Achtsnicht<sup>1</sup>, J. Ser<sup>1</sup>, I. Bouarich<sup>1</sup>, A. Poghossian<sup>3</sup>, P. Wagner<sup>2</sup>,  
M. J. Schöning<sup>1,4</sup>

[karschuck@fh-aachen.de](mailto:karschuck@fh-aachen.de)

<sup>1</sup>Institute of Nano- and Biotechnologies (INB), Aachen University of Applied Sciences, Heinrich-Mußmann-Str. 1, 52428 Jülich, Germany

<sup>2</sup>Laboratory for Soft Matter and Biophysics, KU Leuven, Celestijnenlaan, 3001 Leuven, Belgium

<sup>3</sup>MicroNanoBio, Liebigstr. 4, 40479 Düsseldorf, Germany

<sup>4</sup>Institute of Biological Information Processing (IBI-3), Forschungszentrum Jülich GmbH, Wilhelm-Johnen-Str., 52425 Jülich, Germany

**Abstract:** Portable measurement devices are necessary for point-of-care and in-field applications of biosensors. Here, the thumb-drive sized Sensit Smart potentiostat (PalmSens BV, The Netherlands) was validated for the analysis of single capacitive field-effect sensors by comparing it directly to the stationary electrochemical workstation IM6ex (Zahner Elektrik GmbH & Co. KG, Germany). An almost perfect match of the recorded impedance spectra, capacitance-voltage curves and constant-capacitance measurements was found.

**Keywords:** capacitive field-effect sensor; portable measurement device; enzyme; penicillin; biosensor

## Introduction

Field-effect capacitive electrolyte-insulator-semiconductor (EISCAP) sensors are usually characterized using stationary electrochemical impedance analyzers. In this study, we present a portable measurement device combining the commercial potentiostat “Sensit Smart” from PalmSens BV with a base station for EISCAP characterization (see Figure 1) [1]. A Python script was used to handle the data collection. To compare the performance of the portable and stationary impedance analyzers, Ta<sub>2</sub>O<sub>5</sub>-gate EISCAP pH sensors and biosensors with immobilized penicillinase for the detection of penicillin were selected as example applications [1,2].

## Results and Discussion

Very similar pH sensitivities of  $58 \pm 3$  mV/pH and  $59 \pm 3$  mV/pH were evaluated from the constant-capacitance curves for the same Ta<sub>2</sub>O<sub>5</sub>-gate EISCAP sensor measured with the portable device and the stationary impedance analyzer, respectively. To verify the performance of the portable system for biosensing applications, the sensor surface was functionalized by immobilizing the enzyme penicillinase from *Bacillus cereus*. H<sup>+</sup> ions are produced during the catalysis of penicillin into penicilloic acid by penicillinase, which enabled the detection of penicillin concentrations between 0.2 mM and 2 mM. The penicillin sensitivity was evaluated at  $101 \pm 6$  mV/dec by characterization with the portable device and  $104 \pm 6$  mV/dec for the stationary device, using the same sensor.

## Conclusion

Portable impedance analyzers enable the point-of-care application of EISCAPs for the detection of

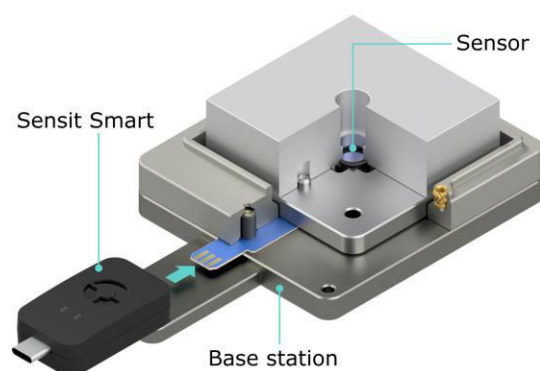


**Figure 1:** Render of the portable single-sensor measurement device with connected Sensit Smart potentiostat from PalmSens BV.

clinically and environmentally relevant analytes. Here, we have validated the performance of the portable “Sensit Smart” potentiostat and compared it directly to a stationary impedance analyzer. Impedance spectra, capacitance-voltage and constant capacitance curves for the same sensor were found to be almost perfectly overlapping.

## References

- [1] T. Karschuck, S. Schmidt, S. Achtsnicht, J. Ser, I. Bouarich, A. Poghossian, P. Wagner, M. J. Schöning, *Manuscript in preparation*
- [2] S. Beging, M. Leinhos, M. Jablonski, A. Poghossian, M.J. Schöning, *Phys. Status Solidi A.* **212** (2015) 1353-1358

## Acknowledgements

Part of this work was funded by the Deutsche Forschungsgemeinschaft (DFG: German Research Foundation)– 445454801.

# Detection of alpha-synuclein with a lipid layer-immobilized light-addressable potentiometric sensor

Minato Matsuda <sup>1</sup>, Minoru Noda <sup>2</sup>, [Carl Frederik Werner](mailto:werner@kit.ac.jp) <sup>1</sup>

[werner@kit.ac.jp](mailto:werner@kit.ac.jp)

<sup>1</sup>Electronics, Kyoto Institute of Technology, Kyoto, Japan

<sup>2</sup>Faculty of Chemistry, Materials and Bioengineering, Kansai University, Osaka, Japan

**Abstract:** Aggregated  $\alpha$ -synuclein ( $\alpha$ Syn), a biomarker for the Parkinson's disease, is a negatively charged protein. In this study a light-addressable potentiometric sensor with an immobilized phospholipid monolayer was used to detect the binding of  $\alpha$ Syn. The measuring solution was adjusted to increase the Debye length and differential measurements show a lower surface potential.

**Keywords:** Parkinson's disease;  $\alpha$ -synuclein; phospholipid layer; light-addressable potentiometric sensor

## Introduction

Parkinson's disease (PD) is an incurable musculoskeletal disorder. It is thought to be caused by mutations or aggregation of  $\alpha$ -synuclein ( $\alpha$ Syn), a causative substance present in the brain. Currently, there are no biomarker tests that can accurately diagnose the "prediagnostic" stage with high sensitivity and specificity [1].

In our previous studies we were able to determine  $\alpha$ Syn fibrils binding to liposomes or phospholipid layer using cantilever biosensors [2] and the LSPR (localized surface plasmon resonance) principle [3]. In this study we attempt to determine  $\alpha$ Syn by detecting its negative charge using a light-addressable potentiometric sensor (LAPS). A LAPS is a semiconductor-based potentiometric sensor [4]. It can detect surface charges in liquid solutions with spatial resolution. The measurement spots on the sensor surface are defined by focused light and the resulting photocurrent depends on the local surface potential.

## Results and Discussion

A LAPS chip with  $\text{Si}_3\text{N}_4$  surface was used. To immobilize the lipid layer, a thin film of an Au pattern was evaporated on some measurement spots. A SAM layer and a DPPC phospholipid monolayer was immobilized on this Au layer. The height of the SAM and lipid monolayer is expected to be 3.2 nm. Diluted PBS buffer with a concentration of 1.5 mM was used as measuring solution to obtain a Debye length of about 10 nm.

The relative change in surface potential over time of two measurement spots with lipid layer and two measurement spots without lipid layer are shown in Fig. 1. First, the measurement was started with PBS solution, at  $t = 0$ ,  $\alpha$ Syn fibrils were added to the solution to achieve a final concentration of 1  $\mu\text{M}$ . The measurement spots with lipid layer show a lower relative surface potential than the spots without lipid layer. The lower surface potential is probably due to the binding of  $\alpha$ Syn fibrils to the lipid layer.

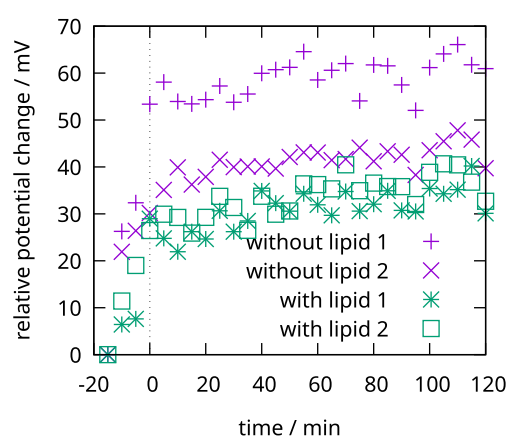


**Figure 1:** Relative change of surface potential over time for measurements spots with and without lipid layer after addition of  $\alpha$ Syn at  $t = 0$ .

## Conclusions

Preliminary measurements show that  $\alpha$ Syn binding to a phospholipid layer can be detected with LAPS due to the negative charge of  $\alpha$ Syn. This may be helpful in the development of a sensor for the early detection of PD.

## References

- [1] E. Tolosa, A. Garrido, S. W. Scholz, W. Poewe. *Lancet Neurol*, 20 (2021), 385, doi: 10.1016/S1474-4422(21)00030-2
- [2] R. Kobayashi, K. Kamitani, M. Sawamura, H. Yamakado, R. Takahashi, M. Sohgo, M. Noda, *IEEE Sensors Journal*, 23 (2023), 12495, doi: 10.1109/JSEN.2023.3272659
- [3] Y. Kimura, K. Kamitani, C. F. Werner, M. Takeda, M. Fukuzawa, M. Noda, *IEEE SENSORS*, (2023), doi: 10.1109/SENSORS56945.2023.10324968
- [4] M. J. Schöning, T. Wagner, A. Poghosian, K. Miyamoto, C. F. Werner, S. Krause, T. Yoshinobu, *Encyclopedia of Interfacial Chemistry*, (2018), 295, doi: 10.1016/B978-0-12-409547-2.13483-3

## Acknowledgements

This research was supported in part by a Grant-in-Aid for Scientific Research (KAKENHI Grant No. 20H00663 and 23K17476) from JSPS.



# Monitoring of saliva pH and buffer capacity using a miniaturized multiwell capacitive sensor

D. Özsoylu<sup>1</sup>, H. Aboelmagd<sup>1</sup>, M. E. Özler<sup>1,2</sup>, G. Conrads<sup>3</sup>, M. J. Schönning<sup>1,4</sup>, T. Wagner<sup>1,4</sup>

[oezsoylu@fh-aachen.de](mailto:oezsoylu@fh-aachen.de)

<sup>1</sup>Institute of Nano- and Biotechnologies (INB), Aachen University of Applied Sciences, Heinrich-Mußmann-Str. 1, 52428 Jülich, Germany

<sup>2</sup>Nanotechnology Engineering Department, Sivas Cumhuriyet University, Yenişehir Mah. Kayseri Cd. No:43 P.K. 58140 Kampus, Sivas, Türkiye

<sup>3</sup>Division of Oral Microbiology and Immunology, Department for Operative Dentistry, Periodontology and Preventive Dentistry, University Hospital RWTH, Pauwelsstraße 30, 52074 Aachen, Germany

<sup>4</sup>Institute of Biological Information Processing (IBI-3), Forschungszentrum Jülich GmbH, Wilhelm-Johnen-Str., 52425 Jülich, Germany

**Abstract:** Present sensors for detecting and monitoring saliva pH and buffer capacity usually require large volumes of saliva samples or do not allow quantitative measurements. In this work, we demonstrate a miniaturized multiwell capacitive sensor that can quantitatively monitor these parameters from only 100  $\mu\text{L}$  of saliva samples.

**Keywords:** Saliva; buffer capacity; pH; multiwell; miniaturization

## Introduction

As a natural buffer, saliva plays an important role in sustaining oral health. The healthy saliva pH range is usually 6.7 to 7.4, and sudden pH change in the oral cavity is resisted and retained, thanks to the buffering capacity of saliva. In addition to regular dental examinations, measurements of saliva pH and buffer capacity could help to maintain optimal dental health. To measure the person's saliva buffering capacity, usually, non-quantitative methods (e.g., colorimetric pH test strips) or methods that require large volumes of saliva (e.g., measurements with conventional pH electrodes) are employed. On the other hand, considering the precise measurements, especially with the samples from pediatric patients where the amount of obtained saliva is limited, developing new diagnostic tools is crucial.

In this work, we fabricated a capacitive electrolyte-insulator-semiconductor (EIS) sensor that can measure pH and buffer capacity from saliva samples (Figure 1). To facilitate the miniaturized multiwell sensor set-up, the sensor surface was patterned photolithographically using a negative photoresist (SU-8 2150) after fabricating the capacitive EIS sensor as described in literature [1]. After that, a micro-agar-salt-bridge was prepared in the tip of a pipette to allow a proper interface between the conventional reference electrode and small saliva droplets. After adding about 100  $\mu\text{L}$  samples of saliva to the wells, an impedance analyzer was used for the signal measurements (e.g., capacitance-voltage curve). After measuring the saliva sample's pH, the samples underwent titration using an HCl solution while monitoring

the change in their pH values. The pH buffer capacity was calculated according to the moles of acid added and the resulting pH change.

## Results and Discussion

The saliva droplets properly stayed inside the wells without overflowing due to the difference in wettability between the transducer and SU-8 passivation layer. It could be demonstrated, using saliva samples from three individuals, that the developed sensor system enables the quantitative assessment of pH and buffer capacity in small saliva samples (around 100  $\mu\text{L}$ ).

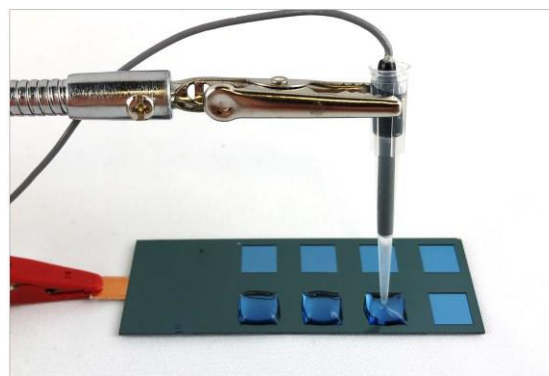


**Figure 1:** Miniaturized multiwell capacitive sensor set-up for saliva pH & buffer capacity measurements.

## References

- [1] A. Poghossian, M. J. Schönning, *Sensors* **20** (2020) 5639, doi: 10.3390/s20195639.

## Acknowledgements

The authors thank H. Iken for technical support.

# Electrochemical degradation of molecularly imprinted polymers for advanced inflammation sensors in cochlear implants

Nguyen, Hai<sup>1</sup>, Adrian Onken<sup>1</sup>, Theodor Doll<sup>1</sup>

nguyen.minh-hai@mh-hannover.de; Onken.Adrian@mh-hannover.de; Doll.Theodor@mh-hannover.de

<sup>1</sup>ORL Department, Hannover Medical School, Carl-Neuberg-Straße 1, 30625 Hannover, Germany

**Abstract:** Inflammation significantly affects the performance of cochlear implants (CIs). To prevent the inflammation, new inflammation sensor such as molecularly imprinted polymers (MIPs) is required. Since CIs must remain in the body for several years, MIPs must fulfil strict requirements, including biocompatibility, biodegradability, and conductivity. In this study, a conductive and biocompatible MIP was characterized and electrochemically degraded using impedance measurement. The degraded molecules in the solution were then analysed using Fourier-transform infrared spectroscopy (FTIR). At 0.205 V a negligible amount of dissolved polymer in addition to the dissolved monomer was measured, which can be defined as the limiting potential.

**Keywords:** Cochlear implant; electrochemical polymerization; MIPs; electrochemical degradation

## Introduction

The CI is a widely used hearing device in which a microelectrode array is surgically inserted directly into the cochlea, ideally remaining there for life. However, statistically, 40% of CI devices fail after implantation, necessitating re-implantation. One potential complication associated with CI is inflammation, which can occur in the first few months [1]. Therefore, information about inflammation is crucial for the timely administration of anti-inflammatory medication. MIP sensors on a CI electrode are suitable for inflammation (e.g. interleukin 6) detection [2, 3]. The requirement for such an inflammation sensor is polymer self-degradation, since stimulation is the intended long-term use for CI. These MIPs could be conductive for further improvement of sensitivity. In this work, conductive MIP and non-MIP (NIP) was deposited onto electrode by electrochemical polymerization. Biotin was first used as a template due to the high cost of interleukin and its epitopes. PEDOT:PSS was selected as a conductive polymer.

## Method

PEDOT:PSS was deposited by cyclic voltammetry onto a platinum electrode. For the biotin sensing, MIPs were washed in acid-base solution and then impedance measurements were conducted in Phosphate-buffered saline (PBS) solution with and without biotin. Paracetamol and ibuprofen were also used to determine cross-sensitivity. Since PEDOT is not biodegradable, the polymer was electrochemically degraded by additional impedance measurements, where the applied voltage was varied to modulate degradation. Finally, to investigate the polymer biocompatibility according to ISO guidelines, the PBS solution containing the degraded monomer molecules was analysed by FTIR.

## Result

The change in impedance of the MIPs demonstrated a successful incorporation of biotin. As expected,

NIPs was not capable of detecting biotin. In addition, no impedance change was observed when the MIPs were immersed in a solution containing paracetamol or ibuprofen. The polymer was then electrochemically degraded by an additional impedance measurement at a differential voltage. In the degradation analysis, fewer dissolved polymers and more degraded monomer molecules were detected with decreasing potential. Below the potential of 205 mV, only dissolved monomer molecules were obtained, which enables renal clearance. An impedance shift during the analysis could also be measured, demonstrating the real-time degradation monitoring (Figure 1). Biocompatibility testing revealed a high biocompatibility for both the polymer and the solution with dissolved monomer molecules. Based on these findings, we have developed conductive, biocompatible and controllably degradable MIPs capable of detecting biotin.

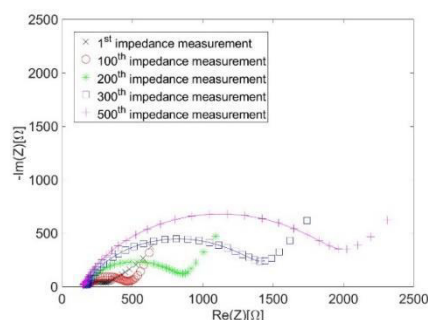


**Figure 1:** Nyquist diagram for the electrical degradation

## References

- [1] J. Anderson, Seminars in Immunology, 2008.
- [2] M. Goncalves et. al., Analytical Letter, 2021
- [3] Gideon Wackers, KU Leuven, 2021.

## Acknowledgements

This study is funded by the “Cluster of Excellence Hearing4All” (EXC2077).

# Investigation on the influence of Ytterbium on potentiodynamic polarization of co-evaporated Magnesium thin-films.

Manuel Hofinger<sup>1</sup>, Hüseyin Zengin<sup>1</sup>, Gianina Popescu Pelin<sup>2</sup>, Gabriel Socol<sup>2</sup> Andrei Ionut Mardare<sup>1</sup>, Achim Walter Hassel<sup>1,3</sup>

manuel.hofinger@jku.at

<sup>1</sup> Institute of Chemical Technology of Inorganic Materials, Johannes Kepler University Linz, Altenberger Straße 69, 4040 Linz, Austria

<sup>2</sup>Lasers Department, National Institute for Lasers, Plasma and Radiation Physics, 077125 Magurele, Romania

<sup>3</sup>Danube Private University, Steiner Landstraße 124, 3500 Krems an der Donau,

**Abstract:** A Magnesium-Ytterbium thin film library was produced by co-evaporation of both metals, covering a compositional gradient from 1 to 10 at.% Yb, identified via scanning Energy Dispersive X-ray Spectroscopy (SEDX). Scanning Electron Microscopy (SEM) revealed a change of the nano structure on the surface over the compositional gradient. Potentiodynamic polarization curves showed a significant change of the behaviour of the library on the as-produced alloy as well as on the anodized one.

**Keywords:** Thin-film library; Tafel-Plots; Magnesium; Ytterbium

## Introduction

Magnesium is an attractive material in many applications due to its low density, high strength and good machinability. Nevertheless, its poor corrosion resistance limits its possible applications as a pure metal. Therefore, different alloying materials and protection strategies are often used to improve the corrosion resistance. Rare-earth elements show a significant potential in Mg alloys. However, there are only limited studies of the influence of Yb as an alloying element with Mg.

## Results and Discussion

A thin film library of Mg-Yb with a compositional gradient was produced, using a self-developed co-evaporation system [1]. For the mapping of the Mg-Yb library SEDX spectroscopy was used. In order to identify the composition along the library, various locations were measured by quantifying the EDX data (IDFix software, remX GmbH) obtained under irradiation with a 20 keV electron beam. Samples with an overall compositional gradient from 1 at.% to 10 at.% Yb were produced SEM showed an increase of nano-structuring in higher Yb contents. Scanning droplet cell microscopy (SDCM) using a 3D-printed cell with a diameter of 2 mm was employed for the investigation of the corrosion properties of different alloys in phosphate-buffered saline (PBS) [2].

Electrochemical investigations of the alloys were done on the as-produced samples as well as on the anodized samples. The anodization was performed potentiostatically for 5 min at 1 V<sub>SHE</sub> in 1 M NaOH. For testing the corrosion properties, potentiodynamic polarization curves were recorded and Tafel plots were investigated for the calculation of

polarization resistance ( $R_p$ ) and the corrosion rate ( $cr$ ).

Figure 1 shows that the anodization of the alloys lowers the  $cr$  and increases the  $R_p$  in higher Yb contents, indicating an improved corrosion resistance. Also, the addition of Yb lowers the corrosion rate significantly in the as-produced as well as in the anodized alloys with an asymptotic behaviour in higher contents.

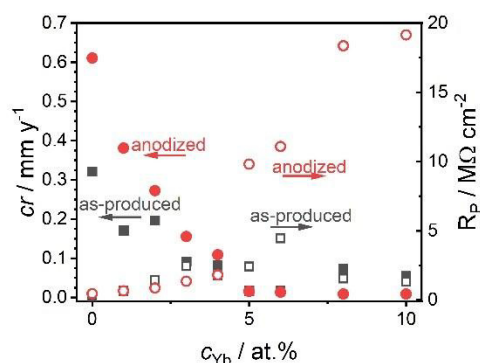


**Figure 1:** Change of corrosion rate and polarization resistance with increasing Yb content.

## Conclusions

It was shown that an increasing content of Yb decreases the corrosion rate of Mg thin-films. Anodization of the alloys give an even better protection of the Mg-Yb thin film library.

## References

- [1] A.I. Mardare, C.D. Grill, I. Pötzelberger, T. Etzelstorfer, J. Stangl, A.W. Hassel, , *J. Solid State Electrochem.* **20** (2016) 1673–1681.
- [2] J.P. Kollender, M. Voith, S. Schneiderbauer, A.I. Mardare, A.W. Hassel, *J. Electroanal. Chem.* **740** (2015) 53–60

## Fibroin as biocompatible and bioabsorbable immobilization matrix for amperometric biosensors?

K. A. Janus<sup>1,2</sup>, S. Achtsnicht<sup>1</sup>, A. Drinic<sup>3</sup>, A. Kopp<sup>3</sup>, M. Keusgen<sup>2</sup>, M. J. Schöning<sup>1,4</sup>

[janus@fh-aachen.de](mailto:janus@fh-aachen.de)

<sup>1</sup>Institute of Nano- and Biotechnologies (INB), Aachen University of Applied Sciences, Heinrich-Mußmann-Str. 1, 52428 Jülich, Germany

<sup>2</sup>Institute for Pharmaceutical Chemistry, Philipps University of Marburg, Wilhelm-Roser-Str. 2, 35032 Marburg, Germany

<sup>3</sup>Fibrothelium GmbH, Philipsstr. 8, 52068 Aachen, Germany

<sup>4</sup>Institute of Biological Information Processing (IBI-3), Forschungszentrum Jülich GmbH, Wilhelm-Johnen-Str., 52425 Jülich, Germany

**Abstract:** Reliable enzyme immobilization represents a crucial challenge in biosensor development. In this work, we studied an enzyme immobilization matrix based on bioabsorbable silk-fibroin, extracted from the silk of the silkworm *Bombyx mori*, for a screen-printed carbon-based amperometric glucose biosensor on a flexible silk-fibroin substrate. The biosensor was characterized for physiological glucose concentrations ranging from 0.5 mM to 10 mM, and the influence of pH, temperature and reproducibility over four days was investigated.

**Keywords:** glucose oxidase; enzyme immobilization; silk-fibroin; bioabsorbable; glucose biosensor

### Introduction

The biosensor performance is profoundly affected by the selected immobilization method for the biological recognition element [1]. A conventional strategy for an amperometric biosensor is embedding the enzyme within a matrix of bovine serum albumin and glutaraldehyde. However, glutaraldehyde as a toxic compound can lead to several health issues and is therefore not suitable for implantable biosensors [2]. Silk-fibroin, on the other hand, is a fully biocompatible and bioabsorbable natural material, which might preserve the enzyme activity and can improve its stability to pH and temperature fluctuations [3].

### Results and Discussion

Silk-fibroin was used as a matrix to immobilize glucose oxidase on a carbon-based, screen-printed electrode on a silk-fibroin substrate. Here, the silk-fibroin content, the enzyme loading and the method to create a water-insoluble immobilization matrix were studied. The optimized silk-fibroin matrix was compared to the established bovine serum albumin & glutaraldehyde one with regard to the ability to withstand pH and temperature variations. The signal evolution of repeated measurement over 4 days was tested.

### Conclusions

Silk-fibroin was successfully implemented as an enzyme immobilization matrix for a screen-printed flexible, bioabsorbable electrode using the model enzyme glucose oxidase, see Figure 1. Silk-fibroin as immobilization matrix shows comparable characteristics to the established bovine serum albumin & glutaraldehyde system. Thus, resigning the usage of toxic chemicals, silk-fibroin represents

a biocompatible, bioabsorbable and sustainable alternative for enzyme immobilization. Highest mean glucose sensitivity resulted for 0.5 wt% silk-fibroin as matrix with 42 and 33 nA mm<sup>-2</sup> mM<sup>-1</sup> for 0.6 U and 1.2 U GOx, respectively, in the glucose concentration range from 0.5 mM to 4 mM.

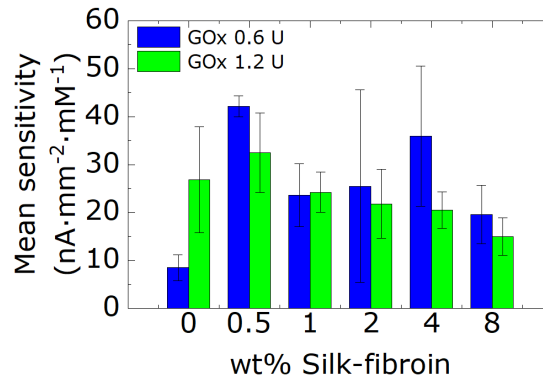


**Figure 1:** Mean glucose sensitivity of screen-printed carbon electrodes on bioabsorbable silk-fibroin, modified with 0.6 U (blue) or 1.2 U (green) glucose oxidase (GOx) and immobilized in a drop-coated silk-fibroin matrix with different silk-fibroin contents (0.5 wt% - 8 wt%).

### References

- [1] A. Sassolas, L. J. Blum, B. D. Leca-Bouvier, *Biotechn. Adv.* **30** (2012) 489-511
- [2] T. Takigawa, Y. Endo, *J. Occup. Health.* **2** (2006) 75-87
- [3] S. Lv, *Molecules* **25** (2020) 4929



## Work Function Tuning by Alloying: Silver – Ln Libraries

Theodor Doll<sup>1,2</sup>, Andrei Mardare<sup>2</sup>, Victor Manuel Fuenzalida<sup>3</sup>, Achim Walter Hassel<sup>2</sup>

[doll.theodor@mh-hannover.de](mailto:doll.theodor@mh-hannover.de)

<sup>1</sup>Biomaterial Engineering, NIFE Institute, Hannover Medical School, Stadtfeldamm 34, 30625 Hannover, Germany; <sup>2</sup>Institute of Chemical Technology of Inorganic Materials, Johannes Kepler University Linz, Altenberger Straße 69, 4040 Linz, Austria, <sup>3</sup>Superficies Lab, FCFM, Universidad de Chile, Santiago, Chile

**Abstract:** The work function of the elements is used in electronics as well as in generation of free electrons, e.g. in air. A work function tuning would be helpful in many cases. With the method of material libraries we find some general correlation between known phase diagrams for the elemental compositions and the corresponding work function. This seems to hold for both eutectic points and intermetallic phases.

**Keywords:** material libraries; work function; phase diagram; eutectic; intermetallic phases;

### Introduction

The work function  $\phi$  is the energy that must be delivered to a solid in order to release a first electron from it to the point where even the image forces that the electron can still cause are overcome. In practice, the work function of metals is used in the design of low-voltage electronics, in the arc ignition of welding electrodes or in completely new applications of chemical analysis technology with free electrons in air [1].

Since the work function of pure substances has been tabulated with a high degree of certainty, one can imagine that ‘work function tuning’ can be carried out by mixing two or more components. This applies almost ideally to continuously miscible elements such as gold and silver, i.e. the mixing ratios are transferred almost linearly to  $\phi$ . On the other hand, it is known from welding electrodes, for example, that the work function of tungsten is so drastically reduced by adding just a few per cent of thorium (today: cerium) that these electrodes can be ignited at all. The question therefore arises as to how the mixing ratio is transferred to the work function.

### Results and Discussion

Although there are few models that attempt to calculate the work function of alloys self-consistently via atomic radii and the refilling of hybrid orbitals with electrons, the Linz method for the production of binary and ternary material libraries with subsequent analytical scanning via the local compositions offers an excellent experimental possibility for verification.

As we are looking for an emitter surface that is as stable as possible in air for applications of electrons in air, silver, which is largely resistant to oxidation, was selected as the starting material. The Ag-Ce-Sm and Ag-Pr-Yb systems were deposited as material libraries, mapped with EDX and the associated emission work in nitrogen and air was measured using the Scanning Kelvin Probe.

On the one hand, we find that the lanthanides in both libraries mix well with each other, i.e. they occur as

a lanthanide sum. What surprises us is the course of the measured work function over the changed system stoichiometries. This appears to be similar to the known phase diagrams for binary alloys with both eutectic points and intermetallic phases. The extent to which further correlations can be found here will be presented at the conference.

The basic understanding of this completely new correlation is as follows: To a first approximation, the work function of a solid is related to the first ionisation energies of the free atoms plus the Energy of Formation. The latter is, to a very rough approximation, linked to the melting points of the solids.

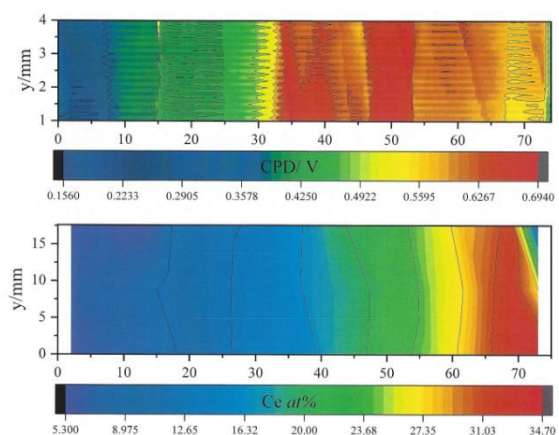


**Figure 1:** AgCe material library on a glass slide: The work function (upper) over the elemental composition (lower) reveals a peak at 22-25 at% Ce.

### Conclusions

It was finally found that the progression of the work function of material libraries is similar to the associated phase diagrams of the systems.

### References

- [1] Doll, T.; Fuenzalida, V.M.; Schütte, H.; Gaßmann, S.; Velasco-Velez, J.J.; Köhler, R.; Kontschew, A.; Haas, T.; Hassel, A.W.; et al. Physical Trace Gas Identification with the Photo Electron Ionization Spectrometer (PEIS). *Sensors* **2024**, *24*, 1256. <https://doi.org/10.3390/s24041256>

# Aluminium-doped manganese dioxide particles “boosting” hydrogen peroxide sensitivity?

S. Achtsnicht<sup>1</sup>, D. Saputri<sup>1</sup>, H. Iken<sup>1</sup>, V. A. Hayrapetyan<sup>2</sup>, M. J. Schöning<sup>1,3</sup>

[achtsnicht@fh-aachen.de](mailto:achtsnicht@fh-aachen.de)

<sup>1</sup>Institute of Nano- and Biotechnologies (INB), Aachen University of Applied Sciences, Heinrich-Mußmann-Str. 1, 52428 Jülich, Germany

<sup>2</sup>Innovation Center for Nanoscience and Technologies, A.B. Nalbandyan Institute of Chemical Physics NAS, 5/2 P. Sevak str., Yerevan, Armenia

<sup>3</sup>Institute of Biological Information Processing (IBI-3), Forschungszentrum Jülich GmbH, Wilhelm-Johnen-Str., 52425 Jülich, Germany

**Abstract:** Hydrogen peroxide vapor is an important agent to sterilize packaging materials in aseptic food industry. In order to monitor such sterilization processes, calorimetric gas sensors can be applied, often utilizing  $\text{MnO}_2$  as catalytically active material to determine the released reaction enthalpy of the exothermal  $\text{H}_2\text{O}_2$  decomposition. In this work, the influence of Al-doped manganese dioxide particles on the sensor behavior of a calorimetric gas sensor was studied.

**Keywords:**  $\text{H}_2\text{O}_2$ ; aseptic packaging; Al- $\alpha$ - $\text{MnO}_2$ ; manganese dioxide; calorimetric gas sensors

## Introduction

Gaseous  $\text{H}_2\text{O}_2$  is widely used in aseptic food packing for sterilization of sensitive foods such as milk or juices. Recently, calorimetric gas sensors were introduced as a differential sensor setup to monitor both the  $\text{H}_2\text{O}_2$  concentration quantitatively and in-line [1]. This setup employs two identical thin-film resistive temperature detectors (RTDs), passivated against  $\text{H}_2\text{O}_2$  by a thermally stable polymer layer. One of the sensor elements (called “active”) is modified with a catalyst, like  $\text{MnO}_2$ . The catalyst enables the reaction of  $\text{H}_2\text{O}_2$  to  $\text{H}_2\text{O}$  and  $\text{O}_2$ , releasing energy in form of a temperature increase. The temperature difference between the active and passive (without catalyst) sensor element serves as  $\text{H}_2\text{O}_2$  concentration-dependent sensor signal.

To improve the lower detection limit of these calorimetric gas sensors and to also study the overall sensor characteristics, a new approach is suggested that is dealing with Al-doped manganese dioxide (Al- $\alpha$ - $\text{MnO}_2$ ) particles. Al- $\alpha$ - $\text{MnO}_2$  is discussed in literature, e.g., as cathodic material in battery research [2,3]. The abundant Mn vacancies resulted in an increase of the specific surface area and pore size, and enabled an increased cycling stability.

## Results and Discussion

Al- $\alpha$ - $\text{MnO}_2$  particles with different doping concentrations of Al have been prepared using the microwave-assisted hydrothermal method. Sensor substrates with Pt-based RTD structures for the calorimetric detection have been produced and passivated by means of thin-film technologies. The

active element was either modified with  $\text{MnO}_2$  powder or Al- $\alpha$ - $\text{MnO}_2$  doped powders. For each calorimetric  $\text{H}_2\text{O}_2$  gas sensor, concentration-dependent temperature measurements have been performed and compared as calibration plots.

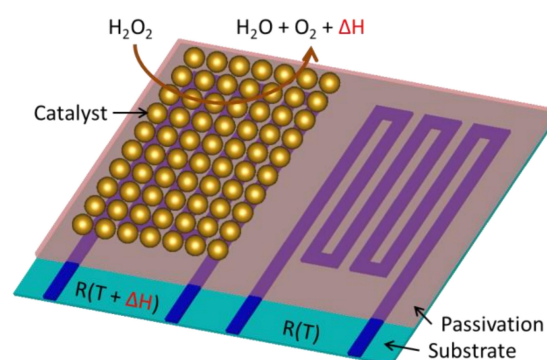


**Figure 1:** Schematic of a calorimetric gas sensor for gaseous  $\text{H}_2\text{O}_2$  detection. The sensor consists of two identical RTD structures (purple) on the same chip with a passivation layer (russet) on top. The active element (left) is modified with the catalyst (gold) enabling the exothermic reaction of gaseous  $\text{H}_2\text{O}_2$  to  $\text{H}_2\text{O}$  and  $\text{H}_2$  that releases additional reaction enthalpy ( $\Delta H$ ).

## References

- [1] F. Vahidpour, J. Oberländer, M. J. Schöning, *Phys. Status Solidi A* **215** (2018) 1800044
- [2] B. He, J. Huang, P. Ji, T. K. Hoang, M. Han, L. Li, L. Zhang, Z. Gao, J. Ma, J. Zhi, P. Chen, *J. Power Sources* **554** (2023) 232353
- [3] S. Huang, J. Sun, J. Yan, J. Liu, W. Wang, Q. Qin, W. Mao, W. Xu, Y. Wu, J. Wang, *ACS Appl. Mater. Interfaces* **10** (2018) 9398–9406

# Exploring 2D material-substrate dielectric interface in MoS<sub>2</sub> liquid-gated transistors

Animesh Pratap Singh<sup>1</sup>, Han Xu<sup>1</sup>, Amir Ghiami<sup>2</sup>, Songyao Tang<sup>2</sup>, Daniyar Kizatov<sup>1</sup>, Andrei Vescan<sup>2</sup>, Sven Ingebrandt<sup>1</sup>, Vivek Pachauri<sup>1</sup>

[singh@iwe1.rwth-aachen.de](mailto:singh@iwe1.rwth-aachen.de)

<sup>1</sup>Institute of Materials in Electrical Engineering 1 and <sup>2</sup>Compound Semiconductor Technology, RWTH Aachen University, Sommerfeldstr. 18-24, 52074 Aachen, Germany

**Abstract:** Two-dimensional (2D) material properties, due to their atomically thin nature, are highly influenced by the underlying substrate. In this work, we study the effect of various substrate dielectrics on molybdenum disulphide (MoS<sub>2</sub>) based liquid-gated transistors. We performed Raman spectroscopy to gain the insights on strain, doping and roughness of transferred MoS<sub>2</sub> layers. Threshold voltage variation in MoS<sub>2</sub> liquid-gated transistors correlated with Raman measurements indicating a significant influence of the underlying substrate on the transistor performance.

**Keywords:** 2D materials; MoS<sub>2</sub>; liquid-gated transistors; Raman spectroscopy

## Introduction

Two-dimensional materials exhibit promising potential for various applications due to their unique properties at atomic scale. Doping, strain [1] and charge transfer mechanism [2] can be tuned by the underlying substrate materials. In liquid-gated transistors, hydrophobicity or hydrophilicity can alter the electrical double layer structure at the 2D-material/liquid interface [3]. In this work, we study the effect of various substrate dielectrics (SiO<sub>2</sub>, Al<sub>2</sub>O<sub>3</sub>, HfO<sub>2</sub> and MgF<sub>2</sub>) on MoS<sub>2</sub> based liquid-gated transistor performance. After transferring MoS<sub>2</sub> grown on sapphire on these substrates using the PMMA-assisted wet transfer method, we performed Raman spectroscopy to characterize strain and doping level in MoS<sub>2</sub> layers. Further, we fabricated MoS<sub>2</sub> transistor arrays to explore the substrate effect in liquid-gate configuration using de-ionised water.

## Results and Discussion

Raman spectroscopy showed the variation of characteristic modes of MoS<sub>2</sub> i.e. E<sup>1</sup><sub>2g</sub> and A<sub>1g</sub> on as grown sapphire and after transfer onto different substrates (Figure 1b). The A<sub>1g</sub> mode, which is more sensitive to doping in MoS<sub>2</sub>, showed higher n-doping compared to the as grown layers. After transfer, due to a substrate-induced charge transfer effect, reduced n-doping was observed for SiO<sub>2</sub> and Al<sub>2</sub>O<sub>3</sub> substrates. For HfO<sub>2</sub> and MgF<sub>2</sub> substrates, the doping level increased. A similar shift trend was observed for the E<sup>1</sup><sub>2g</sub> mode, indicating increasing strain for HfO<sub>2</sub> and MgF<sub>2</sub> substrates. To analyse the substrate-induced effects on MoS<sub>2</sub> liquid-gated transistor performance, we extracted the threshold voltage. For SiO<sub>2</sub>, Al<sub>2</sub>O<sub>3</sub> and HfO<sub>2</sub> substrates, V<sub>th</sub> was positive with a slight change, whereas on the MgF<sub>2</sub> substrate we observed a significant decrease and negative V<sub>th</sub> (Figure 1c). This may be explained by a higher doping in MoS<sub>2</sub> consistent with Raman measurements.

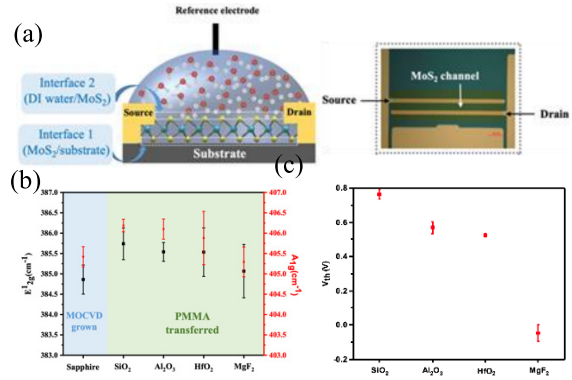


**Figure 1:** (a) Schematics (left) and optical image of MoS<sub>2</sub> liquid-gated transistor having two interfaces. (b) Raman measurements showing variation of E<sup>1</sup><sub>2g</sub> and A<sub>1g</sub> modes on different substrates indicating different doping and strain. (c) Variation of the threshold voltage in MoS<sub>2</sub> liquid-gated transistors on different substrates.

## Conclusions

From these experiments, we conclude that the underlying substrate can significantly alter the properties of atomically thin MoS<sub>2</sub> layers and its transistor performance in DI water. Thus, the choice of substrate becomes crucial, while working with 2D material-based sensor applications.

## References

- [1] Salvatore Ethan Panasci *et al.*, *ACS Applied Materials & Interfaces* 2021 13 (26), 31248-31259
- [2] Park, S., Schultz, T., Xu, X. *et al. Commun Phys* 2, 109 (2019).
- [3] Sun Sang Kwon *et al.*, *Nano Letters* 2019 19 (7), 4588-4593

## Acknowledgements

We gratefully acknowledge the financial support from the DFG project BioNanoLock (grant no. 440055779) and the Federal Ministry of Education and Research (BMBF) project NEUROTEC-II, (grant no. 16ME0399).

## Combinatorial study of aluminium-dysprosium thin films

Lukas Pötscher<sup>1</sup>, Andrei Ionut Mardare<sup>1</sup>, Gianina Popescu-Pelin<sup>2</sup>, Gabriel Socol<sup>2</sup>, Achim Walter Hassel<sup>1,3</sup>

[k11913194@students.jku.at](mailto:k11913194@students.jku.at)

<sup>1</sup>Institute of Chemical Technology of Inorganic Materials, Johannes Kepler University Linz, Altenberger Str. 69, 4040 Linz, Austria

<sup>2</sup>Lasers Department, National Institute for Lasers, Plasma and Radiation Physics, 077125 Magurele, Romania

<sup>3</sup>Danube Private University, Steiner Landstraße 124, Krems and der Donau, Austria

**Abstract:** A combinatorial study of aluminium-dysprosium thin films was conducted to determine the influence of the rare earth element on the aluminium. Therefore, thin films with a compositional gradient of dysprosium in aluminium were produced by thermal co-evaporation onto glass substrates. The compositional gradient was determined by energy dispersive X-ray spectroscopy (EDX). Electrochemical, morphological, structural, and mechanical properties of the thin films were investigated by electrochemical impedance spectroscopy (EIS), scanning electron microscopy (SEM), X-ray diffraction (XRD) and nanoindentation respectively.

**Keywords:** thin films; combinatorial library; electrochemical impedance spectroscopy; anodization

### Introduction

Preceding studies on aluminium-rare earth systems have shown that already low concentrations of the rare earth can have a significant influence on these alloys. For example aluminium-holmium alloys can form an amorphous phase, and the resulting change in morphology leads to decreased oxide formation upon anodization [1]. Nevertheless, different rare-earth elements show dissimilar results for the combinatorial study, as the aluminium-erbium library shows only a reduction in crystallinity but no clearly amorphous phase [2]. Studies on the aluminium-dysprosium system are still missing and therefore the possibility that new properties in this combinatorial library can be found.

### Results and Discussion

A binary thin film library was produced by thermal co-deposition of aluminium and dysprosium onto glass substrates. EDX measurements showed a compositional gradient from 0.2 to 15 at.% dysprosium in aluminium over three produced thin films.

For the electrochemical analysis ten cyclic voltammograms (CVs) were conducted up to 10 V above the open circuit potential (OCP) of each alloy in steps of 1 V. After each anodization step an EIS measurement was done. The data of the CVs was used to calculate the film formation factor of the oxide grown by coulometry, while the data from the EIS resulted in the dielectric constant of the grown oxide. Up to approximately 5 at.% Dy both the film formation factor and dielectric constant stayed rather constant. At concentrations between 5 to 10 at.% Dy very high currents were measured up to the fifth CV which might be due to higher oxide formation because of the effect of the Dy on the surface resulting in a higher roughness or its oxidation behaviour. Above a concentration of 10 at.% Dy the

determination of the film formation is not possible as the CVs are not separated anymore, shown in Figure 1.

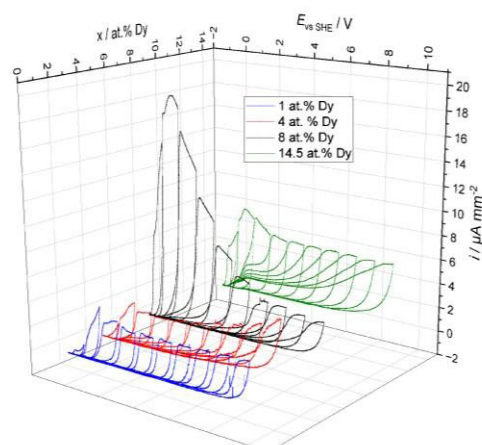


**Figure 1:** CVs at different concentrations in the Al-Dy system.

### Conclusions

The film formation factor and the dielectric constant stay rather constant up to 5 at.% Dy while they show higher values in the range of 5 to 10 at.% Dy even when the very high currents from the first five CVs are neglected. Above a concentration of 10 at.% Dy the determination of the film formation factor is not possible as the CVs are not separated any more.

### References

- [1] K. Shahzad, C. C. Mardare, D. Recktenwald, A. I. Mardare, A. W. Hassel, *Electrochim. Acta*, **297** (2019) 888-904.
- [2] A. I. Mardare, C. C. Mardare, A. W. Hassel, *J. Solid State Electrochem.*, **20** (2018) 869-876.



# Characterization of an Al<sub>2</sub>O<sub>3</sub> extended-gate ion-sensitive field-effect transistor with Nernstian behavior

M. Knoll<sup>1,2</sup>, A. Poghosian<sup>3</sup>, H. Sündermann<sup>1</sup>, S. Meier<sup>4</sup>, E. Müllner<sup>4</sup>, M. Keusgen<sup>2</sup>, M. J. Schöning<sup>1,5</sup>

[Knoll@fh-aachen.de](mailto:Knoll@fh-aachen.de)

<sup>1</sup>Institute of Nano- and Biotechnologies (INB), Aachen University of Applied Sciences, Heinrich-Mußmann Str. 1, 52428 Jülich, Germany

<sup>2</sup>Institute of Pharmaceutical Chemistry, Philipps University of Marburg, Wilhelm-Roser-Str. 2, 35032 Marburg, Germany

<sup>3</sup>MicroNanoBio, Liebigstr. 4, 40479 Düsseldorf, Germany

<sup>4</sup>Texas Instruments Incorporated, Freising, Haggertystr. 1, Germany

<sup>5</sup>Institute of Biological Information Processing (IBI-3), Forschungszentrum Jülich GmbH, Wilhelm-Johnen-Str., 52425 Jülich, Germany

**Abstract:** This work describes a sensing platform containing three extended-gate ion-sensitive field-effect transistors (EG-ISFETs). Each EG-ISFET has an adjustable floating-gate charge, enabling individual calibration. The presented EG-ISFET structure is CMOS- (complementary metal-oxide-semiconductor) compatible and uses atomic layer deposited (ALD) Al<sub>2</sub>O<sub>3</sub> as pH-sensitive material. By means of electrochemical characterization these devices were evaluated in a pH range of pH 2 – 12, in terms of their sensing properties such as drift, pH sensitivity, hysteresis and linear concentration range. The influence of alkaline buffer solutions on the Al<sub>2</sub>O<sub>3</sub> pH-sensitive layer was studied by means of energy-dispersive X-ray spectroscopy.

**Keywords:** extended-gate ISFET; floating-gate; ALD Al<sub>2</sub>O<sub>3</sub>; pH sensitivity; drift

## Introduction

Extended-gate ISFETs (EG-ISFET) are discussed in literature for their improved chemical stability and signal-to-noise ratio as well as their light insensitivity [1,2]. A new chip combining three EG-ISFETs with adjustable floating-gate and an ALD-deposited Al<sub>2</sub>O<sub>3</sub> as pH-sensitive dielectric layer was characterized in terms of its drift behavior, pH sensitivity, hysteresis and linear concentration range. A schematical cross-section of the used EG-ISFET is given in Figure 1.

## Results and Discussion

If necessary, each EG-ISFET was individually tuned by adjusting its floating-gate charge. The drift behavior was observed over 48 h from the initial contact with buffer (pH 7). For the first 24 h, it was found that sensors with an initially low floating-gate charge showed a different signal behavior from those with a sufficient floating-gate charge before calibration. After about 24 hours, all EG-ISFETs possessed a similar, drift of about  $0.6 \pm 0.2$  mV/h. pH characterization was performed by consecutive cycles from pH 2 to pH 12 and vice versa. In the tested pH range all sensors showed an average pH sensitivity of  $58.3 \pm 1.1$  mV/pH. It was observed that the signal increased steadily with each pH cycle. Additional energy-dispersive X-ray spectroscopy studies gave evidence that this change in signal is due to dissolution of the Al<sub>2</sub>O<sub>3</sub> layer in alkaline buffers such as pH 11 and pH 12.

## Conclusions

The tested EG-ISFETs showed a good pH sensitivity with Nernstian behavior. The Al<sub>2</sub>O<sub>3</sub> used turned out to be unstable in highly alkaline pH environment (pH 11 - 12). In the future, automated sensor characterization should allow to study up to 72 EG-ISFETs simultaneously.

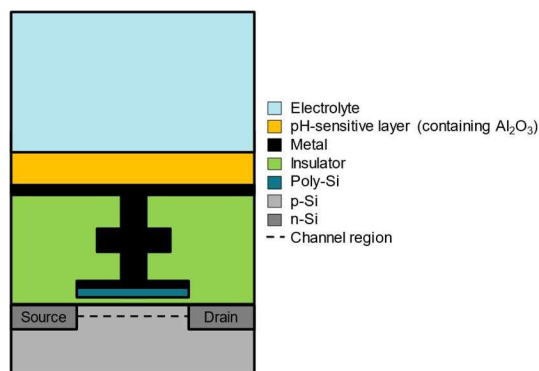


**Figure 1:** Schematic cross-section of the studied Al<sub>2</sub>O<sub>3</sub> EG-ISFET.

## References

- [1] O. Gubanova, A. Poletaev, N. Komarova, V. Grudtsov, D. Ryazantsev, M. Shustinskiy, M. Shibalov, A. Kuznetsov, *MRS* **177**, (2024)
- [2] N. Y. Teng, Y. T. Wu, R. X. Wang, C. T. Lin, *IEEE Sens.* **21**, (2021) 8831-8838

# Combinatorial analysis of silver-gold alloy thin films for possible application in AIMD

Martin Konrad<sup>1</sup>, Gianina Popescu-Pelin<sup>2</sup>, Gabriel Socol<sup>2</sup>, Andrei Ionut Mardare<sup>1</sup>, Achim Walter Hassel<sup>1,3</sup>

martin.konrad@jku.at

<sup>1</sup>Institute of Chemical Technologies of Inorganic Materials (TIM), Johannes Kepler University Linz (JKU), Altenberger Straße 69, 4040 Linz, Austria

<sup>2</sup>Lasers Department, National Institute for Lasers, Plasma and Radiation Physics, 077125 Magurele, Romania

<sup>3</sup>Danube Private University (DPU), Steiner Straße 124, 3500 Krems-Stein, Austria

**Abstract:** Combinatorial analysis is employed to investigate the physical and electrochemical properties of the silver-gold system in the form of a thin film library, using energy dispersive X-ray spectroscopy, scanning electrode microscopy, X-ray diffraction, cyclic voltammetry and electrochemical impedance spectroscopy. This is done to assess the alloys' potential for application in active implantable medical devices such as cochlear implants or cardiac pacemakers.

**Keywords:** combinatorial analysis; silver; gold; thin films; active implants

## Introduction

Active implantable medical devices (AIMD) are employed in a variety of different applications, such as cochlear implants, cardiac pacemakers or glucose sensors [1]. Noble metals and their alloys show promise for use in AIMD due to several properties, including biocompatibility and conductance [2]. In this study, a combinatorial approach was used for screening a silver-gold (Ag-Au) thin film library to assess the aptitude of different Ag-Au alloys for application in AIMD.

## Results and Discussion

A thin film library of the Ag-Au system was prepared via thermal co-evaporation and investigated using energy-dispersive X-ray (EDX) spectroscopy, scanning electron microscopy (SEM) and X-ray diffraction (XRD). Using phosphate buffered saline as electrolyte, cyclic voltammetry (CV) and electrochemical impedance spectroscopy (EIS) were conducted in alternation to investigate the behaviour of the system upon transmitting a signal, mimicking its application as active implant. These measurements were conducted in a three-electrode setup using a scanning droplet cell microscope (SDCM) based on the model described in [3]. EDX spectroscopy was used to determine the composition of the alloys at specific spots of the library. XRD analysis revealed the formation of an FCC crystal structure and the formation of a solid solution. EIS showed stable behaviour of the material up to a polarization voltage of 2 V, followed by a sharp increase in impedance upon subjecting the material to 3 V and more. This suggests the formation of an oxide layer, which was attributed to the oxidation of Ag. The measured impedance was found to remain roughly stable in the range of 1-100 kHz prior to polarization to 3 V. This

stable region is shifted towards lower frequencies with increased polarization voltages, covering the range of 100 Hz-1 kHz in which neural signals are commonly transmitted [2]. The phase shift appeared to stabilize with increased polarization voltages. Calculated capacitances and resistances were found to be acceptable for the desired applications. Overall, a limited aptitude of Ag-Au alloys for use in AIMD is indicated.

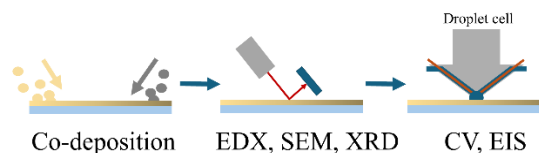


Figure 1: Schematic depiction of the employed combinatorial approach

## Conclusions

Combinatorial analysis of a Ag-Au thin film library was conducted, revealing properties that suggest limited applicability in AIMD.

## References

- [1] D. Fitzpatrick. *Implantable Electronic Medical Devices*, Academic Press, Oxford, UK **2014**
- [2] C. Clément. *Brain-Computer Interface Technologies*, Springer, Cham, Switzerland **2019**
- [3] J. P. Kollender, M. Voith, S. Schneiderbauer, A. I. Mardare, A. W. Hassel. Highly Customisable scanning droplet cell microscopes using 3D-printing. *J. Electroanal. Chem.* **2015**, 740, 53.

## Acknowledgements

The financial support received from the European Union Horizon 2020 through the project Medical Device Obligation Taskforce (MDOT) is gratefully acknowledged.

## Multifunctional bandages as strategy for wound management

Sabine SZUNERITS<sup>1,2</sup>

[sabine.szunerits@univ-lille.fr](mailto:sabine.szunerits@univ-lille.fr) | [Sabine.Szunerits@dp-uni.ac.at](mailto:Sabine.Szunerits@dp-uni.ac.at)

<sup>1</sup> Univ. Lille, CNRS, Centrale Lille, Univ. Polytechnique Hauts-de-France, UMR 8520 - IEMN, Lille, France

<sup>2</sup> Laboratory for Life Sciences and Technology (LiST), Faculty of Medicine and Dentistry, Danube Private University, 3500 Krems, Austria

**Abstract:** Wounds, particularly chronic ones, often exhibit complex biological characteristics that complicate their healing processes. To better address this issue, the development of hydrogels loaded platelet-derived extracellular vesicles (pEVs) presents a promising personalized therapeutic option. These innovative bandages are designed not only to manage inflammation effectively, but also enhance skin regrowth and accelerate the wound's transition into the proliferation phase, often in combination with wound sensors.

**Keywords:** wound healing, field effect transistor, platelet growth factors, personalized therapy

### Introduction

Platelet-derived extracellular vesicles (pEVs) show promising potential in enhancing tissue recovery and healing chronic wounds. They promote neovascularization and cell migration, while reducing inflammation, oxidative stress, and scarring. However, their efficacy in clinical settings is challenged by their susceptibility to washout by wound exudate. Hydrogel-based bandages are effective carriers that stabilize pEVs for personalized wound care. Furthermore, the possibility to integrate sensors in the wound bed enables a theragnostic approach to healing.

### Results and Discussion

Utilizing biologicals like pEVs to counter-balance the patient's deficient biology are appealing options for a personalized treatment. The use of extracellular vesicles, initially an unrealized component of platelet-rich plasma generated by platelet activation, began over ten years ago and has since then made significant progress [1]. While the original discovery of "platelet dust" dates back to 1967, it was from 2016 onwards that platelet-derived wound therapeutics began to be considered [2-6].

It is in addition expected that such therapeutic means, when equipped with (bio)sensors, can ultimately enhance the healing of critical cutaneous wounds [7-9]. This global patient-centric approach has thus the potential to enhance wound management by offering more precise, efficient, and responsive healing strategies



**Figure 1:** "Smart" Wound bandages for personalized treatment of chronic wounds.

### Conclusions

Current approaches for personalized wound movements will be discussed. It will be shown that the successful integration of pEV-loaded hydrogels into clinical practice will ultimately require a coordinated effort among a diverse array of stakeholders, including biomedical engineers, clinicians, blood biotech industry and medical devices experts. Cost considerations and scalability remain formidable challenges. Strategies to optimize production and storage costs will be in addition crucial as these therapies move towards commercial viability.

### References

- [1] T. Burnouf, M.-L. Chou, D. J. Lundy, E.-Y. Chuang, C.-L. Tsend, H. Goubran, *J. Biomed. Sci.* **30** (2023) 79
- [2] M. J. Martinez-Zapata, A. J. Martí-Carvajal, I. Solà, J. Angel Expósito, I. Bolívar, L. Rodríguez, J. Garcia, C. Zaror, *Cochrane Database Syst Rev.* **5** (2016) CD006899.
- [3] J. Etulain, *Platelets* **29** (2018) 556.
- [4] P.-C. Hao, T. Burnouf, C.-W. Chiang, P.-R. Jheng, S. Szunerits, J.-C. Yang, E.-Y. Chuang, *J. Nanobiotechnol.* **21** (2023) 318.
- [5] Y. Wang, Z. Cao, Q. Wei, K. Ma, W. Hu, O. Huang, J. Su, H. Li, C. Zhang, X. Fu, *Acta Biomater.* **147** (2022) 342.
- [6] F. Back, A. Barras, A. Nyam-Erdene, J.-C. Yang, S. Melinte, J. Rumipamba, T. Burnouf, R. Boukherroub, S. Szunerits, E.-Y. Chuang, *Adv. Healthc. Mater.* 2024, submitted revision
- [7] V. Mishyn, M. Aslan, A. Hugo, T. Rodrigues, H. Happy, S. Sanyal, W. Knoll, F. Baudoux, V. Bouchiat, R. O. Bilyy, R. Boukherroub, A. Sanyal, S. Szunerits, *Sens. Diagn.*, **1**, (2022) 739.
- [8] A. Hugo, T. Rodrigues, J. Mader, W. Knoll, V. Bouchiat, R. Boukherroub, A. Sanyal, S. Szunerits, *Biosens. Bioelectron.: X* **13** (2023) 100305.
- [9] Y. Gao, *et al. Sci. Adv.* **7**, (2021) eabg9614.

### Acknowledgements

This work was partly supported by EuroNanomed III-GSkin (ANR-21-ENM3-0002).

## Surface Imprinted Polymers for the Detection of Fungal Spores

Nathalie Philippaerts<sup>1\*</sup>, Rocio Arreguin Campos<sup>1</sup>, Joseph W. Lowdon<sup>1</sup>, Thomas J. Cleij<sup>1</sup>, Hanne Diliën<sup>1</sup>, Kasper Eersels<sup>1</sup>, Bart van Grinsven<sup>1</sup>

[nathalie.philippaerts@maastrichtuniversity.nl](mailto:nathalie.philippaerts@maastrichtuniversity.nl)

<sup>1</sup>Sensor Engineering Department, Faculty of Science and Engineering, Maastricht University,

P.O. Box 616, 6200 MD Maastricht, the Netherlands

**Abstract:** In this study, a cheap, robust and fast detection method for the fungal spores using surface imprinted polymers (SIPs) is in development. Here we provide an overview of the status quo of the sensor progress.

**Keywords:** Biomimetic sensing; Surface Imprinted Polymers; Fungal Spores

### Introduction

In the Netherlands, 9688 ha of greenhouses account for a total energy consumption of 106.8 petajoules and the main portion of this total energy input goes to heating (74%) [1]. Due to the continuous threat of fungal infection to the crop yields, frequent venting and heating is required to ensure a low relative humidity [2]. Detection and continuous monitoring of the fungal spore count in a greenhouse could be a solution to reduce the frequency of venting and heating and thereby reduce the total energy consumption. This study presents the development of a fungal spore sensor based on surface imprinted polymers, a strategy that was successfully employed for the detection of bacteria in prior research [3].

### Results and Discussion

The SIPs were imprinted by the procedure depicted in Figure 1A. Rebinding was assessed using the heat-transfer method (HTM), as shown in Figure 1B.

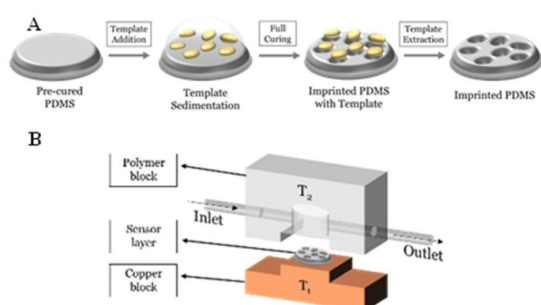


**Figure 1:** Schematic representation of: A) Imprinting procedure, based on [3]. B) Heat-transfer method set-up.

Since fungal spore extraction has proven to be especially challenging, extraction was performed by submersion in 1%SDS 10%HAc for different time periods.

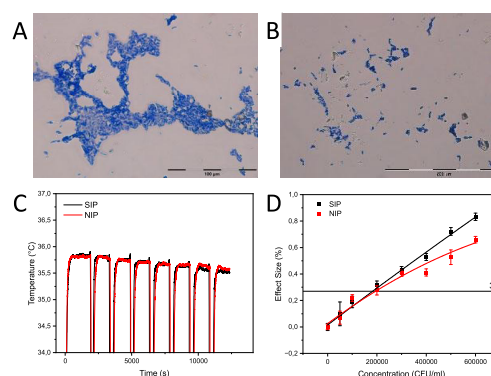


**Figure 2:** A) Imprint with stained template. B) Imprint extracted with 1%SDS 10%HAc. C) HTM rebinding results of the imprint, extracted with 1%SDS 10%HAc.

Preliminary microscopy and HTM investigation showed an ideal incubation time of 20 minutes.

### Conclusions

The preliminary data is promising but further research is needed for the development of a fungal spore sensor.

### References

- [1] Paris, B., et al., Applied Sciences, 2022. 12(10): p. 5150.
- [2] Scarlett, K., et al., European Journal of Plant Pathology, 2015. 141: p. 779-787.
- [3] Arreguin-Campos, R., et al., ACS sensors, 2022.

### Acknowledgements

The authors are grateful for funding of the project "ENERGLIK (Int6B003) by the European Regional Development fund of the E.U. through Interreg via Flanders-the Netherlands.



# New concept for surface-MIPs for bacteria detection: no need for template cell, well-ordered high cavity density

D. Özsoylu<sup>1</sup>, F. Aliazizi<sup>2</sup>, P. Wagner<sup>2</sup>, M. J. Schöning<sup>1,3</sup>

[oezsoylu@fh-aachen.de](mailto:oezsoylu@fh-aachen.de)

<sup>1</sup>Institute of Nano- and Biotechnologies (INB), Aachen University of Applied Sciences, Heinrich-Mußmann-Str. 1, 52428 Jülich, Germany

<sup>2</sup>Department of Physics and Astronomy, Laboratory for Soft Matter and Biophysics, KU Leuven, Celestijnenlaan 200d, B-3001, Leuven, Belgium

<sup>3</sup>Institute of Biological Information Processing (IBI-3), Forschungszentrum Jülich GmbH, Wilhelm-Johnen-Str., 52425 Jülich, Germany

**Abstract:** Surface-molecularly imprinted polymers (surface-MIPs)-based biosensors show great potential in direct detection of target bacteria. However, the major drawbacks of the current fabrication method of surface-MIPs arise from the need for fresh template bacteria, and often low and non-adjustable areal density of the cavities. In this work, we developed a positive master stamp containing bacterial mimics to address the above-mentioned drawbacks.

**Keywords:** Surface-MIPs; bacteria detection; bacterial mimics; template-bacteria-free; high cavity density

## Introduction

In today's globalized world with a highly mobile and interdependent nature, several diseases related to pathogenic bacteria spread rapidly causing a serious global threat to modern health care as well as environment and food safety. As an example, according to the estimations of World Health Organization, every year, 600 million people become ill after consuming contaminated food [1], where most of them are related to pathogenic bacteria [2], and 420,000 people die every year due to contaminated food consumption [1]. Developing advanced diagnostic methods and tools for rapidly detecting and monitoring pathogenic bacteria is crucial to combat this threat.

In this work, we first developed a polydimethylsiloxane-based positive master stamp containing photolithographic structural analogues of the template bacteria (*E. coli* as a model organism). Then, we covalently bound lipopolysaccharides isolated from *E. coli* to the surface of this master stamp. The micro-contact imprinting method was performed using this master stamp and two different polymer types (a photoresist and polyurethane) (Figure 1). This imprinting strategy was employed to interdigitated electrodes and quartz crystal microbalance chips. The obtained surface-MIP sensor samples were characterized by several methods such as scanning electron microscopy (SEM), atomic force microscopy (AFM), Zeta potential measurements, and contact angle measurements. Afterwards, *E. coli*-capturing ability of the developed surface-MIP layers was studied by AFM and SEM methods. Finally, *E. coli* detection feasibility of the developed sensor chips was demonstrated using electrochemical impedance

spectroscopy and quartz crystal microbalance with dissipation monitoring technique.

## Results and Discussion

A high density of biomimetic *E. coli* imprints (around  $10^7$  cavities per  $\text{cm}^2$ ) was achieved without using *E. coli* cells [3]. As a proof-of-concept study, the sensor's *E. coli* detection performance was successfully demonstrated.

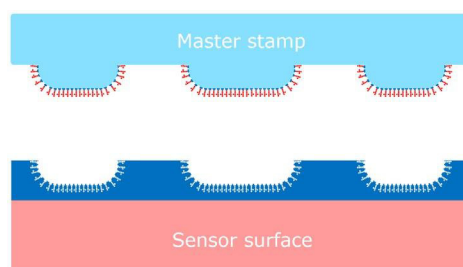


**Figure 1:** Template bacteria-free fabrication concept for surface-MIPs.

## References

- [1] World Health Organization (2022), Food safety, URL: <https://www.who.int/NEWS-ROOM/FACT-SHEETS/DETAIL/FOOD-SAFETY>
- [2] World Health Organization (2015), WHO estimates of the global burden of food-borne diseases, URL: [https://iris.who.int/bitstream/handle/10665/199350/9789241565165\\_eng.pdf?sequence=1](https://iris.who.int/bitstream/handle/10665/199350/9789241565165_eng.pdf?sequence=1)
- [3] D. Özsoylu, F. Aliazizi, P. Wagner, M. J. Schöning, *Biosensors & Bioelectronics* **261** (2024) 116491

## Acknowledgements

The authors thank the German Federal Ministry of Education and Research (project no.: 03F0902A) for funding the ARENA project financed under the 2020 AquaticPollutants Joint call of the AquaticPollutants ERA-NET Cofund (N° 869178). The authors thank H. Iken and D. Rolka for their technical support.

# Bottom-up Assembly of a 3D Structure of Icosahedral Viral Nanoparticles via Specific Binding

Clara Zobeley<sup>1</sup>, Tao He<sup>1</sup>, Mario Braun<sup>2</sup>, Kajohn Boonrod<sup>2</sup>, Christine Müller-Renno<sup>1</sup>,

Gaby Krczal<sup>2</sup>, Christiane Ziegler<sup>1</sup>

zobeley@rptu.de

<sup>1</sup> Department of Physics and Research Center OPTIMAS, RPTU Kaiserslautern, Erwin-Schrödinger Straße 56, D-67663 Kaiserslautern, Germany

<sup>2</sup> RLP Agrosience GmbH, Breitenweg 71, D-67435 Neustadt/Weinstraße, Germany

**Abstract:** Nanotechnology is becoming increasingly important due to the large number of different areas of application. Nano-machines must be built to be able to manipulate nano-matter. Our goal is to create a nano-crane with a bottom-up approach. The prerequisite for this is the production of a structured 3D layer. For this purpose, genetically modified tomato bushy stunt viruses (Strep-Tag II TBSV) and Strep-Tactin<sup>®</sup> are stacked alternately on top of each other to take advantage of the specific interaction. The successful layer formation and the layer height are measured using a scanning force microscope.

**Keywords:** scanning force microscopy; viral-like nanoparticles; bottom-up assembly; Strep-Tactin; Strep-Tag II

## Introduction

Plant viruses have great potential in nanotechnology. Tomato bushy stunt virus (TBSV), the key studying object in this project, is an icosahedral virus of about 33 nm in diameter, particularly applicable for the bottom-up technique due to its uniform size [1]. A genetically modified virus variant with the side chains Strep-Tag II is used. The strong specific key-lock interaction between Strep-Tactin<sup>®</sup> and Strep-Tag II TBSV results in a basic layer with high structural order [2][3]. For further three-dimensional (3D) arrangements, Strep-Tactin<sup>®</sup> and Strep-Tag II TBSV are launched alternately on top of each other to take advantage of the specific interaction.

## Results and Discussion

To build the 3D layer, the first layer of Strep-Tactin is applied to a silicon substrate pre-functionalized with APTES (3-aminopropyltriethoxysilane) and maleimide (=1<sup>st</sup> layer). Then, a layer of Strep-Tag II TBSV is immobilized (= 2<sup>nd</sup> layer) via spin-coating. The specifically strong key-lock interaction between Strep-Tactin<sup>®</sup> and Strep-Tag II TBSV results in a closed and ordered monolayer [3]. In the second step, a further layer of Strep-Tactin<sup>®</sup> is immobilized on the TBSV monolayer (= 3<sup>rd</sup> layer). Afterward, the Strep-Tag II TBSV is spin-coated onto the 3rd layer (= 4<sup>th</sup> layer), as shown in Figure 1. Employing a scanning force microscope, we studied the 3D structures formed by Strep-Tactin and Strep-Tag II TBSV layer by layer.

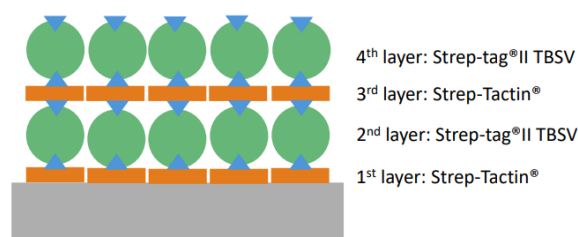


**Figure 1:** Sketch of the 3D structure utilizing Strep-Tag II TBSV particles and Strep-Tactin<sup>®</sup>.

## Conclusions

The layers of Strep-Tactin<sup>®</sup> and Strep-Tag II TBSV (= 3<sup>rd</sup> and 4<sup>th</sup> layer) were successfully prepared. However, it is not a uniformly ordered layer. Our next work will be the optimization of the 3rd layer (particularly the Strep-Tactin<sup>®</sup> on top of the Strep-Tag II TBSV) to reach better uniformity.

## References

- [1] Lüders, A., Müller, C., Boonrod, K., Krczal, G., & Ziegler, C. (2012). *Colloids and Surfaces B: Biointerfaces*, **91**, 154-161.
- [2] Schmidt, T. & Skerra, A. (2015) in: *Affinity Chromatography: Methods and Protocols* (Ed. S. Reichelt), Springer, p. 83-95.
- [3] He, T., Braun, M., Boonrod, K., Müller-Renno, C., Krczal, G., & Ziegler, C. (2024). Pre-published in: *physica status solidi (a)* <https://doi.org/10.1002/pssa.202300864>

## Acknowledgments

We sincerely thank the DFG for funding KR 2242/4-3 and ZI 487/18-3.

# A real-time viscosity technique: from the monitoring of PDMS polymerization to the investigation of biological fluids

Flavia Di Scala<sup>1</sup>, Valerii Myndrul, Margaux Frigoli, Bart Van Grinsven, Kasper Eersels

flavia.discala@maastrichtuniversity.nl

<sup>1</sup>Sensor Engineering (SE), Faculty of Science and Engineering (FSE), Maastricht University, P.O. Box 616, 6200 MD Maastricht, the Netherlands

**Abstract:** In this study we use molecular rotor FCVJ to measure microfluidic viscosity, finding that fluorescence emission increases with viscosity increase and decreases with rising temperature. The goal is to develop a method for measuring viscosity in small biological fluid samples.

**Keywords:** molecular rotors; viscosity; biological fluids; polymerization

## Introduction

Mechanics and fluorescence are commonly used techniques to measure fluid viscosity, but require large samples, which is not always possible for biological samples. This work focuses on the implementation of a technique that measures microfluidic viscosity based on Molecular Rotors (MRs). The fluorescence of MRs depends on the viscosity of the fluid they are in. When a photon is absorbed, the molecule gets excited to a locally excited state. The excited electrons move from donor to acceptor, causing the molecule to twist along bond axes. If the fluid is viscous enough, the molecule will relax back to its ground state by emitting fluorescence. The more viscous the fluid is, the more the molecule's rotation is inhibited, leading to more energy emitted by fluorescence [1].

## Results and Discussion

In this study, we synthesized the molecular rotor FCVJ (2-carboxy-2-cyanovinyl)-julolidine farnesyl ester and tested it in ethylene glycol and glycerol solutions at varying concentrations, as per previous research by Haidekker et al. [2]. Our findings revealed a correlation between an increase in fluorescence emission and an increase in glycerol concentration, which leads to an increase in viscosity. Furthermore, we investigated the temperature dependency of the fluorescence emission, focusing on the behaviour of ethylene glycol-glycerol solutions with the most and least viscosity ratios. Our results indicated a decrease in fluorescence emission with a temperature rise, exhibiting an exponential reduction as described by the Andrade equation, as demonstrated in Figure 1.

Furthermore, we examined the polymerization process of PDMS at different temperatures using FCVJ. We studied how diluting the PDMS solution with tetrahydrofuran (THF) at different concentrations and temperatures affected the process. Through our tests, we discovered that FCVJ reaches a saturation point after 10 hours at 50°C.

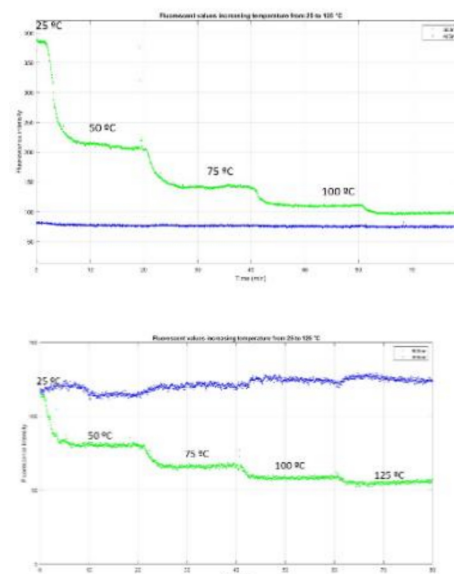


**Figure 1:** Decrease of fluorescent emission in the least viscous and the most viscous samples.

## Conclusions

This study demonstrated the use of the molecular rotor FCVJ to measure viscosity in ethylene glycol and glycerol solutions and to monitor the PDMS polymerization process, investigating the temperature-dependent features.

Although this technique has not yet been tested on biological samples, the goal is to develop a method for measuring viscosity in small biological fluid samples, which could have significant biomedical applications.

## References

- [1] M. A. Haidekker and E. A. Theodorakis, *Journal of biological engineering*, 4(1):11, 2010.
- [2] M. A. Haidekker, T. Ling, M. Anglo, H. Y. Stevens, J. A. Frangos, E. A. Theodorakis, *Chemistry and Biology*, 2000.

## Anodic memristors as future of artificial synapses

Andrei Ionut Mardare, Ivana Zrinski, Dominik Knapic, Achim Walter Hassel

[andrei.mardare@jku.at](mailto:andrei.mardare@jku.at)

Institute of chemical technology of inorganic materials, Johannes Kepler University Linz, Altenberger Str. 69, 4040, Linz, Austria

**Abstract:** The search for the best hardware support for modern artificial intelligence (AI) systems naturally leads to the building of the artificial brain. Observing the tremendous market value increase of Nvidia in 2024, due to fabrication of AI supporting hardware, one can see a strong driving force for developing new technology for AI hardware implementation. This work focuses on developing new memristive thin film composites in a combinatorial approach. The electrical equivalent of Rayleigh-Taylor effect is used for nanoscale structuring of composite oxides, thus intrinsically producing defect-engineered memristors with enhanced electrical capabilities.

**Keywords:** anodic oxides; memristors; defect engineering; thin films; combinatorial libraries

### Introduction

A memristor is defined by an ideal resistor which has a memory about its operational history, its resistive response being a step function between a low and a high resistance state. Switching between these states is obtained via electroforming of a conducting filament which can be erased by a new resistive switching process [1]. Modification at the nanoscale of anodic oxides describes a new route very recently employed in enhancing memristive properties, while leading the way towards composite memristors [2]. Such approach is directly linked to the concept of defect engineering when any lattice modification, interpreted as a defect, may directly influence the behaviour of conductive filaments, and thus the final device capabilities.

### Results and Discussion

There is a strong analogy between the operation of a memristor and that of a synapse, as schematically shown in Figure 1. The electrical equivalent of Rayleigh-Taylor effect is successfully used in anodization of superimposed valve metals for controlled nanostructuring of the resulting oxide. This is not a mixed oxide, but rather a composite one, as already shown in a Hf/Ta system [3]. The interface between both oxides along the formed oxide “fingers” nanocolumns play the role of a large area grain boundary favouring atomic scale transport (e.g. electrolyte species, oxygen vacancies, etc.). Composite anodic oxides obtained on Hf/Ta superimposed layers have a threshold-type memristive behaviour, dependent on the parent metals thickness ratios. This is somehow expected, since this ratio controls the final length and shape of the oxide nanocolumns and their share between both oxidized species. The effect of electrolyte species incorporation on the memristive behaviour is analysed by anodization in different solutions. The influence of citrate and phosphate buffered electrolytes is studied, and the presence of P in the composite anodic oxides is evidenced in the latter case leading to early device failure. Composite

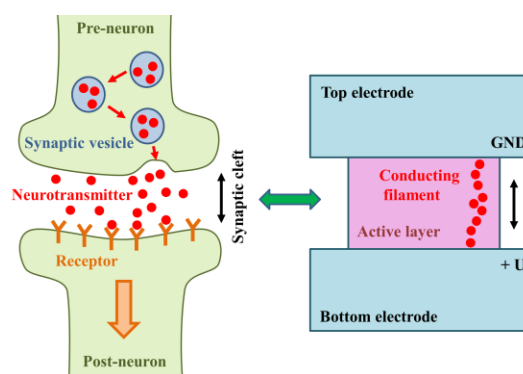


**Figure 1:** Analogy between operation principles of synapse and memristor.

memristors grown in citrate electrolyte show both unipolar and bipolar switching, high stability, very good retention and endurance. The coexistence of both switching mechanisms is related to the special composite oxide nanostructuring.

### Conclusions

Composite memristors based on anodization of Hf/Ta superimposed layers grown in citrate showed a remarkable improvement regarding their resistive state ratio. Non-volatile and threshold characteristics were demonstrated, thus leaving the possibility to apply such memristors for future artificial synapses.

### References

- [1] I. Zrinski, A. Minenkov, C. Cancellieri, R. Hauert, C. C. Mardare, J. P. Kollender, L. P. H. Jeurgens, H. Groiss, A. W. Hassel, A. I. Mardare, *Appl. Mater. Today* **26** (2022) 101270
- [2] I. Zrinski, A. Minenkov, C. C. Mardare, A. W. Hassel, A. I. Mardare, *J. Phys. Chem. Lett.* **12** (2021) 8917–8923
- [3] I. Zrinski, A. Minenkov, J. Duchoslav, C.C. Mardare, H. Groiss, A.W. Hassel, A.I. Mardare, *Phys. Status Solidi A* **219** (2022) 2100751

### Acknowledgements

This research was funded by the Austrian Science Fund (FWF) [P32847-N].



# Development and Calibration of a Sensor System for Assessing the Physical Properties of Water Samples in Aquaculture

Fereshteh Aliazizi<sup>1</sup>, Dua Özsoylu<sup>2</sup>, Soroush Bakhshi Sichani<sup>1</sup>, Mehran Khorshid<sup>1</sup>, Christ Glorieux<sup>1</sup>, Johan Robbens<sup>3</sup>, Michael J. Schöning<sup>2</sup>, and Patrick Wagner<sup>1</sup>

[fereshteh.aliazizi@kuleuven.be](mailto:fereshteh.aliazizi@kuleuven.be)

<sup>1</sup>KU Leuven, Celestijnenlaan 200, B-3000 Leuven, Belgium, <sup>2</sup>FH Aachen, Heinrich-Mußmann-Strasse 1, D-52428 Jülich, Germany, <sup>3</sup>ILVO, Jacobsenstraat 1, B- 8400 Oostende, Belgium

**Abstract:** This work presents a compact, dual-function chip-based sensor that measures temperature and electrical conductivity in water samples. Conductivity is determined via the impedance amplitude using interdigitated electrode structures. Equivalent circuit modelling is not necessary, and the data agree with a reference instrument over several orders of magnitude for fresh and seawater samples. For temperature measurements, we use an on-chip platinum resistance temperature detector (RTD). The sensor is ideal for inline and online monitoring in recirculating aquaculture systems.

**Keywords:** electrical conductivity of liquids; thermometry; impedance spectroscopy; microfluidics; aquaculture; chip-based sensor setup

## Introduction

Aquaculture aims to supply nutrient-rich seafood sustainably, following the European guidelines to minimize ecological impact and manage fish diseases. Hereby, Recirculating Aquaculture Systems (RAS) need precise water management. A major issue regarding aquaculture is antimicrobial resistance, which poses potential risks to human health [1-3]. The ERA-NET project ARENA is developing a modular sensor system for RAS to measure temperature, conductivity, pH and bacteria levels. The present module of the system uses impedance analysis for sensing both conductivity and temperature, which can be upgraded towards bacterial and antibiotic detection, addressing aquaculture's environmental and health challenges [1,4,5]. **Figure 1** shows an overview of the dual function chip, integrated in a microfluidic setup.

## Results and Discussion

First, we examined the relationship between salt concentration  $C$  and electrical conductivity using a SevenCompact Duo meter. Conductivity data, ranging from pure Mili-Q water to 10×PBS, agree with the Kohlrausch formula ( $R^2 = 0.999$ ).

$$\sigma = c. (A_1 - A_2\sqrt{c}) \quad (1)$$

Impedance spectra (100 Hz to 500 kHz) showed capacitive behaviour at low frequencies and resistive behaviour at high frequencies. Conductivity was accurately measured at 46.933 kHz, aligning closely with the reference instrument. Calibration was accurate for river water, water samples from a RAS facility, and seawater. The platinum RTD sensor showed a linear resistance-temperature relationship,

remained unaffected by high conductivity, and demonstrated precision suitable for aquaculture applications [1]. Importantly, the salinity of the liquid does not interfere with the temperature readings that are accurate to  $< 0.5^\circ\text{C}$ .

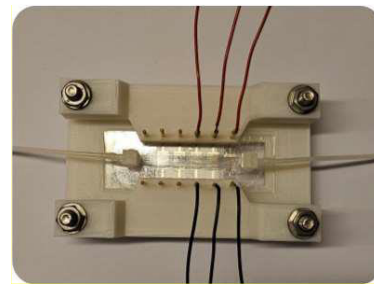


**Figure 1:** Microfluidic channel with connectors for temperature and impedance measurements.

## Conclusions

We developed a sensor system for aquaculture to measure the water parameters, temperature and electrical conductivity, with future upgrades to pH measurements and bacteria detection.

## References

- [1] F. Aliazizi, *et al.*, *Micromachines* 15 (2024) 755.
- [2] N. Ahmed, *et al.*, *J. Clean. Prod.* 297 (2021) 126604.
- [3] G. Suantika, *et al.*, *Aquacult. Eng.* 82 (2018) 12–24.
- [4] C. Huck, *et al.*, *Sens. Actuators B Chem.* 198 (2014) 102-109.
- [5] A. Beutner, *et al.*, *Talanta* 183 (2018) 33-38.

## Acknowledgements

We gratefully acknowledge the support by the ERA-NET ARENA project “Antibiotic Resistance and Pathogenic Signature in Marine and Fresh water Aquaculture Systems.”

# Adjusting the working potential of a bioabsorbable screen-printed carbon-based glucose biosensor on silk-fibroin

K. A. Janus<sup>1,2</sup>, S. Achtsnicht<sup>1</sup>, M. Zach<sup>1</sup>, A. Drinic<sup>3</sup>, A. Kopp<sup>3</sup>, M. Keusgen<sup>2</sup>, M. J. Schöning<sup>1,4</sup>

[janus@fh-aachen.de](mailto:janus@fh-aachen.de)

<sup>1</sup>Institute of Nano- and Biotechnologies (INB), Aachen University of Applied Sciences, Heinrich-Mußmann-Str. 1, 52428 Jülich, Germany

<sup>2</sup>Institute for Pharmaceutical Chemistry, Philipps University of Marburg, Wilhelm-Roser-Str. 2, 35032 Marburg, Germany

<sup>3</sup>Fibrothelium GmbH, Philipsstr. 8, 52068 Aachen, Germany

<sup>4</sup>Institute of Biological Information Processing (IBI-3), Forschungszentrum Jülich GmbH, Wilhelm-Johnen-Str., 52425 Jülich, Germany

**Abstract:** This work describes five different modifications of the carbon working electrode of an amperometric glucose biosensor. The biosensor consists of a screen-printed carbon-based electrode on bioabsorbable silk-fibroin (obtained from the silkworm *Bombyx mori*) modified with a glucose oxidase enzyme cocktail. The modification of the carbon working electrode aims the reduction of the working potential range from 1.2 V to 0.8 V vs. the Ag/AgCl reference electrode. The glucose biosensor performance was studied from 0.5 mM to 10 mM glucose. Moreover, the enzymatic degradation by protease XIV of the biosensor was examined.

**Keywords:** bioabsorbable; silk-fibroin; glucose biosensor; multi-walled carbon nanotubes; protease XIV

## Introduction

To minimize interferences of electroactive species within the working potential “window”, lowering the carbon’s working electrode potential represents a well-known strategy for amperometric biosensors [1]. Discussed research approaches either include the modification of the screen-printed carbon layer by chemical solutions (such as Na<sub>2</sub>CO<sub>3</sub>, KCl or H<sub>2</sub>O<sub>2</sub> [2, 3]), O<sub>2</sub>-plasma treatment [4] or the addition of multi-walled carbon nanotubes to the carbon paste [5]. In the performed experiment, all five modification strategies have been studied systematically.

## Results and Discussion

Post-treatment methods of the screen-printed carbon working electrodes with the chemical solutions Na<sub>2</sub>CO<sub>3</sub>, KCl and H<sub>2</sub>O<sub>2</sub>, as well as the O<sub>2</sub>-plasma treatment did not lead to a reasonable improvement of the biosensor performance (reduction of the working potential). Furthermore, the solvent-based approaches damaged the bioabsorbable carbon working electrode. In contrast, experiments with the carbon-based working electrode filled with 2 wt% multi-walled carbon nanotubes enabled reduction of the applied working potential to 0.8 V vs. the Ag/AgCl reference electrode.

## Conclusions

The applied potential to the screen-printed carbon working electrode on flexible silk-fibroin could be successfully decreased from 1.2 V to 0.8 V vs. the Ag/AgCl reference electrode by adding 2 wt% multi-walled carbon nanotubes to the bioabsorbable carbon paste, see Figure 1. For working potentials of 1.2 V, 1.0 V and 0.8 V, distinct potential steps for varying glucose concentrations were achieved, in

contrast to 0.6 V. Additionally, the complete biodegradation of the carbon nanotubes-modified carbon working electrode within three months was successfully demonstrated.

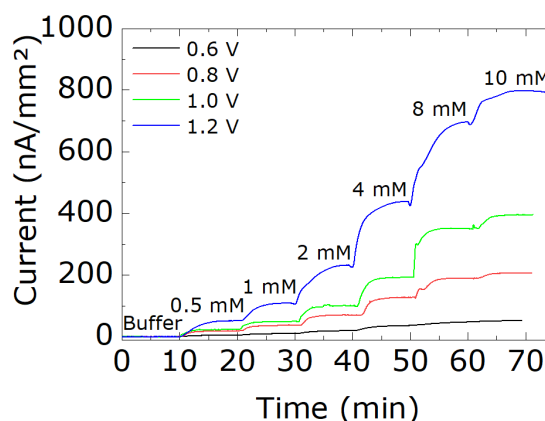


**Figure 1:** Dynamic response of bioabsorbable, screen-printed carbon electrodes on flexible silk-fibroin with immobilized glucose oxidase and modified with 2 wt% multi-walled carbon nanotubes for glucose concentrations between 0.5 and 10 mM, applying different working potentials from 0.6 V to 1.2 V vs. the Ag/AgCl reference electrode.

## References

- [1] J. Wang, *Electroanalysis* **13** (2001) 983-988
- [2] J. Pilas, T. Selmer, M. Keusgen, M. J. Schöning, *Anal. Chem.* **91** (2019) 15293-15299
- [3] M. I. González-Sánchez, B. Gómez-Monedero, J. Agrisuelas, J. Iniesta, E. Valero, *Electrochem. Commun.* **91** (2018) 36-40
- [4] X. Yuan, L. Ma, J. Zhang, Y. Zheng, *Appl. Surf. Sci.* **1** (2021) 148760
- [5] L. Feng, H.-P. Li, K. Galatsis, H. G. Monbouquette, *J. Electroanal. Chem.* **773** (2016) 7-12

## Building a Virus Actuator

Tao He<sup>1</sup>, M. Braun<sup>2</sup>, K. Boonrod<sup>2</sup>, C. Müller-Renno<sup>1</sup>, G. Krczal<sup>2</sup>, C. Ziegler<sup>1</sup>  
hetao@rptu.de

<sup>1</sup> Department of Physics and Research Center OPTIMAS, RPTU Kaiserslautern,  
Erwin-Schrödinger Straße 56, D -67663 Kaiserslautern, Germany

<sup>2</sup> RLP Agrosience GmbH, Breitenweg 71, D-67435 Neustadt/Weinstraße, Germany

**Abstract:** We developed a novel nanoactuator component using genetically modified tomato bushy stunt viruses (Strep-Tag II TBSV) and M13 phages. The genetic modification of the M13 phage enables a classical key-lock interaction with the TBSV monolayer. We investigated the immobilization behavior of the M13 phage on the TBSV monolayer in air. We performed piezoresponse force microscopy (PFM) to measure the deformation of the horizontal M13 phages in response to the applied voltage. We conducted scanning force microscopy (SFM) in a salt solution to capture the uppermost structural characteristics of the vertical standing M13 phages.

**Keywords:** scanning force microscopy; tomato bushy stunt virus; M13 phage; nanoactuator; piezoresponse force microscopy.

### Introduction

Plant viruses are emerging as promising candidates for implementing nanoactuators. This study proposes constructing a nanoactuator component based on the tomato bushy stunt virus (TBSV) and the M13 phage (see Figure 1). TBSV is a ~ 33 nm icosahedron virus, which demonstrates versatile self-assembly behaviors influenced by viral concentration<sup>1,2</sup>, pH value of the viral solution<sup>3</sup>, viral solution drop position, and substrate type<sup>2</sup>. Here, the genetically modified Strep-tag II TBSV is used, which carries a Strep-tag II at each side chain. The M13 is a filamentous bacteriophage with a diameter of ~ 6 nm and a length of ~ 880 nm and piezoelectric properties along the long and short axes. The genetically modified M13 with single-chain variable fragments at the C-terminal establishes a key-lock interaction with the Strep-tag II TBSV. M13 phage is utilized to build a tall structure to achieve a function like a nano lifting platform if they could vertically stand on the TBSV layer<sup>4</sup> (see Figure 1). The reverse piezoelectric effect allows the M13 phage to deform in length by applying a voltage<sup>5</sup>.

### Results and Discussion

In the first step, a monolayer of Strep-Tag II TBSV was immobilized on a Strep-Tactin<sup>®</sup> modified silicon substrate via the specific bonding between the side chain Strep-Tag II (an engineered type of biotin) and the Strep-Tactin<sup>®</sup> (an engineered type of streptavidin). Afterward, the M13 phage was immobilized on top of the Strep-tag II TBSV layer, as shown in Figure 1. The M13 phage topples over on the TBSV layer in air, as we have expected. We investigated the immobilization behavior of the M13 phages on the TBSV monolayer under dry conditions in air, together with the piezoresponse force microscopy measurement of the piezo properties of the M13 phage along the short axis. Notably, we have accomplished the vertical orientation of the M13 phages on TBSV after the sample was immersed in a salt solution, as

evidenced by our experimental progress. Scanning force microscopy (in QI<sup>®</sup> mode) images could demonstrate the height properties and rough top patterns of M13 phages in solution.

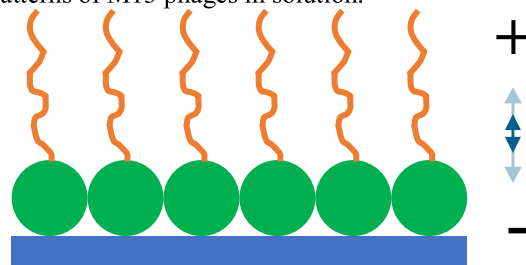


Figure 1. Sketch (not to scale) of a nanoactuator component based on Strep-tag II TBSV and genetically modified M13 phages. The M13 phages produce motion when a voltage is applied along the long axis of the M13 phages.

### Conclusions

We successfully immobilized genetically modified M13 phages on the Strep-tag II TBSV to achieve horizontal structures in air and vertical structures in salt solution. Future research will focus on detecting the piezoelectric properties of the M13 phages via piezoresponse force microscopy (PFM) in the salt solution.

### References

1. Lüders, A., Müller, C., Boonrod, K., Krczal, G. & Ziegler, C. *Colloids Surf B Biointerfaces* **91**, 154–161 (2012).
2. Rink, V. et al. *Physica Status Solidi (C) Current Topics in Solid State Physics* **13**, 163–166 (2016).
3. Rink, V. et al. *Biointerphases* **12**, 04E402 (2017).
4. Salivar, W. O, Tzagoloff, H. & Pratt, D. *Virology* **24**, (1964).
5. Park, I.W. et al. *Nanomaterials* **10**, (2020).

### Acknowledgments

We sincerely thank the DFG: KR 2242/4-3/ZI 487/18-3.

# Turnip vein-clearing virus particles as versatile nanotemplates for the binding of biomolecules on capacitive field-effect sensors

M. Welden<sup>1,2</sup>, A. Alkanoush<sup>1</sup>, T. Wendlandt<sup>3</sup>, M. Keusgen<sup>2</sup>, C. Wege<sup>3</sup>, A. Poghossian<sup>4</sup>, M. J. Schöning<sup>1,5</sup>

[m.welden@fh-aachen.de](mailto:m.welden@fh-aachen.de)

<sup>1</sup>Institute of Nano- and Biotechnologies (INB), Aachen University of Applied Sciences, Heinrich-Mußmann-Str. 1, 52428 Jülich, Germany

<sup>2</sup>Institute of Pharmaceutical Chemistry, Philipps University Marburg, Wilhelm-Roser-Str. 2, 35032 Marburg, Germany

<sup>3</sup>Institute of Biomaterials and Biomolecular Systems, University of Stuttgart, Pfaffenwaldring 57, 70569 Stuttgart, Germany

<sup>4</sup>MicroNanoBio, Liebigstraße 4, 40479 Düsseldorf, Germany

<sup>5</sup>Institute of Biological Information Processing (IBI-3), Forschungszentrum Jülich GmbH, Wilhelm-Johnen-Str., 52425 Jülich, Germany

**Abstract:** The immobilization of *turnip vein-clearing virus* as enzyme nanotemplates on capacitive field-effect sensors is analyzed. The sensors were characterized physically via scanning electron microscopy and atomic force microscopy and electrochemically via leakage-current, capacitance-voltage, and constant-capacitance measurements.

**Keywords:** *turnip vein-clearing virus*; polyelectrolyte; enzyme nanotemplate; capacitive field-effect sensor

## Introduction

The selection of an appropriate enzyme immobilization strategy is of importance in ensuring the reliable performance of enzymatic biosensors. We recently introduced a novel method for enzyme immobilization based on *tobacco mosaic virus* (TMV) particles as enzyme nanocarriers on polyelectrolyte (poly(allylamine hydrochloride), PAH)-modified capacitive electrolyte-insulator-semiconductor (EISCAP) sensors [1]. In that study, enzymes were coupled to the surface of TMV particles via streptavidin-biotin affinity binding. In this study, we employed *S. aureus* protein A-exposing *turnip vein-clearing virus* (TVCV-PA) particles for antibody-mediated enzyme coupling [2]. Al/p-Si/SiO<sub>2</sub>/Ta<sub>2</sub>O<sub>5</sub> EISCAPs were modified with PAH, TVCV-PA, anti-urease IgG, and urease (from *Canavalia ensiformis*) as a model enzyme, thereby realizing a capacitive TVCV-PA-assisted urea biosensor.

## Results and Discussion

The immobilization of TVCV-PA onto PAH-modified Ta<sub>2</sub>O<sub>5</sub>-gate surfaces was systematically studied via scanning electron microscopy (SEM) and atomic force microscopy (AFM) with regard to different TVCV-PA concentrations and immobilization times. Moreover, the coupling of antibodies and enzymes to the TVCV-PA surface was analyzed via SEM and AFM. Figure 1 represents an exemplary SEM image of a PAH/TVCV-PA-modified Ta<sub>2</sub>O<sub>5</sub> gate surface. The TVCV-PA-assisted urea biosensors were characterized via leakage-current, capacitance-

voltage, and constant-capacitance measurements in buffer solution with varying urea concentrations. The results demonstrate the great potential of TVCV-PA-assisted EISCAPs for the application as versatile enzyme biosensors.

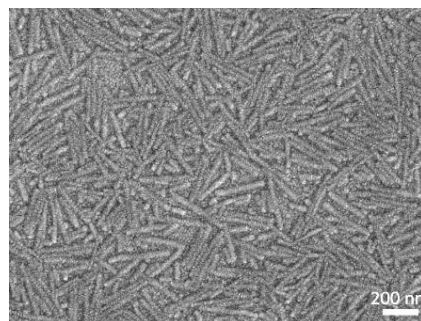


**Figure 1:** SEM image of a PAH/TVCV-PA-modified Ta<sub>2</sub>O<sub>5</sub>-EISCAP surface.

## References

- [1] M. Welden, A. Poghossian, F. Vahidpour, T. Wendlandt, M. Keusgen, C. Wege, M. J. Schöning, *Bioelectrochemistry* **151** (2023) 108397
- [2] T. Wendlandt, C. Koch, B. Britz, A. Liedek, N. Schmidt, S. Werner, Y. Gleba, F. Vahidpour, M. Welden, A. Poghossian, M. J. Schöning, F. J. Eber, H. Jeske, C. Wege, *Viruses* **15** (2023) 1951

## Acknowledgements

This work was funded by the Deutsche Forschungsgemeinschaft (DFG: German Research Foundation)—446507449. The authors thank H. Iken and D. Rolka for technical support.



# PSi/SIP Photonic Composites for the Point-of-Care Diagnosis of Bacterial Urinary Tract Infections

Valerii Myndrul<sup>1</sup>, Rocio Arreguin Campos<sup>1</sup>, Igor Iatsunskyi<sup>2</sup>, Flavia Di Scala<sup>1</sup>, Kasper Eersels<sup>1</sup>

and Bart van Grinsven<sup>1</sup>

valerii.myndrul@maastrichtuniversity.nl

<sup>1</sup> Sensor Engineering Department, Faculty of Science and Engineering, Maastricht University, P.O. Box 616, 6200 MD Maastricht, the Netherlands

<sup>2</sup> NanoBioMedical Centre, Adam Mickiewicz University, 3, Wszechnicy Piastowskiej Str., 61 614 Poznan, Poland

**Abstract:** This study presents a novel method combining porous silicon (PSi) and Surface Imprinted Polymers (SIP) for photoluminescence (PL)-based detection of *E. coli* on PSi/SIP substrates. Using metal-assisted chemical etching (MACE) for PSi fabrication and PDMS-based *E. coli* imprinting, the method offers high reliability, low detection limits, and excellent selectivity. It requires minimal preparation, reducing facility and personnel burden. Detection takes around 20 minutes, making it suitable for point-of-care (PoC) devices utilizing PSi/SIP and PL-based readout for ultra-trace *E. coli* detection.

**Keywords:** porous silicon; surface imprinted polymer; photoluminescence; biosensor

## Introduction

Bacteria are essential to our ecosystem and significantly impact human health. *Escherichia coli* (*E. coli*) is crucial for digestion in the gastrointestinal tract but can cause urinary tract infections (UTIs) when present in other organs [1]. Current UTI diagnostics often use empirical treatment, which contributes to antibiotic resistance and complicates management [2]. This research proposes a user-friendly biosensor based on the Surface Imprinting of Polymers (SIP) technique for detecting uropathogenic *E. coli* (UPEC) [3]. SIP creates artificial recognition layers on photonic transducers, offering scalability, reliability, and simplicity. The biosensor uses porous silicon (PSi) substrates for their high sensitivity and compatibility with SIP layers.

## Results and Discussion

After fabricating PSi using MACE and imprinting *E. coli* with PDMS, the resulting PSi/SIP substrates were rigorously examined using scanning electron microscopy to confirm the formation of cavities essential for *E. coli* re-binding during detection. Initial tests of the samples in PBS with different *E. coli* aliquots revealed a sensitivity to the bacteria, evidenced by changes in PL intensity, which served as the biosensor's response. Selectivity tests demonstrated a high affinity for *E. coli* while effectively disregarding other interfering species. Real-time detection of *E. coli* in urine mirrored the results observed in PBS, with a decrease in PL upon *E. coli* binding to the PSi/SIP substrate. The theoretical limits of detection (LOD) in both PBS and urine were found to vary between 14-17

CFU/mL, indicating excellent reproducibility of the results.

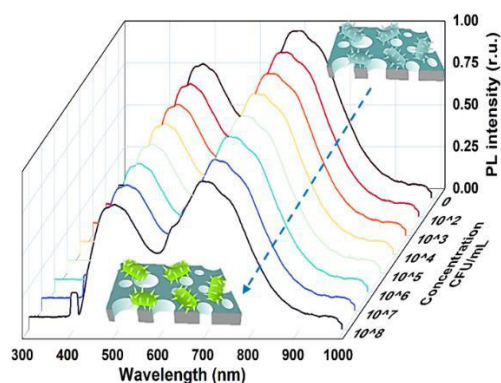


**Figure 1:** The PSi/SIP PL intensity change upon *E. coli* injection into the flow cell. As the concentration of *E. coli* increases, there is a greater decrease in PL intensity.

## Conclusions

The fabricated PSi/SIP photonic substrates exhibited strong affinity and high sensitivity for target bacteria, effectively ignoring the presence of interfering species. Additionally, the proposed PL-based method ensures reliable *E. coli* detection with a very low LOD, ranging from 14 to 17 CFU/mL.

## References

- [1] A.W. Walker, L. Hoyles, Nat. Microbiol. 8 (2023) 1392–1396
- [2] K.M.J. Ganzeboom, et al., Prim. Health Care Res. Dev. 20 (2018) e41.
- [3] W. Stilman, et al., Phys. Status Solidi. 219 (2022) 1–13.

## A heat-transfer biosensor with variable geometry

Csongor Tibor Urban<sup>1</sup>, S. Bakhshi Sichani<sup>1</sup>, D. Yongabi<sup>1</sup>, M. Khorshid<sup>1</sup>, M.P. Lettinga<sup>1,2</sup>, P. Wagner<sup>1</sup>

[csongortibor.urban@kuleuven.be](mailto:csongortibor.urban@kuleuven.be)

<sup>1</sup>KU Leuven, Laboratory for Soft Matter and Biophysics, Celestijnenlaan 200D, 3001 Leuven, Belgium

<sup>2</sup>Research Center Jülich, IBI-4, Wilhelm-Johnen-Straße, 52428 Jülich, Germany

**Abstract:** Cells exposed to temperature gradients using the heat transfer method (HTM), exhibit distinct, spontaneous detachment patterns that allow non-invasive cell identification. This label-free approach enables a universal detection platform of any cell type. We developed a flow cell with adjustable aspect ratios to optimise the detection of cell detachment patterns and move the technology into the industry. We systematically identify the most effective device dimensions for enhancing the sensitivity and accuracy of HTM in cell characterisation.

**Keywords:** biosensor; heat transfer method; cell characterisation; spontaneous cell detachment

### Introduction

The heat-transfer method (HTM) is a thermometric biosensing principle first described in the context of mutation analysis in DNA<sup>1</sup>. A broad range of other bioanalytical applications of HTM has been reviewed<sup>2</sup>. It has been shown that cells spontaneously detach when exposed to a temperature gradient<sup>3</sup>. The timing is highly reproducible for different cell types and can be used to identify and differentiate closely related yeast and cancerous human cell lines. In this project, we focus on maintaining baseline stability and sensitivity. We developed a flow cell with adjustable aspect ratio to optimise and build the next generation of HTM biosensors.

### Results and Discussion

To characterise the cell response to a temperature gradient, HTM uses a tuneable heat source of power,  $P$ . It heats the substrate chip from its underside to a predefined constant temperature,  $T_1$ . The temperature of the liquid,  $T_2$ , is monitored simultaneously (**Fig. 1**). The heat-transfer resistance is the ratio between the temperature difference ( $T_1 - T_2$ ) and the heating power,  $P$ . A decrease in  $T_2$  caused by adhered cells at the substrate-liquid interface corresponds to an increase in the heat transfer resistance,  $R_{th}$ .

The robust design of the device allows for highly sensitive  $R_{th}$  readouts, and the material selection promotes uniaxial heat propagation. The inner height of the device can be adjusted up to 14 mm and the position for  $T_2$  can be adjusted freely within this range. Cell detachment can be read at high fidelity. The nature of this effect is not yet known, but depending on the aspect ratio, fluid convection can be altered in order to determine its relevance for the detection effect.

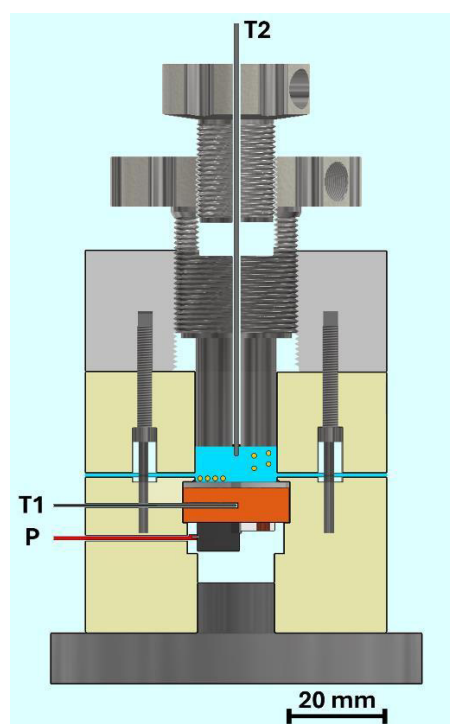


**Figure 1:** Schematic of HTM device with tuneable aspect ratio and position of the  $T_2$  thermocouple.

### Conclusions

We developed a thermal biosensor with highly stable  $R_{th}$  readouts and tuneable device geometries. Stabilisation time and environmental temperature independence will be addressed.

### References

- [1] van Grinsven, B. et al., *ACS Nano* 2012, **6** (3), 2712–2721.
- [2] Wagner, P. et al., *Technisches Messen* 2023, **90** (12), 761–785.
- [3] Yongabi, D. et al., *Advanced Science* 2022, **9** (24).

### Acknowledgements

This work is funded by the KU Leuven project C2E/23/025, titled “Moving thermal-based bio-sensor platforms from principles to application”.

# Whole-Cell Thermal Sensor for the Detection of *P. falciparum*-infected Erythrocytes: Expanding the Boundaries of Imprinted Polymers for the Detection of Malaria

R. Arreguin-Campos<sup>a</sup>, R.M.D.M. Brito<sup>b</sup>, A.R.A. Porto<sup>b</sup>, L.L. Bueno<sup>b</sup>, R.T. Fujiwara<sup>b</sup>, K. Eersels<sup>a</sup>, T. J. Cleij<sup>a</sup>, H. Diliën<sup>a</sup>, B. Grinsven<sup>a</sup>

r.arreguincampos@maastrichtuniversity.nl

<sup>a</sup> Sensor Engineering Department, Faculty of Science and Engineering, Maastricht University, P.O. Box 616, 6200 MD Maastricht, the Netherlands

<sup>b</sup> Laboratory of Immunology and Genomics of Parasites, Department of Parasitology, Institute of Biological Sciences, Universidade Federal de Minas Gerais, Belo Horizonte 07262-130, Brazil

**Abstract:** Malaria is a tropical disease caused by parasites belonging to the *Plasmodium* genus. The infection can be life threatening if not detected on time, but available diagnosis tools hold some limitations. This study presents the surface imprinting of *P. falciparum*-infected red blood cells on a polymeric matrix for the preparation of synthetic receptors that enable the real time detection of the infection employing the Heat Transfer Method as transducing platform. The results highlight the potential prospects that imprinted polymers possess in the development of sensing technologies for parasite-related illness.

**Keywords:** surface-imprinted polymers; parasite detection; malaria; biomimetic sensing

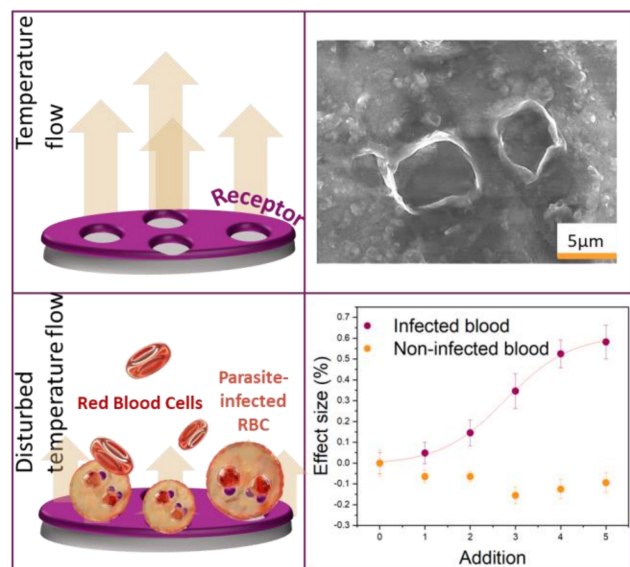
## Introduction

Malaria is a major public healthcare concern worldwide, representing a leading cause of death in specific regions<sup>1</sup>. The gold standard for diagnosis of the infection is microscopic analysis, but this requires a lab setting, trained staff and infrastructure, and is therefore typically slow and expensive. Imprinted polymers (IP) based sensors hold enormous potential as alternative diagnosis technologies. Nonetheless, the development of these materials for large targets (such as parasites) is considerable more challenging when comparing to molecules, limiting their translation into practical technologies. This study aims to provide a proof of concept of the possibility of employing IPs in the detection of the parasite that causes malaria.

## Results and Discussion

The synthetic receptors were prepared *via* the facile interfacial imprinting of polydimethylsiloxane with graphene oxide employing infected red blood cells. The layers were characterized with brightfield and scanning electrode microscopy, exhibiting the successful creation of micro-sized cavities with the morphological features of the target. In order to evaluate the receptor's ability of binding to the target, the films were coupled to the thermal transfer platform.

Results showed the concentration-dependant change of signal from the sensor towards the target in concentrations around 1% parasitemia. In order to depict better a possible real application, experiments with infected and non-infected whole-blood samples were performed in order to assess the limits of the detection tool.



*Schematic representation of cavities on the layer with SEM verification of the receptor film and representative curve of the response of the sensor.*

## Conclusions

This study sheds light on the possibility of employing polymer-imprinting technology for the real-time detection of Malaria. The sensitivity obtained falls within relevant values for the infection, and these results could broaden the perspectives for the development of point of care technologies as alternative diagnosis tools.

## References

[1] World Health Organization (WHO), Malaria. <https://www.who.int/news-room/factsheets/detail/malaria>

## Acknowledgements

This work is funded by the Dutch Research Council (NWO) under the project OCENW.XS23.4.086.

# Detection of C-reactive protein with capacitive field-effect sensors using antibody-functionalized magnetic nanoparticles

T. Karschuck<sup>1,2</sup>, S. Achtsnicht<sup>1</sup>, J. Ser<sup>1</sup>, I. Bouarich<sup>1</sup>, G. Aboutass<sup>1</sup>, F. Eivazi<sup>3</sup>, A. Poghossian<sup>4</sup>, H.-J. Krause<sup>1,3</sup>, P. Wagner<sup>2</sup>, M. J. Schöning<sup>1,3</sup>

[karschuck@fh-aachen.de](mailto:karschuck@fh-aachen.de)

<sup>1</sup>Institute of Nano- and Biotechnologies (INB), Aachen University of Applied Sciences, Heinrich-Mußmann-Str. 1, 52428 Jülich, Germany

<sup>2</sup>Laboratory for Soft Matter and Biophysics, KU Leuven, Celestijnenlaan, 3001 Leuven, Belgium

<sup>3</sup>Institute of Biological Information Processing (IBI-3), Forschungszentrum Jülich GmbH, Wilhelm-Johnen-Str., 52425 Jülich, Germany

<sup>4</sup>MicroNanoBio, Liebigstr. 4, 40479 Düsseldorf, Germany

**Abstract:** The aim of this study is the detection of C-reactive protein (CRP), an inflammation biomarker, with antibody-functionalized magnetic nanoparticles on capacitive field-effect sensors. This was examined by comparing the sensor signals after the immobilization of particles with and without bound CRP.

**Keywords:** capacitive field-effect sensor; C-reactive protein; magnetic nanoparticle; antibody

## Introduction

Field-effect devices have been developed for the direct detection of different nanomaterials and proteins by their intrinsic charge [1]. However, when working with real blood samples, the non-specific adsorption of blood cells and other proteins on the sensor surface may result in erroneous signals. Selective binding of target biomarkers to be detected from complex solutions using antibody-functionalized magnetic nanoparticles (MNP) and their magnetic separation is a promising strategy in immuno-sensing. It allows the immobilization and detection of MNPs with bound biomarkers in experimental conditions, optimized in terms of ionic strength and pH value of the solution.

This study is focussing on the detection of C-reactive protein, a well-known biomarker for inflammation monitoring, which can be used as a predictor for vascular events [2].

## Results and Discussion

For the detection of CRP with capacitive electrolyte-insulator-semiconductor (EISCAP) sensors, 70 nm particles were functionalized with monoclonal antibodies (Ab<sub>m</sub>) against CRP (micromod Partikeltechnologie GmbH, Germany). The CRP solution was prepared with a concentration of 100 mg/L. After binding CRP and purifying the solution, comparative measurements between the field-effect sensors with immobilized MNP-Ab<sub>m</sub> and MNP-Ab<sub>m</sub>-CRP were performed at acidic (pH 5.5), neutral (pH 7.2) and alkaline (pH 9.1) pH values.

First, a baseline measurement was performed with blank sensors. To immobilize the MNPs, a magnet was placed under the sensor. During the immobilization, no datapoints were collected. The ConCap signal of a SiO<sub>2</sub>/p-Si/Al EISCAP after the immobilization of MNP-Ab<sub>m</sub> or MNP-Ab<sub>m</sub>-CRP is shown in Figure 1. A signal difference of

$7.9 \pm 1.8$  mV between MNP-Ab<sub>m</sub> and MNP-Ab<sub>m</sub>-CRP was recorded in pH 5.5 solution.

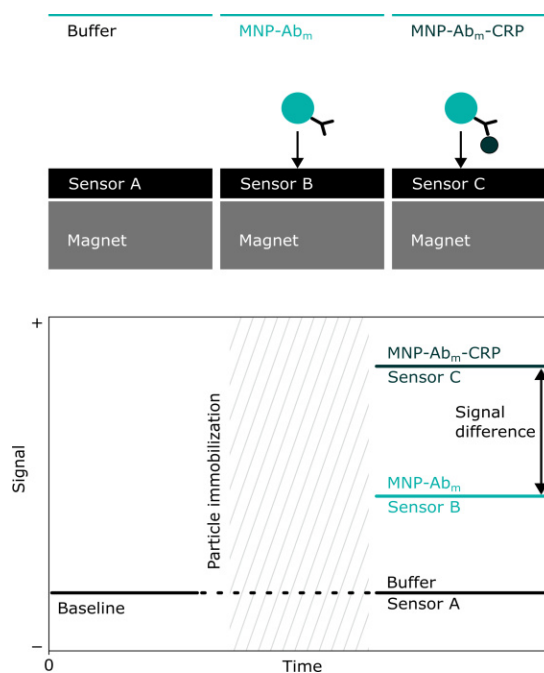


**Figure 1:** Schematic of CRP detection with signals of the capacitive field-effect sensors after immobilization of MNP-Ab<sub>m</sub> and MNP-Ab<sub>m</sub>-CRP.

## References

- [1] A. Poghossian, M.J. Schöning, *Electroanalysis*. **26** (2014), 1197-1213
- [2] P.M. Ridker, J.D. Silvertown, *J. Periodontol.* **79** (2008), 1544-1551

## Acknowledgements

This work was funded by the Deutsche Forschungsgemeinschaft (DFG: German Research Foundation)– 445454801.



# Design and implementation of a wafer-scale process for SiC microwire aiming for biochemical sensing applications

Xuan Thang Vu<sup>1\*</sup>, Tuan Khoa Nguyen<sup>2</sup>, Denis Besedin<sup>1</sup>, Zhongxin Zhao<sup>1</sup>, Minh Anh Huynh<sup>2</sup>, Nam Trung Nguyen<sup>2</sup>, Sven Ingebrandt<sup>1</sup>

\*[vu@iwe.rwth-aachen.de](mailto:vu@iwe.rwth-aachen.de)

<sup>1</sup>Institute of Materials in Electrical Engineering 1, RWTH Aachen University, Sommerfeldstr. 24, 52074 Aachen, Germany

<sup>2</sup>Queensland Micro and Nanotechnology Centre, Griffith University, Nathan, Queensland, 4111, Australia

**Abstract:** 3C-SiC is highly valued across multiple fields for applications, including biosensing, pH sensing, temperature sensing, and pressure sensing, due to its pivotal role in biology, medicine, and industrial engineering. The work aims to develop a wafer-scale fabrication of silicon carbide devices for biosensor and bioelectronics applications.

**Keywords:** Silicon carbide; biosensors; field-effect transistors

## Introduction

Being a wide band gap material, silicon carbide (SiC) has been demonstrated to be robust and multifunctional in biosensors and bioelectronics for advanced biomedical applications. This is attributed to its excellent biocompatibility and electronic properties as well as the maturity of material growth and fabrication technologies. Current research on SiC suggests it is a promising material platform for high-performance bioelectronics and biosensors that can solve the major mismatch in biocompatibility and electronic functionality [1]. This work will explore a new capability of low dimensional SiC-based biosensors (i.e. microwires) to achieve high sensing performance while maintaining good consistency and stability.

## Results and Discussion

We have successfully developed a wafer-scale fabrication process using laser lithography and RIE etching processes for the production of 3C-SiC microwires. First, the 3C-SiC was grown on the p-type silicon substrate using a low-pressure chemical vapour deposition process at 1250°C. Laser lithography was then used to define the size of the microwire, and a protocol for etching the SiC using SF<sub>6</sub> plasma was developed to precisely control the etching process. Subsequently, an Al/Ti/Au stack was deposited on top of the contact line to reduce the serial contact resistance. A 300 nm PECVD SiO<sub>2</sub> layer was deposited on the wafer as the passivation layer. The micro window and the contact pads were opened by another lithography step and subsequently etched in HF 1%. We also investigated different gate dielectric layers using ion-beam deposition techniques. The chips were then

characterized in different configurations, both in dry conditions and in contact with an electrolyte solution.

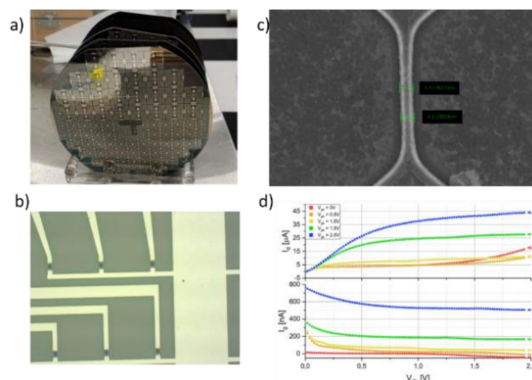


**Figure 1:** (a) wafer-scale processed SiC devices, (b,c) Optical and SEM images of the SiC microwire, (d) electrical characteristic of the SiC microwire

## Conclusions

The fabrication of a wafer-scale of SiC devices has been successfully completed, with different configurations such as varying the doping concentration of SiC. Further electrical characterization and improvements for device performance will be carried out for bio-chemical sensing applications.

## References

- [1] N.-K. Nguyen, *ACS Appl. Electron. Mater.* 2021, 3, 5, 1959–1981

## Acknowledgements

We acknowledge financial support from the DAAD (project ID 57655030), and RWTH Aachen University.

# Tutorial Lecture C

## Characterization of working electrochemical interfaces with X-ray spectroscopies and electron microscopy

Juan Jesús Velasco Vélez

[jvelasco@cells.es](mailto:jvelasco@cells.es)

ALBA Synchrotron, Carrer de la Llum 2-26, 08290 Cerdanyola del Valles, Spain

**Abstract:** An in depth understanding of the atomistic mechanism underlying electrochemical interfaces requires recording large set of data under operando conditions. Unfortunately, the analytical techniques able to provide interface information are very limited and hardly compatible with liquids leading to a loss of important information as in many case the desired information cannot be “quenched” in post process analysis. In this talk I will present new approaches that allow the investigation of working electrochemical interfaces. These approaches will be validated using as a research topics the electrocatalytic CO<sub>2</sub> reduction reaction.

**Keywords:** In-situ/operando, X-ray spectroscopy, electron microscopy, CO<sub>2</sub>RR, copper electrodes

### Introduction

Copper has become the subject of widespread interest because of its unique ability to facilitate the electrochemical reduction of CO<sub>2</sub> to valuable hydrocarbons and alcohols at high Faradaic efficiency under mild conditions [1]. This makes Cu-based catalysts critical in the emerging circular clean carbon economy, where CO<sub>2</sub> and H<sub>2</sub>O are the cornerstone molecules [2] that are electro-reduced using renewable energy. Different models have been developed in an effort to explain the uniqueness of copper and its ability to electrochemically produce C<sub>2+</sub> [3] and oxygenated hydrocarbon products, unfortunately however, a complete description of the electronic factors making copper active in CO<sub>2</sub> reduction remains elusive. To solve this conundrum, *in situ* characterization of the working copper/electrolyte interface during the cathodic CO<sub>2</sub> reduction reaction (CO<sub>2</sub>RR) is necessary where the combination of X-ray spectroscopy with electron microscopy is a valuable method to ascribe the variation in the electronic structure with the changes observed in the material morphology during its operation.

### Results and Discussion

It was found that the copper electrode electrified interface is ruled by the formation of reduced copper as shown in Figure 1, being thermodynamic stable and active during the cathodic reduction of CO<sub>2</sub> to hydrocarbons [4]. This finding is in good agreement with the expected thermodynamics equilibrium under such condition in the respective Pourbaix diagram. These results imply that copper oxides can be only stabilized due to kinetics and they are not stable at high cathodic potentials required to perform the CO<sub>2</sub>RR. Also, changes in the electronic structure are accompanied by a reconstruction in the electrode surface changing

from a flatter surface to a more stepped one (see Figure 1), which in last term controls the dissociation barrier and thus the activity, selectivity and stability.

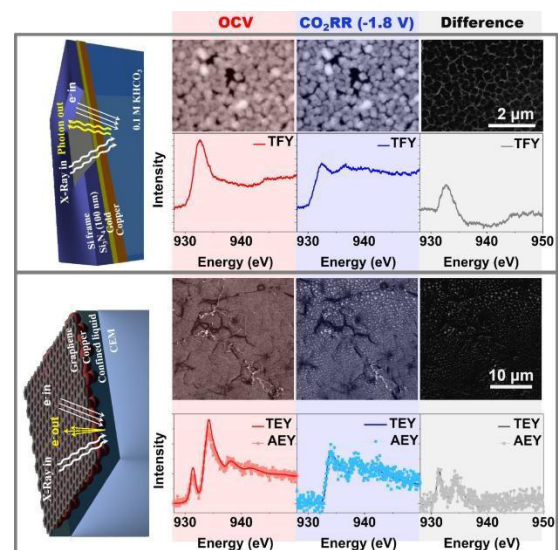


**Figure 1:** Detection scheme and *in situ* AEY-XAS/TEY-XAS and ECSEM measurements of the CO<sub>2</sub>RR onto an *in situ* electrodeposited copper electrode collected under OCV and CO<sub>2</sub>RR [4].

### Conclusions

The surface morphology and electronic structure of the electrode catalyst play a key role in the transport process and governs the electrocatalytic CO<sub>2</sub>RR performance on copper electrodes.

### References

- [1] A. A. Peterson, J. Phys. Chem. Lett. 2012, 3, 251
- [2] R. Schlögl, Green 2012, 2, 1
- [3] Y. Zheng, JACS 2019, 141, 7646
- [4] J.J. Velasco-Velez, J.J. ACS En. Lett. 2020, 5, 2106

# *In-situ* measurement of the work function of steel surface by photoelectron yield spectroscopy under atmospheric condition

Ko-ichiro Miyamoto<sup>1</sup>, Tatsuo Yoshinobu<sup>1</sup>

koichiro.miyamoto.d2@tohoku.ac.jp

<sup>1</sup> Department of Electronic Engineering, Tohoku University,  
6-6-05, Aramaki-Aza-Aoba, Aoba-ku, Sendai, JAPAN

**Abstract:** Photoelectron yield spectroscopy (PYS) is able to measure the work function of a surface under atmospheric conditions. In this study, the PYS technique was applied to a steel surface. Taking advantage of PYS, the work functions of a dry surface, a wet surface, and a surface in the drying process were monitored.

**Keywords:** work function; photoelectron yield spectroscopy; atmospheric conditions

## Introduction

The work function (WF) is one of the most fundamental indices of surface properties. However, conventional XPS, UPS, or AES require vacuum conditions. To overcome this problem, photoelectron yield spectroscopy (PYS) has been proposed by Ishii *et al.* [1]. In this study, we utilized the PYS technique for *in-situ* measurement of WF of steel surface.

## Experiment

In the PYS measurement (see Fig. 1), an excitation light from a monochromator illuminates the surface of the specimen. By applying a negative bias voltage to the specimen, the emitted photoelectrons are collected by a ring-shaped electrode. By scanning the excitation wavelength, the emission yield spectrum of iron is obtained.

## Results and Discussion

Fig. 2a shows a typical emission yield spectrum of a polished iron surface under the atmospheric condition. By extrapolating the slope, the WF was estimated to be 4.76 eV.

In addition to the polished surface, PYS measurement was performed on a wet surface. Fig. 2b shows a plot of WFs before and after dropping an aliquot of diluted H<sub>2</sub>SO<sub>4</sub> (3.6 mM, 20  $\mu$ L). Even when the whole surface of the specimen was covered with a thin water layer, the measurement could be performed. The results of the *in-situ* monitoring of WF indicated that the surface state was changing during the drying process.

## Conclusions

The measurement of WF under atmospheric conditions was demonstrated. The WFs of dry and wet surfaces could be monitored. It can be a powerful tool to probe surface properties. In our poster, we will also discuss the WF changes induced by hydrogen entry into steel.

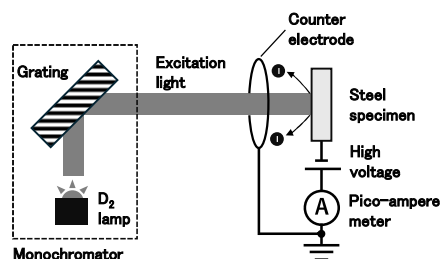


Fig.1 Measurement system of photoelectron yield spectroscopy (PYS).

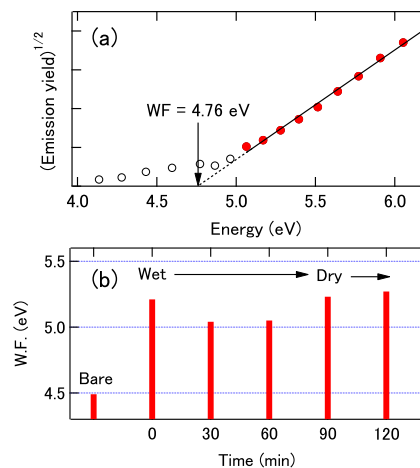


Fig.2 (a) Emission yield spectrum of iron surface. (b) Variation of iron WF in dry – wet – dry states.

## References

[1] H. Ishii *et al.*, *J. Surf. Sci. Soc. Jpn.*, 28 (2007), p264-270.

## Acknowledgments

This study was supported by JSPS KAKENHI (22H01826) and Nippon Steel Corporation.

## Ohmic contacts in tellurium nanowires semiconductor devices

Heping Cui<sup>1</sup>, Kai Zheng<sup>2</sup>, Sven Ingebrandt<sup>1</sup>

[heping.cui@iwe1.rwth-aachen.de](mailto:heping.cui@iwe1.rwth-aachen.de)

<sup>1</sup>Institute of Materials in Electrical Engineering 1, RWTH Aachen University, Sommerfeldstr. 24, 52074 Aachen, Germany

<sup>2</sup>School of Electrical Engineering and State Key Laboratory of Power Transmission Equipment & System Security and New Technology, Chongqing University, 400044, Chongqing, China

**Abstract:** Semiconductor nanowires have gained strong interest as a class of nanoscale building blocks for electronic devices. With the unique 1D van der Waals structure, tellurium nanowires (TeNWs) exhibit appealing optoelectronic and transport properties. However, an Ohmic contact between metal and TeNWs remains a significant challenge even it is crucial for the performance of electronic devices. In this work, Au-TeNW interfaces were studied using density functional theory (DFT) combined with experiments. The results of DFT revealed that gold (Au) showed great potential to form favourable contact with TeNW due to the strong interaction and high orbital overlapping. Subsequently, we characterized the morphology and crystallinity of TeNWs and fabricated electronic devices. Electrical characterization showed good Ohmic contacts between Te and Au.

**Keywords:** TeNWs; semiconductor devices; DFT; Ohmic contact; hydrothermal synthesis

### Introduction

Tellurium (Te) is a p-type semiconductor belonging to the chalcogenide group. Its crystal structure is composed of 1D atomic chains held together by weak van der Waals forces resulting in a surface free of dangling bonds. This distinctive anisotropic crystal structure gives Te high intra-chain hole mobility and enables it to support high current densities [1]. With its straightforward synthesis and the ability for direct low-temperature growth, TeNWs have recently gained significant attention in the field of nanoelectronic devices. The nature of the contact—whether Ohmic or Schottky—significantly influences the electronic properties of these devices. Achieving low-resistance Ohmic contact remains a significant challenge due to the strong Fermi level pinning (FLP) effect at the interface [2]. In this study, we studied Au-TeNWs interfaces using both DFT theoretical modelling and experimental methods for later use in field-effect transistors.

### Results and Discussion

TeNWs were prepared by hydrothermal synthesis. We verified morphology and single-crystal nature of TeNWs by characterization with scanning (SEM), high-resolution transmission (HRTEM) and selected area diffraction (SAED) electron microscopy. The results indicated a good material compatibility, allowing an efficient charge transfer with orbital overlapping with no tunneling or Schottky barriers [2]. Chips with 4×4 arrays of gold microelectrodes were fabricated and electrical characterization indicated a good Ohmic contact between Te and Au, which is matching well with the results from the DFT modelling.

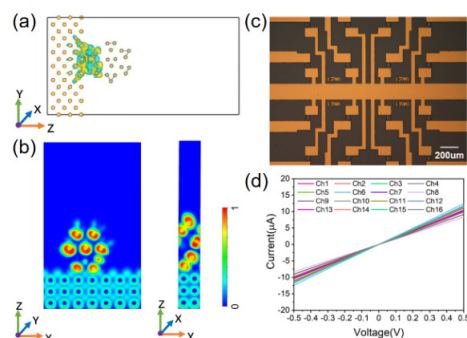


**Figure 1:** (a-b) Charge density difference and electron localization function at Au-TeNW interface. (c-d) TeNWs devices and electrical characterization.

### Conclusions

TeNWs were successfully synthesized by a hydrothermal method. SEM, HRTEM and SAED characterization techniques confirmed the ultrathin morphology and single-crystal nature of TeNWs. The combination of theoretical modelling and electrical characterization revealed good Ohmic contacts. In future, TeNWs will be used to fabricate liquid-gated field-effect transistors.

### References

- [1] J. K. Qin, P. Y. Liao et al. Nature Electronics, 2020, 3(3): 141-147.
- [2] T. Shen, J. C. Ren et al. Journal of the American Chemical Society, 2019, 141(7): 3110-3115.

### Acknowledgements

Financial support for this project came from RWTH Aachen University. H.C. thanks for the financial support from the Chinese Scholarship Council Fellowship (no. 202006050050).



## 3D Photoelectrochemical Imaging

Jiazhe Zhao<sup>1</sup>, Bo Zhou<sup>1</sup>, Ruixiang Li<sup>1</sup>, Joe Briscoe<sup>1</sup>, Ana Belén Jorge Sobrido<sup>1</sup>, Steffi Krause<sup>1</sup>

[jiazhe.zhao@qmul.ac.uk](mailto:jiazhe.zhao@qmul.ac.uk)

<sup>1</sup> School of Engineering and Materials Science, Queen Mary University of London, Mile End Road, E1 4NS London, UK

**Abstract:** A 3D photoelectrochemical imaging system (PEIS) for investigating local electrochemical activity in complex porous electrode structures will be presented. Porous ITO coated with hematite via electrodeposition was fabricated and used as the light addressable electrode. Photocurrents were excited with a two-photon effect using a focused, modulated 780 nm fs laser to provide depth resolution. The scans were performed by moving the sample holder with respect to the laser beam with a mechanical positioning system. The variation of the photocurrents collected in different depths of the photoelectrode demonstrates the potential of 3D photoelectrochemical imaging.

**Keywords:** light-addressable electrochemistry; 3D photoelectrochemical imaging; porous semiconductor electrode.

### Introduction

Electrochemical imaging techniques are powerful tools to investigate topography, charge, and catalytic activity of surfaces and for label-free imaging of cellular processes with high resolution<sup>1</sup>. Current electrochemical imaging technologies have been limited to probing thin films or the outer surfaces of living cells. Here, we present a novel 3D imaging technology that is expected to aid in-situ functional imaging in 3D tissue culture in the future. Hematite has been used as semiconductor substrate for cell imaging<sup>2</sup> and is also an excellent photocatalyst for photoelectrochemical water splitting<sup>3</sup>. In this work, photocurrents were excited in a 3D porous electrode of ITO coated with hematite. Depth resolution was achieved by exciting photocurrents using a two-photon effect using light with an energy smaller than the bandgap of hematite (Fig. 1).

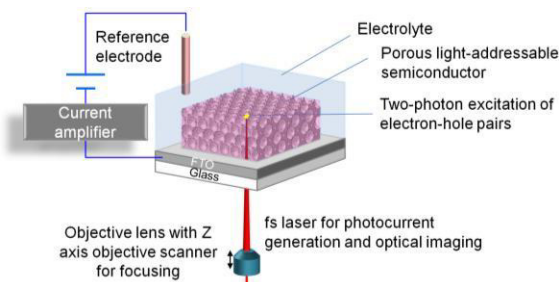


**Figure 1:** A schematic of the setup for 3D photoelectrochemical imaging.

### Results and Discussion

The ITO-hematite porous electrode with interconnected pores and a well-connected interface with the substrate (Fig 2a and b) was fabricated successfully. Photocurrent images of the porous structure were taken on both the XY plane and the XZ plane (Fig. 2c and d). The photocurrent was significantly larger when the laser was focused on the pore wall rather than the cavities of the structure, both in the XY scan (Fig. 2c) and an XZ area scan (Fig 2d). The image reveals discernible features showing the shape and size of the observed pores.

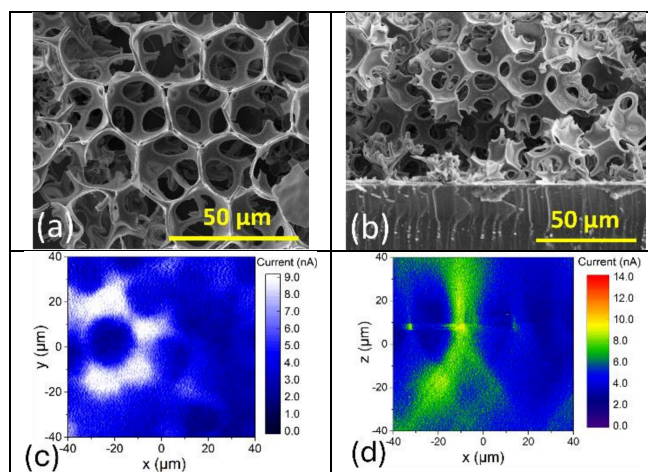


**Figure 2:** (a) SEM image of the ITO-hematite photoelectrode; (b) SEM image of the ITO-hematite electrode cross section; (c) Photocurrent image of the XY plane; (d) Photocurrent image of the XZ plane.

### Conclusions

Porous ITO-hematite scaffold was used successfully as a photoelectrode for 3D photoelectrochemical imaging. Our photoelectrochemical imaging system is able to capture images of pores in the Z-direction, thereby demonstrating the significant potential of this technique for in-situ 3D functional imaging in 3D tissue culture or electrochemical processes in energy harvesting devices.

### References

- [1] Richter A.P. et al. *Langmuir* 2016; 32:6468-77.
- [2] Zhou B. et al. *Biosensors and Bioelectronics* 2021; 180:113121.
- [3] Brillet J. et al. *Nano letters* 2010; 10:4155-60

### Acknowledgements

The authors are grateful to the China Scholarship Council for providing Jiazhe Zhao with a PhD studentship, and to EPSRC (EP/V047523/1) for funding.



## Combinatorial property mapping of a Al-Eu Compositional Thin Film Library

A. Greul<sup>1</sup>, G. Popescu-Pelin<sup>2</sup>, G. Socol<sup>2</sup>, A. I. Mardare<sup>1</sup>, A. W. Hassel<sup>1,3</sup>

[andreas.greul@jku.at](mailto:andreas.greul@jku.at)

<sup>1</sup>Institute of Chemical Technologies of Inorganic Material (TIM), Johannes Kepler University, Altenberger Straße 69, 4040 Linz, Austria

<sup>2</sup>Laser Department, National Institute for Lasers, Plasma and Radiation Physics, 077125, Romania

<sup>3</sup>Danube Private University (DPU), Steiner Landstraße 124, 3500 Krems an der Donau, Austria

**Abstract:** A Al-Eu compositional thin film library was fabricated via thermal co-evaporation, covering 0.5-5.0 at.% Eu, identified by Scanning Energy Dispersive X-ray Spectroscopy (SEDX). Atomic Force Microscopy (AFM) and Scanning Electron Microscopy (SEM) revealed significant nanostructuring around the eutectic point at 2.25 at.% Eu. Contact angle measurements showed notable changes in wetting behaviour at this composition. Electrochemical testing indicated that even minimal Eu concentrations significantly affect Al matrix stability. Ongoing experiments using Deep-Level Transient Spectroscopy (DLTS) aim to characterize defect energy levels and temperature coefficients of electrical resistivity.

**Keywords:** nano-structuring; combinatorial; electro chemistry; thin film

### Introduction

Previous research on the influence of rare earth metals on the electrochemical and crystallographic properties of aluminium revealed notable effects [1]. For the case of the Al-Eu system, there is lack of comprehensive studies examining the influence of europium on the electrochemical and structural properties of aluminium. There are three intermetallic compounds and two eutectic points identified for this system [2]. The aim of this study is to identify promising compositions and potential applications of Al-Eu thin films. Utilizing compositional thin film libraries enables investigation broad compositional ranges in an effective manner.

### Results and Discussion

Al-Eu compositional thin films were produced using thermal co-evaporation. The covered compositional range was 0.5-5.0 at.% of Eu, identified by SEDX. Investigations using AFM and SEM revealed pronounced nano structuring around the first eutectic point at 2.25 at% Eu. Furthermore, contact angle measurements showed significant changes in the wetting behaviour of the film at this composition. A SEM image of this composition can be seen in **Figure 1**. Electrochemical testing so far revealed that Eu strongly influences the stability of the Al matrix even in the smallest concentrations. Current investigations involve DLTS to characterize energy levels of possible defects and to determine the temperature coefficient of the electrical resistivity [3].

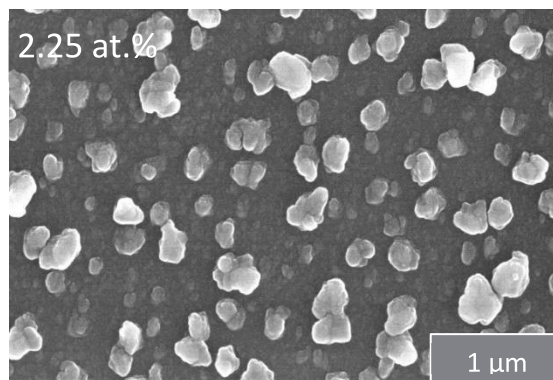


**Figure 1:** SEM image of the Al-Eu compositional library at 2.25 at.% Eu.

### Conclusions

This study represents a starting point in understanding the influences of Eu on an Al matrix. First significant influences of Eu have been revealed and warrant further electrochemical investigations which might lead to the discovery of promising material candidates for industry.

### References

- [1] A.I. Mardare, C.D. Grill, I. Pötzelberger, T. Etzelstorfer, J. Stangl, A.W. Hassel, *J Solid State Electrochem* **20** (2016) 1673-1681
- [2] H. Okamoto, *JPE* **12** (1991) 499-500.
- [3] J. Lauwaert, S. Khelifi, In *Capacitance Spectroscopy of Semiconductors*. Taylor and Francis, Oxfordshire UK, 2018, p. 61-84

# Thermal Detection of Riboflavin in Almond Milk Using Molecularly Imprinted Polymers

G. van Wissen <sup>1</sup>, J.W. Lowdon, T.J. Cleij, H. Diliën, K. Eersels and B. van Grinsven

[g.vanwissen@maastrichtuniversity.nl](mailto:g.vanwissen@maastrichtuniversity.nl)

<sup>1</sup> Department of Sensor Engineering, Faculty of Science and Engineering, Maastricht University, Duboisdomein 30, 6229 GT Maastricht, the Netherlands.

**Abstract:** Riboflavin is an essential vitamin in our diet and a powerful freshness indicator in food quality control. Given its significance, accurate riboflavin determination in complex food samples is indispensable. A promising sensor is based on molecularly imprinted polymers (MIPs), which are coupled to a low-cost thermal readout device to detect riboflavin in almond milk with minimal pretreatment steps. The sensor performance was assessed by loading assays with aqueous riboflavin solutions, selectivity studies with nutrients commonly found in almond milk and for real-life applicability for determination of riboflavin in almond milk. Most importantly, the sensor exhibits a LOD of 3.1  $\mu\text{M}$  in almond milk and the riboflavin content can be calculated using a calibration curve with an accuracy of 95.6%.

**Keywords:** Vitamin Sensing; Molecularly Imprinted Polymers; Heat-transfer Method; Food Analysis

## Introduction

Riboflavin, also called vitamin B2 is an essential part of our diet and its deficiency is widespread among different cultures [1]. A promising solution that allows for direct on-site measuring are molecularly imprinted polymers (MIPs). MIPs are highly cross-linked synthetic polymeric materials, able to selectively bind specific targets [2]. A recently developed readout technology is the heat-transfer-method (HTM) based on the change of thermal resistance upon analyte binding [3]. In this research, riboflavin imprinted MIPs were prepared and implemented into the thermal sensing platform to detect vitamin B2 in almond milk with minimal pretreatment steps.

## Results and Discussion

In the first step, the MIP composition was optimized by investigating monomer type, crosslinker, solvent amount and rebinding conditions with the best performing MIP showing an IF of 1.33. This MIP was implemented into the HTM setup by microcontact stamping. The sensor performance was scrutinized using loading assays, selectivity studies with other compounds commonly found in almond milk and the detection of riboflavin in almond milk. Out of vit. B3 and E, and sucrose as possible interferents, the sensor showed the highest affinity towards vit. B2 even at low concentrations. Lastly, centrifuged almond milk was investigated for its riboflavin content and compared to the loading assays and a LOD of 3.1  $\mu\text{M}$  was obtained. Quantification using the calibration allowed for a 96% accuracy in determining the riboflavin content of the almond milk.

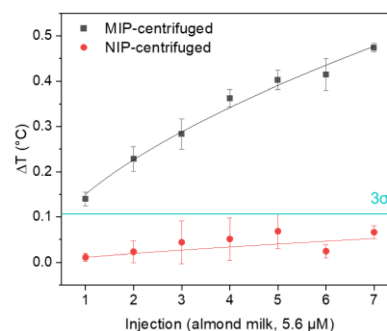


**Figure 1:** Dose-response curve of centrifuged almond milk with 5.6  $\mu\text{M}$  vitamin B2 content.

## Conclusions

The imprinting of vit. B2 was successful and after optimization the best performing MIP was implemented into the HTM setup. Both sensitivity and selectivity and a real-life sample were investigated with a final LOD of 3.1  $\mu\text{M}$  in almond milk and an accuracy of 96% for vit. B2 quantification.

## References

- [1] K. Thakur et al., Crit. Rev. Food Sci. Nutr. 2017, 57:17, 3650-3660
- [2] J. W. Lowdon et al., Sens. Actuators B Chem. 2020, 325, 128973.
- [3] B. van Grinsven, K. Eersels et al., ACS Appl. Mater. Interfaces, 2014, 6 (16), 13309-13318

## Acknowledgements

This work was supported by the European Regional Development Fund through the Interreg VA Euregion Meus Rhine program. Project name: Food Screening EMR, project number: EMR159.

# Exploring of a multi-sensor array system for on-site monitoring of groundwater quality

D. Özsoylu<sup>1</sup>, V. Kajonrungsilp<sup>1</sup>, S. Achtsnicht<sup>1</sup>, E. Börmann-El Kholly<sup>1</sup>, M. J. Schöning<sup>1,2</sup>

[oezsoylu@fh-aachen.de](mailto:oezsoylu@fh-aachen.de)

<sup>1</sup>Institute of Nano- and Biotechnologies (INB), Aachen University of Applied Sciences, Heinrich-Mußmann-Str. 1, 52428 Jülich, Germany

<sup>2</sup>Institute of Biological Information Processing (IBI-3), Forschungszentrum Jülich GmbH, Wilhelm-Johnen-Str., 52428 Jülich, Germany

**Abstract:** Over 60% of available drinking water in Germany is obtained from groundwater. Nevertheless, groundwater could contain dangerous levels of heavy metals, toxins, and ions. Therefore, its quality control is vital to preventing potential hazards to human health and the environment as well as to supply healthy water to the community. This project deals with the development of a multi-sensor array system for continuous monitoring of important water parameters indicating groundwater quality.

**Keywords:** Ion-selective electrode (ISE); water quality; continuous monitoring; ground water

## Introduction

Up to 62% of an adult body consists of water [1] and around 1 to 1.5 liters of drinking water on average is consumed per day [2]. The scarcity of fresh water on Earth is also steadily worsening. Hence, the development of reliable water quality control proves vital on a global scale. On the other hand, commercially available devices for on-site continuous monitoring of groundwater quality are rare. Therefore, the service for obligated regular screening of groundwater samples is outsourced to central laboratories, which does not ensure cost-effective and continuous monitoring.

In this project, the suitability of different commercially available ion-selective electrodes (ISEs) is explored to develop a multi-sensor array system (Figure 1) for continuous monitoring of important water parameters such as lead, chloride, fluoride, nitrate, and arsenic. The key parameters for the first screening process of suitable electrodes include detection range, optimal working conditions (e.g., pH and temperature), cost-effectiveness, and compatibility being a multi-sensor array set-up. For the literature search, the reports from the last 10 years were carefully evaluated, also considering industrial sensors.

## Results and Discussion

The following challenges were found to be critical for the realization of the multi-parameter ISE-based sensing system allowing continuous, on-site, online and long-term monitoring: *i*) interference of non-target ions, *ii*) sensor drift, and *iii*) requirement for periodic sensor calibrations. Current work focuses on expanding the sensor system with the help of

training data and machine learning algorithms together with our project partners.

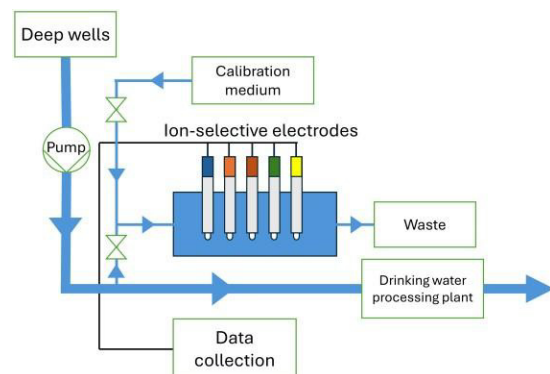


**Figure 1:** Flowchart concept of the multi-sensor array system for monitoring groundwater quality.

## References

- [1] H. Lu, E. Ayers, P. Patel, and T. K. Mattoo, *Kidney Res. Clin. Pract.* **42** (2023) 340–348
- [2] L. Barraj, C. Scrafford, J. Lantz, C. Daniels, and G. Mhlan, *J. Expo. Sci. Environ. Epidemiol.* **19** (2009) 382–395

## Acknowledgments

The authors thank the Central Innovation Program (project number:16KN0996445) for small and medium-sized enterprises (SMEs) funded by the German Federal Ministry for Economic Affairs and Climate Action (BMWK). The authors would also like to thank the project partners, INCOstartec GmbH, LANTECH Informationstechnik GmbH, Fraunhofer IGB, and Stadtwerke Klingenberg.

# Live Cell Imaging with Photoelectrochemical Imaging and Scanning Ion Conductance Microscopy

Ruixiang Li<sup>1</sup>, Jiazhe Zhao<sup>1</sup>, Yunpeng Fang<sup>1</sup>, Bo Zhou<sup>1</sup>, Jon Gorecki<sup>1</sup>, Anirban Das<sup>1</sup>, Nivethitha Kota Lakshminaraasimulu<sup>1</sup>, Andrew Shevchuk<sup>2</sup>, Thomas Iskratsch<sup>1</sup>, Steffi Krause<sup>1\*</sup>

[s.krause@qmul.ac.uk](mailto:s.krause@qmul.ac.uk) (Corresponding e-mail address)

<sup>1</sup>School of Engineering and Materials Science, Queen Mary University of London, Mile End Road, London, E1 4NS, UK.

<sup>2</sup>Department of Medicine, Imperial College London, Du Cane Road, London, W12 0NN, UK

**Abstract:** A setup that combines photoelectrochemical imaging (PEI) and scanning ion conductance microscopy (SICM) is introduced as new method for high resolution cell imaging and biosensing applications. A7R5 cells were cultured on a hematite substrate for simultaneous PEI and SICM measurements, resulting in morphological and electrochemical images. The setup will be used for action potential monitoring of cells for the investigation of drug-induced cell responses.

**Keywords:** photoelectrochemical imaging; scanning ion conductance microscopy; cell imaging; action potential

## Introduction

Recent developments in electrochemical measurements highlight photoelectrochemical imaging (PEI) and Scanning Ion Conductance Microscopy (SICM) as tools for functional and morphological cell imaging. PEI is based on the excitation of local photocurrents in a semiconductor electrode and measures localized electrochemical activity with on the basal side of cells with micron resolution, while SICM offers detailed topographical analysis of the apical side of cells by detecting ion currents through a nanopipette.<sup>1,2</sup> A new setup was built combining PEI and SICM in a single instrument for simultaneous imaging.

Hematite ( $\alpha\text{-Fe}_2\text{O}_3$ ) was electrodeposited onto fluorine doped tin oxide (FTO) coated glass adapting a previously described method.<sup>1</sup> The hematite film was used as the working electrode (WE) for PEI to generate local photocurrents under the cells. A Nanopipette with a tip diameter of 50 nm was used for topography imaging with SICM. Vascular smooth muscle cells (A7R5) were cultured on the hematite substrate for imaging. Figure 1a shows the setup for simultaneous PEI and SICM measurements.

## Results and Discussion

The resolution of PEI was determined to be  $1.6\ \mu\text{m}$  by scanning the laser across the edge of a photoresist pattern. Simultaneously recorded PEI and SICM images of a single A7R5 cell are presented in figures 1b and c. The attachment of the cell to the substrate was monitored with PEI, and the morphology of the cell was measured with SICM showing a clear edge of the cell and the shape of the nucleus, indicating good spatial resolution of both methods. To stimulate the cells, we will release Yoda-1 calcium ions channel opener through the SICM nanopipette while continuous imaging the cells with PEI.

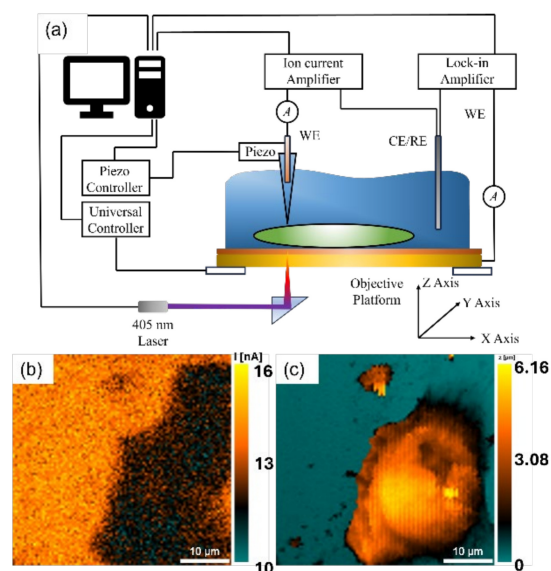


Figure 1. (a) Schematic of simultaneous PEI and SICM measurement setup. (b) PEI imaging of A7R5 cell and (c) SICM measurement of the same cell simultaneously.

## Conclusions

A new setup combining PEI and SICM was presented. Simultaneous images of photoresist patterns and A7R5 cells were recorded with good spatial resolution. The new setup will be used to measure the electrochemical responses of individual cells.

## References

- Bo Zhou et al. Biosensors and Bioelectronics 2021; 180:113121.
- Bednarska et al. Journal of Microscopy 2021; 282:21-29.



# Colorimetric detection of veterinary tranquilizer in adulterated alcoholic beverages

Ramiro Marroquin-Garcia <sup>1</sup>, Gil van Wissen, Thomas Cleij, Kasper Eersels, Bart van Grinsven, and Hanne Dillën

r.marroquingarcia@maastrichtuniversity.nl

<sup>1</sup>Sensor Engineering Department, Faculty of Science and Engineering, Maastricht University, 6200, MD, Maastricht, the Netherlands

**Abstract:** The use of the veterinary-tranquilizer xylazine as an adulterant poses a major health problem in the world. Involuntary consumption in alcoholic beverages leads to potential loss of consciousness and even death. In this work, a probe for the fast, visual detection of xylazine in alcoholic beverages is proposed. The molecularly imprinted polymer (MIP)-based sensor was evaluated in a real gin and tonic sample and displayed a linear regime of 1.5–4 mM and a LOD of 1.36 mM. Implementation of the assay in a portable device resulted in fast xylazine detection (< 30 s) in a spiked gin & tonic.

**Keywords:** Molecularly imprinted polymers; Xylazine; Dye displacement assay; Beverage adulteration

## Introduction

The use of molecularly imprinted polymers (MIPs) for the detection of drugs is well-established in the literature.<sup>1</sup> Advances in the MIP field have enabled the production of colorimetric probes for the detection of various drugs such as diarylethylamines and amphetamine. In this case, a dye molecule is introduced in a specific drug-designed MIP. The dye contains similar functionalities as the drug, allowing it to bind loosely to the cavity of the MIP and then is displaced in the presence of the target (Figure 1).

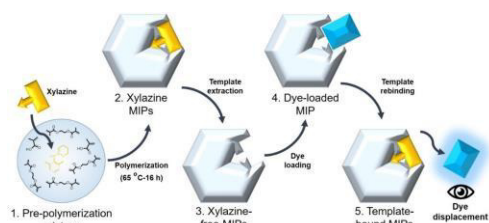


Figure 1: MIP synthesis and dye displacement

The colorimetric probes, combine both the fast and specific detection of MIPs with the easy visual detection provided by the dye. This technology could potentially provide a solution to several drug-related crimes such as drug facilitated sexual abuse (DFSA). In this work, we present the advances in the development of a colorimetric test for detecting xylazine adulteration in alcoholic beverages.

## Results and Discussion

The MIPs were synthesized *via* bulk polymerization and using an optimized molar ratio of 1:2:4 (xylazine:methylmethacrylate:egmda). The porogen consisted of a 1:3 volume mixture of chloroform:toluene. The materials displayed an

imprinting factor of 2 in water (See Figure 1).

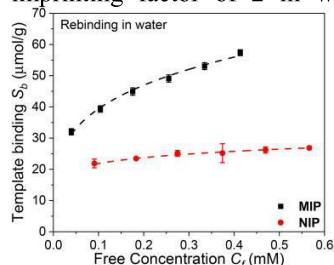


Figure 1. Binding isotherm of the optimized MIP using xylazine HCl concentrations from 0.7-0.2 mM in water.

Dye selection was conducted by testing the MIPs against 4 compounds at the same concentration of the template (0.7-0.2 mM). Methylene blue was selected as it displayed a very similar binding factor (still lower) than xylazine (see Figure 2.)

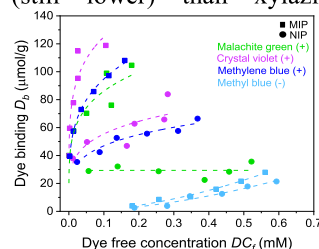


Figure 2. Dye binding isotherm of the optimized MIP using dyes (0.7-0.2 mM) in water

## Conclusion

The optimized dye loaded sample was evaluated in a real sample (gin and tonic) where a low limit of detection LoD of 1.36 mM was achieved. Furthermore, the material was incorporated into a device with the ability to detect xylazine within 20 seconds using small volume of sample.

## References

Marroquin-Garcia. R. *et al.* *Food Control*, 161, 110403



# Detection of urea in artificial urine using capacitive field-effect biosensors modified with a stacked polyelectrolyte-enzyme bilayer

A. Tsokolakyan<sup>1</sup>, Ts. Poghosyan<sup>1</sup>, V. A. Hayrapetyan<sup>1</sup>, D. Petrosyan<sup>1</sup>, K. Simonyan<sup>1</sup>, A. Badasyan<sup>2</sup>, V. Buniatyanyan<sup>1</sup>, T. Karschuck<sup>3</sup>, M. Welden<sup>3</sup>, H. Iken<sup>3</sup>, M. J. Schöning<sup>3</sup>, M. Yeranossyan<sup>1</sup>, A. Poghosian<sup>4</sup>

[astghik.tsokolakyan@edu.isec.am](mailto:astghik.tsokolakyan@edu.isec.am)

<sup>1</sup>A.B. Nalbandyan Institute of Chemical Physics NAS RA, P. Sevak 5/2, 0014, Yerevan, Armenia

<sup>2</sup>Materials Research Laboratory, University of Nova Gorica, Vipavska 13, 5000, Slovenia

<sup>3</sup>Institute of Nano- and Biotechnologies, Aachen University of Applied Sciences, Heinrich-Mussmann-Str. 1, 52428, Jülich, Germany

<sup>4</sup>MicroNanoBio, Liebigstr. 4, 40479, Düsseldorf, Germany

**Abstract:** Capacitive field-effect biosensors modified with a stacked polyelectrolyte/enzyme urease bilayer were applied for the detection of the urinary biomarker urea in phosphate buffer and artificial urine. A theoretical kinetic model of the biosensor was developed and compared with the experimentally observed results.

**Keywords:** field-effect sensor; urea biosensor; polyelectrolyte; urease; artificial urine

## Introduction

Detection of clinically relevant biomarkers in urine opens new prospects in the development of point-of-care urine analysis devices for medical diagnostics [1]. The urine sample is an ideal liquid excretion compared to other biofluids such as saliva, tears or blood, allowing the collection in large quantities and enabling easy handling and low risk of infections.

In this study, Ta<sub>2</sub>O<sub>5</sub>-gate electrolyte-insulator-semiconductor capacitors (EISCAPs, [2]) modified with a bilayer of poly(allylamine hydrochloride) (PAH)/enzyme urease (Figure 1) were utilized for urinary biomarker (urea) detection in phosphate buffer (PBS) and artificial urine (AU).

## Results and Discussion

With the aim to achieve a dense immobilization of enzymes and thus, to enhance the biosensor performance, the enzyme urease was immobilized onto the pH-sensitive Ta<sub>2</sub>O<sub>5</sub>-gate EISCAP surface modified with the positively charged PAH layer. The modified EISCAP surface was physically characterized by atomic force microscopy and scanning electron microscopy. The PAH/urease bilayer-modified EISCAP biosensors were characterized in PBS and AU samples with different urea concentrations between 0.1 mM – 50 mM via capacitance-voltage and constant-capacitance (ConCap) methods. The AU solution was prepared according to the protocol published in [3]. The urea sensitivity was 34 mV/dec and 27 mV/dec in PBS and AU, respectively. To demonstrate reproducibility of the EISCAP urea biosensor, the ConCap signal was repeatedly recorded in PBS and in 25 mM urea AU samples in alternating order (Figure 1). Finally, the urea biosensor response was modelled (using a kinetic approach proposed in [4]) and compared with the experimentally observed results.

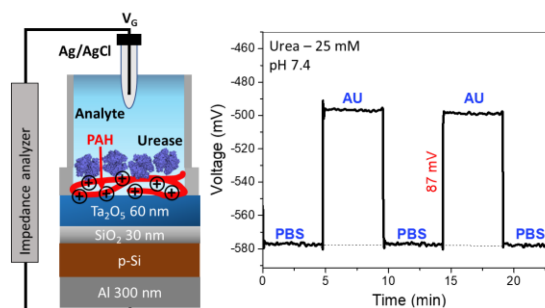


**Figure 1:** Schematic of the measurement setup (left) and ConCap response of the EISCAP biosensor in AU containing 25 mM urea (right).

## Conclusions

The obtained results demonstrate the suitability of PAH/urease bilayer-modified EISCAPs for the urea detection in AU samples.

## References

- [1] Singh, S.; Sharma, M.; Singh, G. IET Nanobiotechnol, 15, 358 (2021). [doi.org/10.1049/nbt2.12050](https://doi.org/10.1049/nbt2.12050)
- [2] Poghosian, A.; Schöning, M.J. Sensors, 20, 5639 (2020). [doi.org/10.3390/s20195639](https://doi.org/10.3390/s20195639)
- [3] Sarigul, N.; Korkmaz, F.; Kurultak, İ. Scientific reports, 9(1), 20159 (2019). [doi.org/10.1038/s41598-019-56693-4](https://doi.org/10.1038/s41598-019-56693-4)
- [4] Glab, S.; Koncki, R.; Hulanicki, A. Analyst, 116, 453 (1991). [doi.org/10.1039/AN9911600453](https://doi.org/10.1039/AN9911600453)

## Acknowledgements

This research was supported by the Higher Education and Science Committee of MESCS RA (Research project № 22rl-056).

# Temperature and solvent effect on the electrical characteristics of two-dimensional metal-organic frameworks

Huijie Jiang,<sup>1</sup> Işıl Berfin Sönmez,<sup>1</sup> Sven Ingebrandt,<sup>1</sup> Vivek Pachauri<sup>1\*</sup>

[huijie.jiang@iwe1.rwth-aachen.de](mailto:huijie.jiang@iwe1.rwth-aachen.de)

<sup>1</sup>Institute of Materials in Electrical Engineering 1, RWTH Aachen University, Sommerfeldstr. 24, 52074 Aachen, Germany

**Abstract:** Two-dimensional conjugated metal-organic frameworks (MOFs) represent a novel class of functional materials that integrate electrical conductivity and a coordinated crystal structure, exhibiting considerable promise in the fields of electronics and sensors. In this study, we examine the impact of synthetic solvents and temperatures on the electrical transport characteristics of  $\text{Cu}_3(\text{HHTP})_2$  (HHTP = 2,3,6,7,10,11-hexahydroxytriphenylene) thin films fabricated using layer-by-layer liquid phase epitaxy in confined microfluidic channels. Our findings indicate that thin MOF films exhibit higher conductivity than vertically aligned nanoflake arrays.

**Keywords:** metal-organic frameworks; thin films; liquid-phase epitaxy; electrical characteristics

## Introduction

Two-dimensional conjugated metal-organic frameworks (2D c-MOFs) are a type of layer-stacked materials constructed of organic ligands and square-planar metal ions through coordination bonds.<sup>1</sup> These materials exhibit structural similarities to graphite and other van der Waals layer-stacked compounds. In recent years, such MOFs have been demonstrated with conductivity values reaching up to  $2500 \text{ S}\cdot\text{cm}^{-1}$ , which is a notable improvement over conventional 3D MOFs.<sup>2</sup> 2D c-MOFs also exhibit anisotropic electrical transport, attributed to their layered lattice structure. For example, in-plane conductivity differs from out-of-plane conductivity, whereby it is critical to control the morphology of the 2D c-MOFs during growth.<sup>3</sup> In this study, a microfluidics-assisted layer-by-layer liquid-phase epitaxy is employed for controllable growth of  $\text{Cu}_3(\text{HHTP})_2$  thin films while precisely varying solvents and temperature conditions. Finally, the electrical characteristics were evaluated using I-V measurements with a two-probe configuration.

## Results and Discussion

In this study, pure ethanol and the mixture of deionized water and ethanol with volumetric ratios of 1:1, 4:1 and 9:1 were utilized as solvents. Besides, three different temperatures (20, 50 and 80°C) were applied during the growth of  $\text{Cu}_3(\text{HHTP})_2$  thin films in microfluidic channels. In the case of using ethanol as synthetic solvents at varying temperatures, as characterized by high-resolution scanning electron microscopy (HR-SEM), larger crystallites were observed at elevated temperatures without a change in morphology or introduction of oxides. Besides, more current was recorded from the thin-film samples grown at higher temperatures, while no significant change was observed by increasing growth temperature from 50°C to 80°C. We studied the solvent effect by adding different amount of

water keeping the synthetic temperature of 80°C. Apparently, we observed a slight drop in current amplitudes by increasing the water content from 50% (v:v) to 80% (v:v). With 90% (v:v) of water in the solvent, the morphology was changed from flat thin films to vertically aligned nanoflake arrays. In this case the current decreases dramatically, which is probably due to the discontinuity of the layer or the existence of non-conducting oxides.

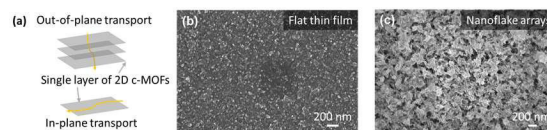


**Figure 1:** (a) Charge carrier transport pathways in 2D c-MOFs. (b, c) HR-SEM images of a smooth thin film and a nanoflake-like 2D c-MOF.

## Conclusions

By systematically varying the synthetic solvents and temperatures, it is possible to regulate the morphology and electrical characteristics in 2D c-MOFs. However, it is essential to rule out the influence of unexpected oxides in  $\text{Cu}_3(\text{HHTP})_2$  thin film to ensure that the only electrical contribution is from intrinsic 2D c-MOFs.

## References

- [1] M. Wang, R. Dong and X. Feng, *Chem Soc Rev*, **50** (2021) 2764-2793.
- [2] Z. Jin, J. Yan, X. Huang, W. Xu, S. Yang, D. Zhu and J. Wang, *Nano Energy*, **40** (2017), 376-381.
- [3] Z. Z. Ma, Q. H. Li, Z. Wang, Z. G. Gu and J. Zhang, *Nat Commun*, **13** (2022), 6347

## Acknowledgements

This project is supported by the DFG-DBT project MOFSens (grant No. 445865083). H.J. thanks for the financial support from the Chinese Scholarship Council Fellowship (no. 202004910374).

## Fluidic setup for automated electrochemical characterization of extended-gate ISFETs

M. Knoll<sup>1,2</sup>, A. Poghosian<sup>3</sup>, N. Biegus<sup>1</sup>, S. Meier<sup>4</sup>, E. Müllner<sup>4</sup>, M. Keusgen<sup>2</sup>, M. J. Schöning<sup>1,5</sup>

[Knoll@fh-aachen.de](mailto:Knoll@fh-aachen.de)

<sup>1</sup>Institute of Nano- and Biotechnologies (INB), Aachen University of Applied Sciences, Heinrich-Mußmann Str. 1, 52428 Jülich, Germany

<sup>2</sup>Institute of Pharmaceutical Chemistry, Philipps University of Marburg, Wilhelm-Roser-Str. 2, 35032 Marburg, Germany

<sup>3</sup>MicroNanoBio, Liebigstr. 4, 40479 Düsseldorf, Germany

<sup>4</sup>Texas Instruments Incorporated, Freising, Haggertystr. 1, Germany

<sup>5</sup>Institute of Biological Information Processing (IBI-3), Forschungszentrum Jülich GmbH, Wilhelm-Johnen-Str., 52425 Jülich, Germany

**Abstract:** This work proposes and evaluates a fluidic setup for automated pH characterization of extended-gate ion-sensitive field-effect transistors (EG-ISFET). Each characterized chip contains three EG-ISFETs with adjustable floating-gate charge and pH-sensitive Al<sub>2</sub>O<sub>3</sub> dielectric layer. The fluidic setup allows measurements with up to 14 different solvents, such as pH buffers, and automatically collects metadata during the measurement, enabling an automated evaluation of each experiment.

**Keywords:** extended-gate field-effect transistor; fluidic setup; Al<sub>2</sub>O<sub>3</sub>; multiple pH sensors

### Introduction

Individual characterization of extended-gate ISFETs (EG-ISFETs) is time-consuming, automation can increase productivity and quality standards as well as reduce the time required for manual laboratory routines [1,2]. Using fluidic setups, standard electrochemical measurements can be automated, monitoring important data on sensor properties such as drift, hysteresis, pH sensitivity and stability to be collected with consistent quality. The here characterized sensing platform combines three EG-ISFETs with a pH-sensitive Al<sub>2</sub>O<sub>3</sub> dielectric layer on one chip. Without the pauses that occur when manually changing buffers, e.g., by pipetting, the fluidic measuring system enables continuous measurement in which the response behavior to each pH change can be examined.

### Results and Discussion

A fluidic measuring system was built up and validated. In automated measurements, the pH sensitivity, hysteresis and stability of EG-ISFETs were studied by use of multiple pH cycles in alkaline (pH 4-6-7-8-10) and acidic direction (pH 10-8-7-6-4). A schematic of the developed fluidic setup is given in Figure 1. At the beginning of each pH stage, the system is sufficiently flushed with the respective pH buffer, after which the flow is stopped, allowing a “go-stop” operation mode. All valve states are simultaneously recorded during the measurement, so each measuring point can be clearly assigned to the particular pH buffer (change). Automated calculation of pH sensitivities in each individual pH cycle is done.

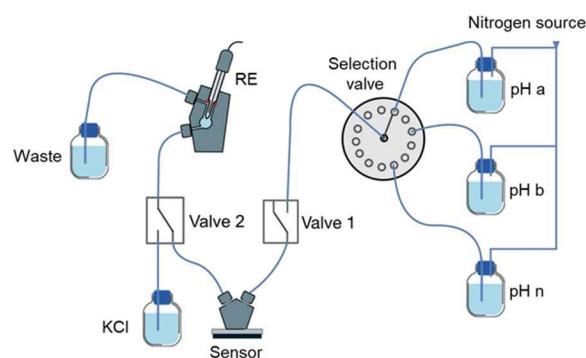


**Figure 1:** Schematic of the fluidic setup for automated characterization of extended-gate ISFETs

### Conclusions

Compared to manual, individual sensor characterization, the combined automation of both the measurement routine and the evaluation represents distinct progress with regard to reduction of workload and improving quality of standards. Future work will deal with increasing the number of sensors, which can be characterized in parallel in the automated fluidic setup.

### References

- [1] M. Wurster, B. Häfner, D. Gauder, N. Stricker, G. Lanza, *Procedia CIRP* **97**, (2020)
- [2] S. Y. Nof, *Springer Handbook of Automation*, 2<sup>nd</sup> ed.; Springer: Switzerland, (2023)

# Development towards a novel screening method for nipecotic acid bioisosteres using molecular imprinted polymers (MIPs) as alternative to *in vitro* cellular uptake assays

Niels Knippenberg<sup>1</sup>, Joseph W. Lowdon<sup>1</sup>, Margaux Frigoli<sup>1</sup>, Thomas J. Cleij<sup>1</sup>, Kasper Eersels<sup>1</sup>, Bart van Grinsven<sup>1</sup>, Hanne Diliën<sup>1</sup>

[niels.knippenberg@maastrichtuniversity.nl](mailto:niels.knippenberg@maastrichtuniversity.nl) (Corresponding e-mail address)

<sup>1</sup>Sensor Engineering Department, Faculty of Science and Engineering, Maastricht University, P.O. Box 616, 6200 MD Maastricht, The Netherlands

**Abstract:** The development of radioligands targeting GABA transporter 1 (GAT1) is highly desired to allow for better diagnosis and treatment of CNS diseases. To increase the brain-uptake of GAT1 radioligands, the use of nipecotic acid bioisosteres is an important strategy. In order to screen these isosteres for their binding to GAT1 in a time- and cost-effective manner, this research aims to develop a molecular imprinted polymer (MIP) that mimics the natural binding site of GAT1 and can act as an alternative screening tool to the current cellular-based assays. To that end, nipecotic acid MIPs are developed and analysed using electrical impedance spectroscopy (EIS).

**Keywords:** nipecotic acid; bioisostere; molecular imprinted polymer; electropolymerization

## Introduction

The development of radioligands addressing GABA transporter 1 (GAT1) is highly desirable, as they could allow for better treatment and diagnosis options for various CNS diseases. As such, several lipophilic nipecotic acid analogues have been developed, but suffer from low brain uptake due to the zwitterionic behaviour of the nipecotic acid group (structure visible in Figure 1) [1].

To develop more viable GAT1 radioligands in the future, the use of nipecotic acid bioisosteres is an important strategy to increase brain uptake [1]. However, this requires knowledge on the binding of these isosteres to GAT1. To obtain this information and screen isosteres for their affinity to GAT1, a nipecotic acid imprinted polymer was developed with a view to generating an artificial mimic of the GAT1 binding site (Figure 1). It is expected that bioisosteres that bind well to the MIP should also bind well to GAT1 and could function as viable isosteres.

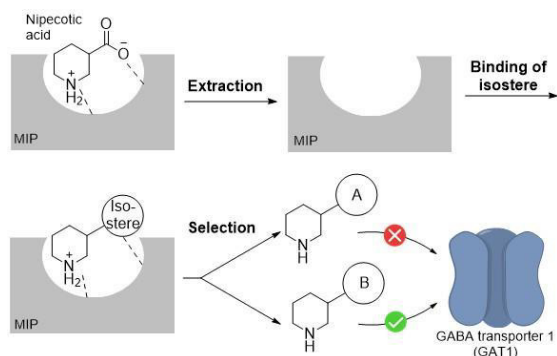


**Figure 1:** Schematic overview of the screening of nipecotic bioisosteres using MIPs. After synthesis, nipecotic acid is extracted and the binding of isosteres is evaluated. Well-binding isosteres are expected to bind to the natural GAT1 as well.

## Results and Discussion

Nipecotic acid MIPs were created through electropolymerization of *ortho*-phenylenediamine (oPD) by cyclic voltammetry (CV) [2]. The optimization of the generated receptor layer was achieved by varying the scan rate and number of CV cycles, yielding an optimized MIP with an average imprinting factor of 2.6 as analysed by electrical impedance spectroscopy (EIS). Selectivity studies facilitated the determination of the major binding interactions between the MIP and substrate. As such, the substrate carboxylic acid group was shown to play a more important role in binding than an amine group [3].

## Conclusions

Despite the successful synthesis of a nipecotic acid MIP, it was found that the developed MIP did not exhibit all the major binding interactions that can be seen in the natural GAT1 binding site. This shows that efficient mimicking of dynamic natural receptors and remains difficult, and smart monomer and template selection are critical in the process.

## References

- [1] N. Knippenberg, M. Bauwens, O. Schijns, G. Hoogland, A. Florea, K. Rijkers, T.J. Cleij, K. Eersels, B. van Grinsven, H. Diliën, *EJNMMI Res.* **2023**, *13*, 42
- [2] X. Zheng, R. Lin, X. Zhou, L. Zhang, W. Lin, *Anal. Methods* **2012**, *4*, 482-487
- [3] N. Knippenberg, J.W. Lowdon, M. Frigoli, T.J. Cleij, K. Eersels, B. van Grinsven, H. Diliën, *Talanta* **2024**, *in press*

## Acknowledgements

The project was funded by the Sensor Engineering department, Faculty of Science and Engineering, Maastricht University.



# A portable platform for the multiplexed characterization of 16 capacitive field-effect sensors

S. Schmidt<sup>1,2</sup>, T. Karschuck<sup>1,3</sup>, S. Achtsnicht<sup>1</sup>, A. Poghossian<sup>4</sup>, M. Keusgen<sup>3</sup>, M. J. Schöning<sup>1,5</sup>

[s.schmidt@fh-aachen.de](mailto:s.schmidt@fh-aachen.de)

<sup>1</sup>Institute of Nano- and Biotechnologies (INB), Aachen University of Applied Sciences, Campus Jülich, Heinrich-Mußmann-Str. 1, 52428 Jülich, Germany

<sup>2</sup>Institute of Pharmaceutical Chemistry, Philipps University of Marburg, Wilhelm-Roser-Str. 2, 35037 Marburg, Germany

<sup>3</sup>Laboratory for Soft Matter and Biophysics, KU Leuven, Celestijnenlaan, 3001 Leuven, Belgium

<sup>4</sup>MicroNanoBio, Liebigstr. 4, 40479 Düsseldorf, Germany

<sup>5</sup>Institute of Biological Information Processing (IBI-3), Forschungszentrum Jülich GmbH, Wilhelm-Johnen-Str., 52425 Jülich, Germany

**Abstract:** A portable measurement platform for 16 capacitive field-effect sensors was developed and tested by means of a pH characterization. An almost ideal Nernstian pH sensitivity of  $58.5 \pm 0.6$  mV/pH (mean  $\pm$  standard deviation,  $n = 16$ ) was achieved for Ta<sub>2</sub>O<sub>5</sub>-gated sensors, which is in good agreement with values for individual sensors reported in literature.

**Keywords:** capacitive field-effect sensor; pH sensing; multiplexed measurement setup; portable platform

## Introduction

Capacitive field-effect sensors with an electrolyte-insulator-semiconductor (EISCAP) structure are used in a variety of chemo- and biosensing applications, by virtue of their easy customizability through surface modifications [1]. Recently, our group presented a multiplexed system for the characterization of 16 EISCAP sensors consisting of a measurement cell and a base station which are connected to an external electrochemical workstation IM6eX (Zahner-Elektrik GmbH & Co. KG, Kronach, Germany) [2]. By integrating an EmStat Pico MUX16 (PalmSens BV, Houten, The Netherlands) into a slightly modified base station, the platform was enhanced to become a USB-powered, portable device (see Figure 1), independent from a complex, stationary electrochemical workstation. The dimensions of the fully mounted device (excluding reference electrode) are 19.7 cm  $\times$  10.3 cm  $\times$  5.5 cm.

## Results and Discussion

The novel portable platform was compared to the established stationary one by pH characterizations of 16 EISCAP sensors with Ta<sub>2</sub>O<sub>5</sub> as pH-sensitive layer. The same sensors were measured with both devices in different Titrisol buffers using a sequence of pH 7 $\rightarrow$ 6 $\rightarrow$ 5 $\rightarrow$ 6 $\rightarrow$ 7 $\rightarrow$ 8 $\rightarrow$ 9 $\rightarrow$ 8 $\rightarrow$ 7. Per pH step, the measurements in the two platforms occurred in immediate succession by simply swapping the measurement cell between the base stations. The pH sensitivity was calculated by linear regression per sensor and device. For the portable platform, a mean pH sensitivity of  $58.5 \pm 0.6$  mV/pH was determined and  $59.0 \pm 0.3$  mV/pH for the stationary one. The characteristics were almost identical, with the results being in good accordance with literature [1, 3].

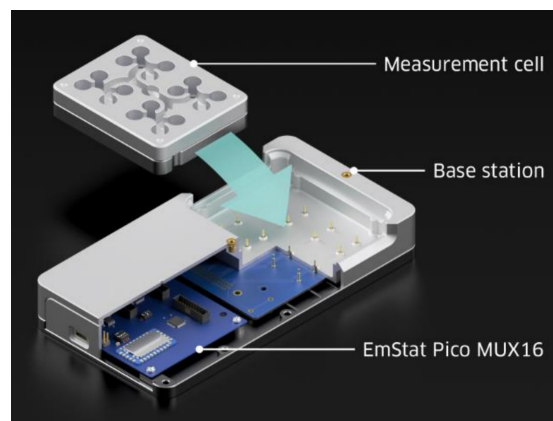


**Figure 1:** Section through the portable platform. The CAD model of the EmStat Pico MUX16 developer board was downloaded from the product website of PalmSens BV.

## Conclusions

The novel portable platform is a step forward towards affordable, stand-alone EISCAP sensor measurements and has proven to deliver results that can compete with larger, stationary devices. Future iterations may include a battery as power source and wireless connectivity for control via a smartphone.

## References

- [1] A. Poghossian, M. J. Schöning, *Sensors*, **20** (2020) 5639
- [2] T. Karschuck, S. Schmidt, S. Achtsnicht, A. Poghossian, P. Wagner, M. J. Schöning, *Phys. Status Solidi A*, **220** (2023) 2300265
- [3] M. Chen, Y. Jin, X. Qu, Q. Jin, J. Zhao, *Sens. Actuators B*, **192** (2014) 399-405



# Combinatorial screening of titanium-based ultra-thin anodic memristors

Elena Atanasova<sup>1</sup>, Dominik Knapic<sup>1</sup>, Andrei Ionut Mardare<sup>1</sup>, Achim Walter Hassel<sup>1,2</sup>

[elena.atanasova@jku.at](mailto:elena.atanasova@jku.at)

<sup>1</sup>Institute of Chemical Technologies of Inorganic Material (TIM), Johannes Kepler University, Altenberger Straße 69, 4040 Linz, Austria

<sup>2</sup>Danube Private University (DPU), Steiner Landstraße 124, 3500 Krems an der Donau, Austria

**Abstract:** Memristors on a Nb-Ti thin film combinatorial library, ranging from 22 to 64 at% Ti, were evaluated for stability in endurance and retention up to 106 cycles. All compositions exhibited multilevel switching capabilities, but the Nb-46 at% Ti alloy emerged as the optimal composition, showing significant multilevel switching and the highest HRS/LRS ratio of  $5 \cdot 10^5$ . This alloy also displayed self-rectifying characteristics and an interfacial switching mechanism, confirmed via High-Resolution Transmission Electron Microscopy (HR-TEM) and Schottky emission. The Nb-46 at% Ti composition was developed into a memristive pH sensor, showing promising results for medical applications, regarding its sensitivity to variations in pH values.

**Keywords:** memristors; titanium; sputtering; anodic oxide

## Introduction

Memristors are metal/insulator/metal devices that can alter their resistance by application of an external electrical field. This allows the devices to retain and recall their resistance state, exhibiting resistive switching behaviour. The switching mechanism can be filamentary. This type is associated with the migration of oxygen vacancies within the metal oxide layer. Switching can also be non-filamentary relying on interfacial mechanisms, such as Schottky barrier formation. Memristors are of significant importance in fields such as sensors and neuromorphic computing [1,2].

## Results and Discussion

A Nb-Ti thin film combinatorial library was evaluated ranging from 22 to 64 at% Ti. All compositions demonstrated stability in endurance and retention measurements up to 106 cycles. Additionally, all devices exhibited multilevel switching behaviour, which is crucial for increased data storage capacity. Notably, the Nb-46 at% Ti alloy, was identified as the optimal composition, due to significant multi-level switching capabilities and the highest HRS/LRS ratio, of  $5 \cdot 10^5$ , across the library. The Nb-46 at% Ti device exhibited self-rectifying characteristics during I-U scans, with asymmetry and current suppression. Building on previous studies of Ti-based anodic memristors, an interfacial switching mechanism was proposed and confirmed via HR-TEM, which revealed no conductive filament formation [3]. Consequently, Schottky emission was identified as the dominating switching mechanism via current conduction analysis. The device was classified as a volatile self-rectifying memristor, making it a promising candidate for crossbar array architectures to reduce sneak path currents.

Utilizing the Nb-46 at% Ti alloy, crossbar arrays for memristive sensing applications were fabricated. The sensing capabilities were evaluated by exposing the device's active layer to Ringer's solution of varying pH values (3.0,5.0,7.0,9.0,11.0). The sensor was calibrated to pH responses through HRS/LRS ratios, given by I-U curves. The gradual opening of the hysteresis of the sweeps indicates sensitivity to OH<sup>-</sup> ions. X-ray Photoelectron Spectroscopy (XPS) further confirmed OH<sup>-</sup> diffusion into the oxide, validating the sensing mechanism. The sensor's Limit of Detection (LOD) and Limit of Quantification (LOQ) were characterized to be 0.4 pH and 1.2 pH, respectively, with a sensitivity of 0.5 pH corresponding to 3.5 mM OH<sup>-</sup>. These results suggest that the Nb-46 at% Ti pH sensor holds significant promise for medical applications.

## Conclusions

A Nb-Ti combinatorial library and a Nb-Ti pH sensor were successfully developed. All devices exhibited self-rectifying qualities based on an interfacial switching mechanism governed by Schottky emission. Such devices demonstrate significant potential for applications in biomedical sensing. Further, they show promising results for neuromorphic computing, possibly enhancing performance and reliability in the advancement of computing memories.

## References

- [1] A.G. Isaev, O.O. Permyakova, A.E. Rogozhin, Russian Microelectronics 52, 2023,74
- [2] D. Knapic, A. Minenkov, E. Atanasova, I. Zrinski, A.W. Hassel, A.I. Mardare, Nanomaterials 14, 2024, 381
- [3] D. Knapic, E. Atanasova, I. Zrinski, A.W.Hassel, A.I. Mardare, Coatings 14, 2024, 446

## A project introduction "PFAS-resolve": On-site monitoring of *per- and polyfluoroalkyl substances (PFAS) in soil and wastewater*

Torsten Wagner<sup>1</sup>, Jürgen Pettrak<sup>2</sup>, Michael J. Schöning<sup>1</sup>, Sofie Thijs<sup>3</sup>, Dupont François<sup>4</sup>, Stoukatch Serguei<sup>4</sup>, Jean-M. Redouté<sup>4</sup>, Marta Popova<sup>5</sup>, Björn Scheepers<sup>6</sup>, Thomas-B. Seiler<sup>7</sup>, Marcos d. R. Fernandes<sup>7</sup>, Patricia P. Moreno<sup>7</sup>, Ananthan Padma<sup>7</sup>, Bart van Grinsven<sup>8</sup>, Kasper Eersels<sup>8</sup>

torsten.wagner@fh-aachen.de

<sup>1</sup>Institute of Nano- and Biotechnologies (INB), FH Aachen, Heinrich-Mussmannstr. 1, 52428 Jülich, Germany;

<sup>2</sup>Institute of Applied Polymer Chemistry (IAP), FH Aachen, Heinrich-Mussmannstr. 1, 52428 Jülich, Germany;

<sup>3</sup>Bio2Clean B.V., Mombeekdreef 44, 3500 Hasselt, Belgium;

<sup>4</sup>Microsys, University of Liège, Allée de la Découverte 10 4000 Liège, Belgium;

<sup>5</sup>SPAQUE, Avenue Maurice Destenay 13 4000 Liège, Belgium;

<sup>6</sup>Geonius Groep B.V., De Asselenkuil 10, 6161 RD Geleen, Netherlands;

<sup>7</sup>Hygiene-Institut des Ruhrgebiets (Hyg), Rotthausen Str. 21, 45879 Gelsenkirchen, Germany;

<sup>8</sup>Sensor Engineering Department, Maastricht University, Duboisdomein 30, 6229 GT Maastricht, Netherlands

**Abstract:** "PFAS-resolve" is a recently started project, which aims to develop a new sensor system to detect per- and polyfluoroalkyl (PFAS) substances which are widely used in different products. PFAS is known for its long chemical stability, the subsequent accumulation in the food chain and the associated health issues. A risk assessment is currently only possible, following laboratory analyses. "PFAS-resolve" has set the goal of developing a fast, uncomplicated and favourable on-site analysis.

**Keywords:** PFAS; polyfluoroalkyl; field-effect sensors; molecular imprinted polymers; phytoremediation

### Introduction

Per- and polyfluoroalkyl substances, known as PFAS, are commonly used in the textile and packaging industries for their ability to repel dirt, grease, and water. They are also used in various industrial processes such as automotive, protective coatings, and firefighting foam, due to their high thermal and chemical stability. Despite their usefulness and cost-effectiveness, PFAS have significant drawbacks. They are hardly biodegradable, earning them the nickname 'forever chemicals.' They have been suspected to be carcinogenic and linked to various diseases [1,2]. PFAS can accumulate in soil, water, animals, plants, and the human body, including in blood, liver, and kidneys, and can be passed through breast milk. Many countries have issued guidelines and limits for PFAS handling, but the extent of contamination from sources like wastewater discharge, biosolids fertilization, and erosion remains unclear [3]. Brownfield sites undergoing cultivation are often found to have widespread PFAS contamination.

To address this transnational issue, the Interreg-funded "PFAS-resolve" project aims to develop a sensor platform that can prepare and analyze water and soil samples using chemical sensors. Project partners are exploring semiconductor-based sensors combined with molecular imprinted polymers. These sensors will be an integral component of a customized on-field capable sample preparation and fluidic set-up, augmented by precisely crafted

measurement and control electronics. Additionally, industrial partners will provide certified laboratory analysis methods based on the current state-of-the-art as well as real samples. Furthermore, the project will investigate the feasibility of cultivating suitable plants to absorb PFAS from soil and water. The PFAS-enriched plants could then be harvested, treated, and disposed of. This method, known as phytoremediation, could be used alongside the introduced sensor technology to create a close-loop real-time monitoring, thereby allowing for the cleaning of large areas in a sustainable and environmentally friendly manner.

### References

- [1] K. Steenland, A. Winquist, PFAS and cancer, a scoping review of the epidemiologic evidence. *Environ Res.* (2021), doi: 10.1016/j.envres.2020.110690
- [2] K.E. Pelch, A. Reade, T.A.M. Wolffe, C.F. Kwiatkowski. PFAS health effects database: Protocol for a systematic evidence map. *Environ Int.* (2019) doi:10.1016/j.envint.2019.05.045
- [3] G.R. Johnson, PFAS in soil and groundwater following historical land application of biosolids. *Water* (2022) doi:10.1016/j.watres.2021.118035

### Acknowledgements

This will be supported by Intereg Meuse-Rhine (NL-BE-DE) program under IMR6-00027.

# Tutorial Lecture D

## Surface modifications of implants for tailored osseointegration properties

Christoph Kleber<sup>1</sup>

[christoph.kleber@dp-uni.ac.at](mailto:christoph.kleber@dp-uni.ac.at)

<sup>1</sup> Department of Physics and Chemistry of Materials, Danube Private University, 3500 Krems-Stein, Austria

**Abstract:** With the growing elderly population the demand for the medical implants and especially dental implants is growing. Moreover, keeping in mind the development of current technologies and techniques, it is necessary to carry on with the improvements of commonly used and available materials and equipment to ensure a proper osseointegration. Recent attempts to further improve the osseointegration properties of dental implants, are based on 3D printing and composite coating of electrochemically precipitated implants [1] or the surface modification by laser treatment [2].

**Keywords:** atomic force microscopy; dental implants; surface modification; 3D-printing

### Introduction

The research in surface modification of the implants is aimed in increasing their success rate and healing time. Treatment with laser of the implant surface is of interest for pure Ti as well as for Ti based alloys such as Ti-6Al-4V whereby a micro-nano scale modification of the surface is achieved [2,3]. Such modifications of the surface lead to a significant enhancement of the cell adhesion on the surface. Moreover, increased roughness and cell adhesion led to lower surface toxicity and increase of antibacterial properties. It is also proven that neodymium-doped yttrium aluminium garnet lasers are able to generate osseointegrating surfaces [4].

### Results and Discussion

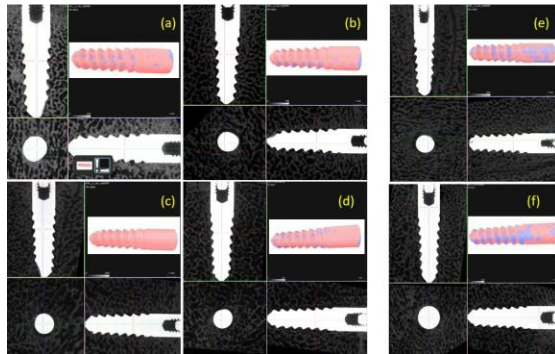


**Figure 1:**  $\mu$ -CT images of laser treated implants (a-d) on the left side and only sand-blasted implants on the right side (e and f) as reference. The red/blue colored images in every upper right corner depicts a reconstruction of the surface coverage of the implant surface (blue) with bone material (red). It is clearly visible that the laser treated implants show a higher coverage compared to the sand blasted ones.

To prove the advanced osseointegration properties of the laser treated implants they were placed in the

frontal bone of a domestic pig and were left there for a healing period of eight weeks. The statistical evaluation was done by the analysis of more than 800 single cross section slides of the implants resulting in statistical relevant numbers. T-test showed statistically significant higher rates of 3D-BIC% ( $p < 0.05$ ) for the laser treated implants, compared to the control group.

### Conclusions

Laser-treatment of Ti Grade 4 implants improves the osseointegration abilities mainly caused by roughness higher than observed on machined Ti or 3D-printed ceramic implants. The laser-treated surfaces show characteristic micro- and nanostructures on the surface affecting the osseointegration properties as proven in animal experiments.

### References

- [1] Yang, C., Yu, Z., Long, Y., & Chen, L. (2020). *Science Of Advanced Materials*, 12(10), 1492-1501. doi: 10.1166/sam.2020.3844
- [2] W. Luczak, C. Reiner-Rozman, M. Muck, J. Heitz, G. Mitov, F. Pfaffeneder, C. von See, A.W. Hassel, C. Kleber, *Physica Status Solidi (a)*, 220 (2023) 10.1002/pssa.202200605
- [3] Eghbali, N., Naffakh-Moosavy, H., Sadeghi Mohammadi, S., & Naderi-Manesh, H. (2021). *Dental Materials*, 37(3), 547-558. doi: 10.1016/j.dental.2020.12.007
- [4] Olsson, R., Powell, J., Palmquist, A., Brånemark, R., Frostevarg, J., & Kaplan, A. (2018). *Journal Of Laser Applications*, 30(4), 042009. doi: 10.2351/1.5078502

### Acknowledgements

This work was supported by the EU Horizon 2020 research and innovation program no. 951730.

# TM-AFM analysis of laser-treated surface compared to 3D-printed ceramic and titanium dental implants

Wiktor Łuczak<sup>1</sup>, Achim Walter Hassel<sup>1,2</sup>, Caroline Steiner<sup>1</sup>, Christoph Kleber<sup>1</sup>

[wiktor.luczak@dp-uni.ac.at](mailto:wiktor.luczak@dp-uni.ac.at)

<sup>1</sup> Department of Physics and Chemistry of Materials, Danube Private University, 3500 Krems-Stein, Austria

<sup>2</sup> Institute of Chemical Technology of Inorganic Materials, Johannes Kepler University, 4040 Linz, Austria

**Abstract:** Surface modification of the dental implants is proven to greatly affect the interaction between the implant itself and the surrounding biological matrix, hence influencing its osseointegration abilities. Surface analysis by atomic force microscopy (AFM) allows investigation of the surface roughness modified with laser, in comparison to standard titanium (Grade 4) and 3D-printed ceramic implants. Surface modifications by laser treatment leads to the creation of nanostructures, increasing the roughness of the material. Therefore, increased osseointegration is expected for the implants with modified surface, reducing the healing time.

**Keywords:** atomic force microscopy; dental implants; surface modification; 3D-printing

## Introduction

The research in surface modification of the implants is aimed in increasing their success rate and healing time. Implants can undergo processes such as sandblasting, etching or short-pulsed laser-treatment [1, 2]. Moreover, in recent years zirconia implants have been shown to possess similar functionality to titanium implants [3]. However, each method as well as material along with advantages has its disadvantages [4]. Additionally, the implants in European Union need to fulfil very strict requirements to be allowed for a commercial use [5]. Therefore, despite decades of research, there is still a need for further progress.

## Results and Discussion

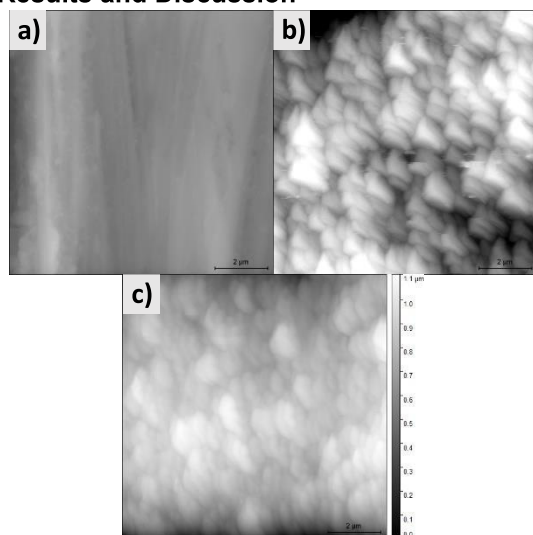


**Figure 1:**  $10 \times 10 \mu\text{m}^2$  TM-AFM images of the three compared types of surfaces (a) machined titanium, (b) laser-treated SLA titanium, (c) 3D printed ceramic implant. As clearly visible each surface has distinctive characteristics and features influencing the osseointegrative properties.

The surfaces of the three different types of implants have been analysed with AFM. Laser-treated surfaces show the highest value of RMS of height irregularities ( $394.8 \pm 149.8 \text{ nm}$ ), while machined implant shows lowest value ( $62.1 \pm 21.2 \text{ nm}$ ). Both, the laser-treated and 3D-printed implants have surface covered by the distinctive nanostructures – even though they are different materials – which might promote improved osseointegration after implantation.

## Conclusions

Laser-treatment of Ti Grade 4 implants causes roughness higher than observed on machined Ti or 3D-printed ceramic implants. 3D-printed ceramic and laser-treated metallic samples show characteristic nanostructures on the surface – even though different in shape and size – which affect the wettability and hence the osseointegration properties.

## References

- [1] J. Zhang, J. Liu, C. Wang, F. Chen, X. Wang, K. Lin, *Bioact. Mater.* **5** (2020) 9-16, doi: 10.1016/j.bioactmat.2019.12.008
- [2] Seo, B.Y.; Son, K.; Son, Y.-T. et al., *J. Funct. Biomater.* **14** (2023) 297, doi: 10.3390/jfb14060297
- [3] S. Roehling, K.A. Schlegel, H. Woelfler, M. Gahlert, *Clin. Oral Implants Res.* **29** (2018) 135-53, doi: 10.1111/clr.13352
- [4] G. Zhu, G. Wang, J. J. Li, *Mater. Adv.* **2** (2021) 6901-27, doi: 10.1039/D1MA00675D
- [5] D. Mohn, M. Zehnder, *Front. Dent. Med.* **4** (2023), doi: 10.3389/fdmed.2023.1155820

## Acknowledgements

This work was supported by the EU Horizon 2020 research and innovation program no. 951730.



## Interaction of Dextran with Dental Surfaces

Anastasija Link<sup>1</sup>, Swen Ehnert<sup>1</sup>, Christine Müller-Renno<sup>1</sup>, Matthias Hannig<sup>2</sup>, Christiane Ziegler<sup>1</sup>  
link@rptu.de

<sup>1</sup> Department of Physics and Research Center OPTIMAS, RPTU Kaiserslautern,  
Erwin-Schrödinger Straße 56, D-67663 Kaiserslautern, Germany

<sup>2</sup> Clinic of Operative Dentistry, Periodontology and Preventive Dentistry, Saarland University Hospital,  
66421 Homburg, Germany

**Abstract:** Understanding biofilm formation inside the oral cavity is an important task. Proteins and polysaccharide are the two main components of the conditioning film, the first step of biofilm formation. Microbes colonize this biofilm and cause a variety of dental diseases and the detachment of dental implants. It is important to mention that, unlike other human tissues, the enamel cannot be restored. Whereas the influence of proteins is widely studied, research on polysaccharides is underrepresented in oral biofilm research. Therefore, the interaction of the polysaccharide dextran with dental-relevant titanium was investigated using scanning force spectroscopy (SFS), while surrounding conditions were changed and data were compared with reference materials.

**Keywords:** scanning force microscopy (SFM); scanning force spectroscopy (SFS); dextran; oral cavity; pH value; biofilm

### Introduction

Our goal is to monitor the interaction of dextran with different dental-relevant materials to better understand the development of various dental diseases. The focus has been on titanium [1], while further measurements with enamel are currently performed. Dental gold and silicon were used as reference materials for comparison. Force-distance curves, investigated by scanning force spectroscopy (SFS), were measured to determine the adhesion forces of dextran on dental materials. Parameters such as the pH value and contact time were varied to mimic different conditions inside the oral cavity. Zeta potential measurements of the dextran were performed to investigate the resulting charge of the dextran as a function of the pH value.

### Results and Discussion

Zeta potential measurements of the dextran indicate an uncharged stage at a pH between 4.5 and 11, and a slightly negative charge at pH 13 due to deprotonation. For further experiments with SFS, the dextran was covalently coupled to the colloidal probe of an SFM cantilever [2]. Sawtooth-shaped retract curves in force-distance measurements exhibit interaction events between dextran and dental surfaces. The adhesion force increases with contact time, followed by a steady state for all measured pH values at about 40 s. Measurements with increasing (pH 4.5 to pH 13) and decreasing (pH 13 to pH 4.5) values were taken to exclude the influence of the pH order on the adhesion force. It could be observed that the pH order had no influence on the adhesion values, and as a function of pH value, all adhesion forces are comparable within the error bars. The adhesion force measurements were also performed on dental gold and silicon reference materials. Here, dental gold demonstrates an increased adhesion strength compared to the other materials. This can be caused by the hydroxyl groups of the dextran, which interact very well with the gold surface.

First measurements on natural enamel show a smaller interaction of dextran with the substrate than with titanium and the reference material.

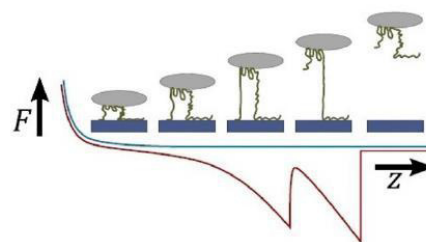


**Figure 1:** Postulated adhesion mechanism, which leads to sawtooth-shaped force-distance curves.

### Conclusions

It has been successfully evidenced that dextran adheres to dental materials. The adhesion force increases with time, followed by saturation. This is caused by conformational change of the dextran during interaction. Dextran shows lower adhesion forces on dental surfaces compared to proteins, i.e., bovine serum albumin. The adhesion force does not depend on the pH value, mainly because dextran is nearly uncharged over the entire pH range. The adhesion force on titanium and silicon is comparable while increased on gold. Further measurements with enamel will be performed, which is relevant to understand the development of dental diseases.

### References

- [1] Link, A.; Ehnert, S.; Müller-Renno, C.; Hannig, M.; Ziegler, C.; prepublished in *Physica Status Solidi A* <https://doi.org/10.1002/pssa.202400209>
- [2] Ehnert, S.; Müller-Renno, C.; Hannig, M.; Ziegler, C.; *Physica Status Solidi A* **220** (2023) 2200834.

### Acknowledgments

Funding by the DFG within project Zi 487/23-1 is gratefully acknowledged.



## Medical-grade liquid-infused titanium for biofilm reduction

Nils Heine<sup>1,3\*</sup>, Katharina Doll-Nikutta<sup>1,3\*</sup>, Elena Fadeeva<sup>2</sup>, Kestutis Kurselis<sup>2</sup>, Carina Mikolai<sup>1,3</sup>, Boris N. Chichkov<sup>2,3</sup>, Meike Stiesch<sup>1,3</sup>

[heine.nils@mh-hannover.de](mailto:heine.nils@mh-hannover.de)

\*equally contributing authors

<sup>1</sup>Department of Prosthetic Dentistry and Biomedical Materials Science, Hannover Medical School, Carl-Neuberg-Str. 1, 30625 Hannover, Germany

<sup>2</sup>Institute of Quantum Optics, Leibniz University of Hannover, Welfengarten 1, 30167 Hannover, Germany

<sup>3</sup>Lower Saxony Center for Biomedical Engineering, Implant Research and Development (NIFE), Stadtfelddamm 34, 30625 Hannover, Germany

**Abstract:** To reduce adherent biofilm and subsequent infection development on dental implants, surface modification by laser-structuring and lubricant application to create slippery liquid-infused porous surfaces (SLIPS) is a promising approach. In this study, a titanium SLIPS functionalization using medical-grade silicone oil was developed and analysed in complex *in vitro* models. Oral mono- and multispecies biofilm growth was reduced by 95% and 60% in a static environment and under flow conditions, respectively. Additionally, the antiadhesive effect was maintained in a 3D mucosa-implant-biofilm coculture model.

**Keywords:** oral biofilm; antiadhesive surface; slippery liquid-infused porous surface; implant

### Introduction

Bacterial biofilms on dental implants are the major cause for highly prevalent and difficult to treat peri-implantitis [1]. Therefore, inhibiting biofilm formation by implant surface modification is a promising approach. A possible modification is the “slippery liquid-infused porous surface” (SLIPS), for which a lubricant is immobilized on a structured substrate. On titanium, a widely used material for dental implants, antiadhesive SLIPS have already been created using lubricants that are not biocompatible [2, 3]. This study aimed to develop biofilm-reducing SLIPS on titanium with a lubricant approved as medical product and further test its clinical applicability in complex *in vitro* models.

### Results and Discussion

SLIPS were created on titanium specimens by ultra-short pulsed laser ablation to generate a combined micro/nano-structure and applying silicone oil (Fig.1A). The resulting SLIPS were stable in air and in phosphate buffer. The contact angle hysteresis of approx. 2 ° aligned with previous characteristics [4]. Bacterial biofilm formation by the oral commensal *Streptococcus oralis* was significantly reduced by 95% (Fig.1B, C). For an oral multispecies biofilm grown in a saliva flow-simulating flow chamber system, resulting biofilm volume was reduced by 60%, indicating supportive interspecies interactions. This reduction was also confirmed in a complex 3D mucosa-implant-biofilm coculture model, while no signs of cytotoxicity were observed.

### Conclusions

We could successfully create stable SLIPS on titanium using a lubricant approved as medical

product. Biofilm formation of oral bacteria was significantly reduced in clinically relevant *in vitro* settings including multispecies interactions, saliva flow and tissue integration.

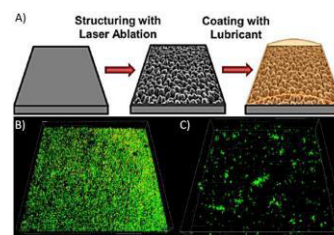


**Figure 1:** A) Schematic of SLIPS creation. Modified from [3]. 3D CLSM images of *S. oralis* on titanium (B) and SLIPS (C). Green – living bacteria, Red – dead bacteria. Edge length 190 µm.

### References

- [1] Dreyer, H. *et al.* Periodontal Res. 2018, 53, 657–681. <https://doi.org/10.1111/jre.12562>.
- [2] Doll, K. *et al.* ACS Appl. Mater. Interfaces 2017, 9, 9359–68. <https://doi.org/10.1021/acsami.6b16159>.
- [3] Doll, K. *et al.* ACS Appl. Mater. Interfaces 2019, 11, 23026–38. <https://doi.org/10.1021/acsami.9b06817>.
- [4] Wong, T.-S. *et al.* Nature 2011, 477, 443–447. <https://doi.org/10.1038/nature10447>.

### Acknowledgements

The work was funded by the Deutsche Forschungsgemeinschaft (DFG, German Research Foundation) under the Collaborative Research Center SFB/TRR-298-SIIRI (Project ID 426335750) and by the German Society for Dental Prosthetics and Biomaterials (DGPro).

## Study of spontaneous cell detachment using a multiparametric biosensing platform based on HTM, EIS, and QCM-D

Soroush Bakhshi Sichani<sup>1</sup>, Mehran Khorshid, Derick Yongabi, Csongor Tibor Urbán,

Michael J. Schöning, Peter Lieberzeit, and Patrick Wagner

[soroush.bakhshisichani@kuleuven.be](mailto:soroush.bakhshisichani@kuleuven.be)

<sup>1</sup> Laboratory for Soft Matter and Biophysics, ZMB, Department of Physics and Astronomy, KU Leuven, Celestijnenlaan 200 D, B-3001 Leuven, Belgium

**Abstract:** This article introduces a bioanalytical sensor device incorporating three transducer principles: electrochemical impedance spectroscopy (EIS), quartz-crystal microbalance with dissipation monitoring (QCM-D), and the heat transfer method (HTM). Using a single chip, it enables simultaneous measurements of HTM, EIS, and QCM-D parameters. The device was validated by monitoring eukaryotic-cell detachment under influence of a temperature gradient, distinguishing yeast strains with different flocculation genes.

**Keywords:** Multiparametric biosensor; HTM; EIS; QCM-D; Spontaneous cell detachment

### Introduction

Label-free biosensing techniques such as QCM, EIS, SPR, and HTM, enable critical insights into cell-material interactions and the dynamic effects of physico-chemical factors at the cellular level [1]. These methods surpass traditional techniques such as microscopy and flow cytometry by offering real-time, cost-effective monitoring without the need for labels that can alter cellular behaviour. Our work focuses on a Triple-Device platform that combines QCM-D, EIS, and HTM, allowing multiparametric analysis of spontaneous cell detachment under temperature gradients [2]. A schematic illustration of the device is shown in **Figure 1**. This novel approach enhances our understanding of cellular responses and optimizing bioprocesses [3].

### Results and Discussion

In this work, we studied the temperature-dependent spontaneous detachment of baker's yeast and two *S. cerevisiae* strains (1278b and S288C) using the Triple Device platform: We observed that increasing the chip temperature from 27°C to 37°C consistently reduces the detachment time ( $t_d$ ) across all methods. The detachment was tracked by measuring changes of the heat transfer resistance, impedance amplitude, and the resonance frequency and dissipation signals. Notably, detachment times varied significantly between the yeast strains, with strain 1278b detaching fastest and S288C the slowest, likely due to genetic differences affecting cell adhesion properties. SEM imaging supported these findings, showing distinct morphological differences and cell-cell interactions among the strains. Our results demonstrate that cell detachment can be effectively monitored using these combined sensing techniques, highlighting the influence of temperature and the genome profile on cell behaviour.

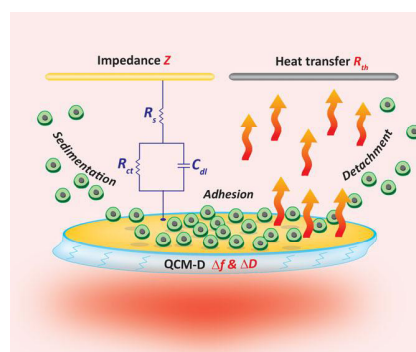


**Figure 1:** Triple Device: A gold-coated QCM crystal serves as a QCM-D sensor and the working electrode for impedance measurements. A gold wire used as the counter electrode of EIS. For HTM, a contactless heater and two thermocouples are used to measure temperatures.

### Conclusions

We developed a multiparametric biosensor that measures QCM parameters, impedance signals, and thermal resistance independently. We found that the yeast detachment time decreases with increasing temperature and HTM is the best way to monitor detachment. Detachment times is related to cell viability and cell-cell interaction.

### References

- [1] A. Sabot; S. Krause. *Anal. Chem* **2002**, 74, 3304-3311.
- [2] D. Yongabi, *et al.*, *Adv. Sci.* **2022**, 9, 1–24.
- [3] E. Briand, *et al.*, *Analyst* **2010**, 135, 343–350.

### Acknowledgements

This work was financed by the project SmartNano G.0E3618.18N of FWO in cooperation with the FWF, project no. I3568-N28. Furthermore, acknowledge funding by the KU Leuven, grant number C24E/23/025.

## Cell adhesion and behaviour on micro-nano-structured glass surfaces produced by wet etching

Muhammad Usman Anwar<sup>a</sup>, Celine Buchmann<sup>a</sup>, Christine Müller-Renno<sup>b</sup>, Christiane Ziegler<sup>b</sup>, Bernd Bufe<sup>a</sup>,  
Monika Saumer<sup>a</sup>

E-Mail: [muhammadusman.anwar@hs-kl.de](mailto:muhammadusman.anwar@hs-kl.de)

<sup>a</sup>University of Applied Sciences Kaiserslautern, Zweibrücken, 66482, Germany

<sup>b</sup>Kaiserslautern-Landau, Department of Physics and Research Center OPTIMAS, 67663 Kaiserslautern, Germany

**Abstract:** This study examines how micro and nanometre-scale topography on Borofloat 33 glass surfaces affects cell adhesion and behaviour. Using isotropic wet etching, spherical microstructures with diameters of 15, 30, 60, and 100  $\mu\text{m}$  and a depth of 12  $\mu\text{m}$  were created on 5x5 mm<sup>2</sup> glass chips to enhance cell adhesion for biosensing applications. Different etching masks, including organic adhesion promoters and metal stacks, were tested to achieve this depth. The microstructures were analysed using optical microscopy, atomic force microscopy, and profilometry. Cell experiments with various cell lines demonstrated improved adhesion and viability, indicating potential for advanced biosensing platforms.

**Keywords:** surface modification; microstructures; profilometry; cell adhesion; profilometry; scanning force microscopy; collagen.

### Introduction

Surface topography is vital for cellular response to substrate materials and is essential for cell adhesion and growth [1]. Recent studies have focused on how surface features at various scales affect cell adhesion and proliferation [2]. Micro-scale structures may enhance cell adhesion, while nano-scale bio-collagen structures significantly impact cell adhesion [3].

### Results and Discussion

Isotropic wet etching with hydrofluoric acid was used to create hemispherical (figure 1) microstructures in glass with diameters of 15, 30, 60, and 100  $\mu\text{m}$  and depths of 12  $\mu\text{m}$ , resulting in 5x5 mm<sup>2</sup> chips to enhance the cell adhesion for biosensing applications.

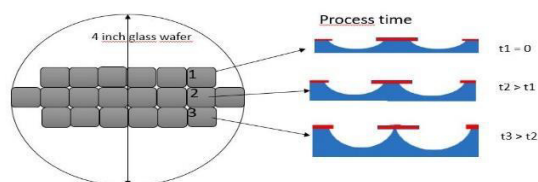
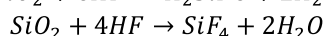
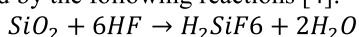


Figure 1: Schematic representation of the microstructured glass fabrication process.

Figure 2(a) illustrates the isotropic etching of glass, where 100  $\mu\text{m}$  diameter was precisely controlled to achieve varying depths and surface roughness. Borofloat 33 glass is selected for this process due to its superior transparency, chemical stability, and biocompatibility. Silicon fluoride compounds are generated by the following reactions [4]:



The initial etching process used organic adhesion promoters and photoresists ARP 5910 as an etching mask for 0.6  $\mu\text{m}$  depth. By using a metal stack Cr/Ni etching mask, a 12  $\mu\text{m}$  depth was achieved. Nano-scale roughness and topography with collagen were also explored. Figure 2(b) presents the three-dimensional surface profiles of bio-collagen fibers

deposited on microstructured glass. The glass was coated using slow spin coating techniques to ensure the optimal adhesion of the collagen fibers. Surface topography was characterized by optical microscopy, scanning force microscopy, and profilometry. Cell culture experiments with the cell lines HEK294T, THP1, U937 and SIM-A9 may show different adhesion and viability depending on the diameter of the hemispherical microstructures.

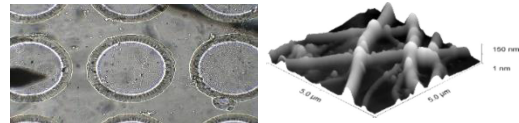


Figure 2:(a) 100  $\mu\text{m}$  diameter microstructured glass with collagen (b) 3D surface profile of scanning force microscopy measurement of natural collagen fibres coated inside the microstructured glass.

**Conclusions** In this study, we fabricated micro- and nano-structured surfaces of Borofloat 33 glass by wet chemical etching. Utilizing advanced characterization techniques and cell experiments, this study enhances the understanding of the interplay between engineered surface topography and cellular behaviour and shows the potential for biochip applications.

### References

- [1] Lord, M., Foss, M., & Besenbacher, F. (2010). Nano Today, 5(1), 66-78. <https://doi.org/10.1016/j.nantod.2010.01.001>
- [2] Simon, K., Burton, E., Han, Y., Li, J., Huang, A., & Luk, Y. (2007). Journal of the American Chemical Society, 129(16), 4892-4893.
- [3] Chen, P., Aso, T., Sasaki, R., Ashida, M., Tsutsumi, Y., Doi, H., & Hanawa, T. (2018). Journal of Biomedical Materials Research Part A, 106(10) 2735-2743.
- [4] Park, H., Cho, J. H., Jung, J. H., Duy, P. P., Le, A. H. T., & Yi, J. (2017). Current Photovoltaic Research, 5(3), 75-82.

### Acknowledgements

This work is funded by the Ministry of Science and Health of Rhineland-Palatinate (Project MultiSensE).

# Design of a microfluidic channel system for real-time monitoring of the perilymphatic fluid of the inner ear using molecularly imprinted polymers

Kevin Brunke<sup>1</sup>, Adrian Onken<sup>1</sup>, Helmut Schütte<sup>2</sup>, Theodor Doll<sup>1</sup>

[brunke@stud.uni-hannover.de](mailto:brunke@stud.uni-hannover.de)

<sup>1</sup>ORL Department, Hannover Medical School, Carl-Neuberg-Straße 1, 30625 Hannover, Germany

<sup>2</sup>Department of Engineering, Jade University of Applied Sciences, 26382 Wilhelmshaven, Germany

**Abstract:** Inflammation causes tissue growth, significantly affecting impedance and consequently the performance of cochlear implants (CIs). To address this issue, incorporating an inflammation sensor based on molecularly imprinted polymers (MIPs) onto CI electrodes should be considered. Since only 2–3  $\mu\text{L}$  of perilymph fluid can be extracted from the cochlear during the operation, in-vitro testing must be conducted in an appropriately scaled down size. In this study, we designed a microfluidic channel system to analyse the perilymph fluid with MIPs each specialised for different inflammations. To reduce the fluid volume, a control setup using air bubbles was realized.

**Keywords:** microfluidic; microengineering; PDMS; cochlear implant;

## Introduction

The peculiar behaviour of fluids in small-scale environments has long since been successfully harnessed as a base for applications such as lab-on-a-chip-systems [1]. Most prominently, these can be designed as detection devices requiring only minuscule input sizes or low concentrations of what it is designed to react to. Using an electrochemical microfluidic chip [2], the presence of a particular component within a passing fluid can be detected due to a change in conductivity.

## Method

Based on established design principles [3], material pairings of PMMA, glass and PDMS have been considered. The upper half consists of PDMS with an etched-in canal system. The lower half, on the other hand, was varied to accommodate either sputtered Pt-electrodes in a plasma-bonded glass-PDMS-combination or thin sheet electrodes lodged between two PDMS bodies. Fluid movement within the 300 x 300  $\mu\text{m}$  cross-section canal was controlled using two air or water-filled pumps at opposite ends of the system.

## Result and Conclusion

A microfluidic device has successfully been designed as an experimental setup for further research. Although promising due to the otherwise preferable nature of sheet electrodes, sealing a PDMS-PDMS-system using applied pressure instead of bonding proved to be difficult given the surface roughness achieved by using milled PMMA masters for casting. Therefore, further research will be conducted using the plasma bonded glass-PDMS-variant.

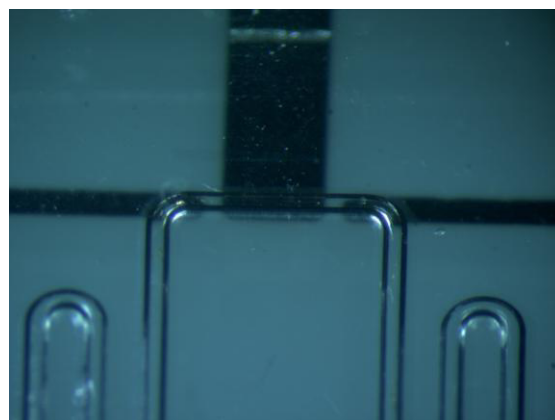


**Figure 1:** Sputtered Pt-Electrodes in a plasma bonded PDMS-Glass microfluidic system

## References

- [1] *Microsystem engineering of lab-on-a-chip devices* (Hrsg.: O. Geschke), Wiley-VCH, Weinheim, **2004**.
- [2] Y. Xie, X. Zhi, H. Su, K. Wang, Z. Yan, N. He, J. Zhang, Di Chen und D. Cui, *Nanoscale research letters* **2015**, *10*, 477, DOI: 10.1186/s11671-015-1153-3.
- [3] J. Castillo-León und W. E. Svendsen, *Lab-on-a-Chip Devices and Micro-Total Analysis Systems*, Springer International Publishing, Cham, **2015**.

## Acknowledgements

This study is funded by the “Cluster of Excellence Hearing4All” (EXC2077)



# Gold screen-printed electrodes coupled with molecularly imprinted conjugated polymers for ultrasensitive detection of streptomycin in milk

Margaux Frigolia<sup>1</sup>, Manlio Caldara<sup>1</sup>, Jeroen Royakkers<sup>1</sup>, Joseph W. Lowdon<sup>1</sup>, Thomas J. Cleij<sup>1</sup>, Hanne Diliën<sup>1</sup>, Kasper Eersels<sup>1</sup>, Bart van Grinsven<sup>1</sup>.

[m.frigoli@maastrichtuniversity.nl](mailto:m.frigoli@maastrichtuniversity.nl)

<sup>1</sup>Sensor Engineering Department, Faculty of Science and Engineering, Maastricht University, P.O. Box 616, 6200 MD Maastricht, the Netherlands

**Abstract:** Antibiotic resistance is a global health threat challenging environmental and food safety. This study introduces an electrochemical method for detecting streptomycin sulfate using gold screen-printed electrodes functionalized with a naphthalene diimide-based monomer. The sensor enables rapid detection of streptomycin via Differential Pulse Voltammetry, with a LoD of  $0.190 \pm 0.005$  pM. It shows selectivity for streptomycin even in the presence of common milk interferents. Successful testing in whole cow milk demonstrates its potential for rapid, portable antibiotic residue detection in food.

**Keywords:** Antibiotic detection; Food safety; Streptomycin; Milk detection; Screen-printed electrodes

## Introduction

Antibiotic resistance is an escalating global health threat, complicating treatment options and endangering food safety. Effective detection of antibiotic residues in food products is crucial to managing this issue. Innovative methods such as electrochemical-based biosensors are needed to quickly and accurately monitor these residues, ensuring safer consumption and helping to combat the spread of resistant bacteria (Figure 1).

## Results and Discussion

This study introduces an electrochemical detection method for streptomycin sulfate, utilizing gold screen-printed electrodes (Au-SPE) functionalized via electropolymerization of a custom-made naphthalene diimide-based conjugated monomer (Th2-NDI-PIA).[1] This modification creates specific binding sites for streptomycin, allowing a rapid detection of the antibiotic. The sensor's response to different concentrations of streptomycin was studied via Differential Pulse Voltammetry (DPV) in a wide linear range from  $10^{-13}$  M to  $10^{-9}$  M, with a limit of detection (LoD) of  $0.190 \pm 0.005$  pM (Figure 1).

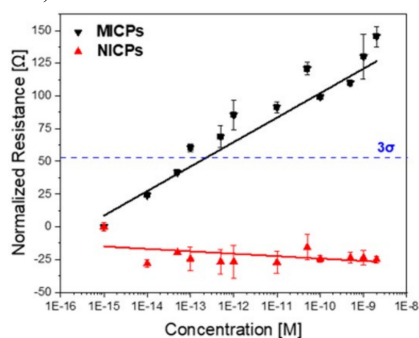


**Figure 1:** Dose-response curve for molecularly imprinted conjugated polymer (black line) and non-imprinted conjugated polymer (red line) after exposure to different concentrations of streptomycin.

The imprinted electrode demonstrates selectivity to other antibiotics, such as vancomycin and amoxicillin, but also to common interferents that can be found in milk such as lactose, glucose, riboflavin and bisphenol A. Successful proof-of-principle in whole cow milk highlights the sensor's efficacy in detecting antibiotic residues in food samples, offering a promising alternative for a rapid and portable detection technique.

## Conclusions

In this study, we demonstrated the detection of streptomycin in milk using functionalized gold screen-printed electrodes (Au-SPEs). The sensor exhibited excellent sensitivity and selectivity, detecting streptomycin sulfate at levels below regulatory limits, and its successful application in cow milk samples shows its potential for quality control in the dairy industry and point-of-care applications.

## References

[1] M. Frigoli et al, *Microchemical J.* 2024, <https://doi.org/10.1016/j.microc.2024.110433>

## Acknowledgements

This work was supported by the European Regional Development Fund through the AgrEU food project, 446 funded by the Interreg VA Flanders-The Netherlands program, CCI grant no. 2014TC16RFCB046.



# Concept of foldable active intraocular implants for artificial vision with enhanced spatial resolution

Eashika Ghosh<sup>1</sup>, Ziyu Gao<sup>1</sup>, Xuan Thang Vu<sup>1</sup>, and Sven Ingebrandt<sup>1</sup>

[ghosh@iwe1.rwth-aachen.de](mailto:ghosh@iwe1.rwth-aachen.de)

<sup>1</sup>Institute of Materials in Electrical Engineering 1, RWTH Aachen University, Sommerfeldstr. 24, 52074 Aachen, Germany

**Abstract:** A novel flexible implant is designed and fabricated following an Origami-like technique to fold it during implantation and unfold it before attachment to the retina. This concept should in future be utilized in novel, active epiretinal implants to improve the spatial resolution and field of view for patients suffering from degenerative diseases like Retinitis Pigmentosa and age-related macular degeneration.

**Keywords:** epiretinal implant; flexible microelectrode arrays; spatial resolution; active addressing

## Introduction

Visual impairment and blindness caused by degenerative diseases of the eye, such as Retinitis Pigmentosa and age-related macular degeneration, affect millions of people worldwide [1, 2]. The disease damages the photoreceptors in the retina gradually leading to complete blindness. Restoring the loss of vision is very challenging and many teams worldwide are working on engineering concepts, genetic cell therapies and autologous stem cell approaches. Although many different concepts have been developed around the world, previous attempts to cure the disease or manage the symptoms have been unsuccessful. Among the technical approaches, implantation of visual prostheses in the form of implants has shown optimistic results in restoring vision, but with the limitation of resolution and field of view.

## Results and Discussion

A functional epiretinal implant has been developed utilizing an Origami-inspired concept to enhance the field of view and reduce complications inherent to major surgical procedures. The implant's flexibility is achieved through a bi-layer configuration consisting of 3 $\mu$ m thick polyimide (PI) layers. Embedded between these layers are 30 $\mu$ m diameter gold microelectrodes and 4 $\mu$ m thick gold interconnecting wires, fabricated via electroplating to ensure structural integrity and prevent cracks upon folding and unfolding. Despite the presence of 480 microelectrodes, our current characterization was limited to 32 electrodes due to the conventional 1:1 wiring methodology. To overcome these limitations and enhance spatial resolution, a prototype for a large matrix of 32 $\times$ 32 electrodes was developed in parallel using a two-layer metallization in a CMOS-compatible fabrication route with silicon-on-insulator (SOI) wafers. We aim to use the top-silicon as an active layer for active addressing after transfer into the PI, while sustaining the flexibility and foldability of the implants.

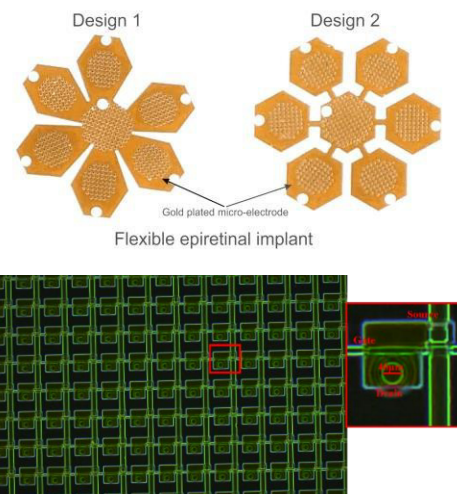


**Figure 1a:** Functional epiretinal implant concept based on an Origami approach. **1b:** Active 32 $\times$ 32 transistor matrix for retinal stimulation. An enlarged picture of one of the pixel is shown with the selection transistor realized in an SOI process.

## Conclusion

We have developed an epiretinal implant concept that can accommodate a high density of active stimulating electrodes, which shall improve spatial resolution and expand the field of view in future implants. The accessible field of view is enhanced by the introduction of a CMOS-compatible SOI technology encapsulated in a flexible PI foil.

## References

1. Duncan, J.L., et al., Clin Exp Optom, 2017. **100**(2): p. 144-150.
2. Behrend, M.R., et al., IEEE Trans Neural Syst Rehabil Eng, 2011. **19**(4): p. 436-42.

## Acknowledgements

We acknowledge financial support by the Deutsche Forschungsgemeinschaft (DFG) for funding this research with grant number 424556709/GRK2610.

# Investigating Diffusion-Triggered Corrosion in AIMD

Adrian Onken<sup>1</sup>, Christian Angerer<sup>2</sup>, Helmut Schütte, Thomas Stieglitz, Sabine Hild<sup>2</sup>, Theo Doll<sup>1</sup>

[Onken.Adrian@mh-hannover.de](mailto:Onken.Adrian@mh-hannover.de)

<sup>1</sup>Hannover Medical School

<sup>2</sup>Johannes Kepler University Linz, Institute of Polymer Science

**Abstract:** The ingress of bodily fluids into active implantable medical devices (AIMDs) poses a significant risk of failure. Delamination progresses along metal-polymer junctions of electrodes and conductive pathways leading to leakage currents and insulation faults, potentially causing device failure. To address this challenge a test method and specimen were developed to investigate diffusion-based delamination processes of the polymer-metal interface. A suitable tool to enlighten diffusion induced chemical changes within the specimen is Confocal Scanning Raman Microscopy (CSRM). CSRM offers detailed chemical information corresponding to a material, in combination with a high spatial resolution, resulting in high quality Raman images.

**Keywords:** Delamination; AIMD; interface diffusion; degradation; PDMS; Raman microscopy

## Introduction

A standardized test method and specimen were developed to investigate diffusion in the interfacial layer. Medical grade materials were chosen for better transferability to real AIMD. The silicone Sylgard 184 was chosen as flexible encapsulation for a platinum electrode which was sputtered onto a glass wafer. Since the test uses a chemical reaction of the metallic surface to visualize diffusion in the silicone-platinum-interface, an indicator structure was added onto the platinum using PVD (Fig. 1a) Copper was chosen as it yields an intense color change in the chemical reactions and allows the corrosion process to be visualized without the use of hazardous chemicals. The test-specimens were immersed in a potassium sulfide solution serving as corroding agent and images were taken with a time-lapse camera, showing the progressing diffusion front in the interface.

## Results and Discussion

The experiments showed a high permeability and diffusion rate for ionic molecules that penetrate from the water into the interface. The indicator structure was suitable to visualize and investigate the diffusion processes in the silicone-platinum interface by visual color change (Fig.1 a). First Raman experiments prove the diffusion of sulfides in the polymer and indicate an unequal deposition of copper sulfides throughout the setup. Green areas in figure 1d correlate with  $\text{Cu}_x\text{S}_y$  compounds. Further, high resolution imaging has to be done in order to provide more in-depth information concerning the physio-chemical processes during diffusion and delamination.

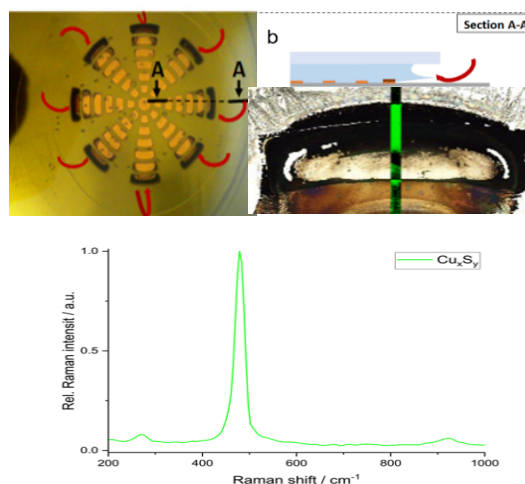


**Figure 1:** Schematic and experimental setup of the test structure (a & b). (c) Microscopy image of the test sample after immersion in potassium sulfide solution reveals formation of dark spots of CuS. Green bar in (c) indicates the Raman imaging area. The graph (d) shows the corresponding Raman spectrum of Cu sulfides with Raman bands at 265 and 475  $\text{cm}^{-1}$  used for constructing the Raman image (b).

## Conclusions

The developed diffusion test in combination with spectroscopy characterization has the potential to provide a better understanding of the degradation processes in the metal-polymer interface of AIMD.

## References

- [1] Boehler, C.; Carli, S.; Fadiga, L.; Stieglitz, T.; Asplund, M.: Guidelines for standardized performance tests. *Nat. Protoc.* **2020**

## Acknowledgements

DFG; MDOT; Hearing4all

# Quantification of the Titanium Dissolution during a new Explantation Procedure

A. Greul<sup>1</sup>, V. Alevizakos<sup>2</sup>, M. Hofinger<sup>1</sup>, C. Kleber<sup>2</sup>, C. von See<sup>2</sup>, A. W. Hassel<sup>1,2</sup>

[andreas.greul@jku.at](mailto:andreas.greul@jku.at)

<sup>1</sup>Institute of Chemical Technologies of Inorganic Material (TIM), Johannes Kepler University, Altenberger Straße 69, 4040 Linz, Austria

<sup>2</sup>Danube Private University (DPU), Steiner Landstraße 124, 3500 Krems an der Donau, Austria

**Abstract:** The motivation of this study is a newly developed explantation method for titanium dental implants. This method involves the application of a high-frequency current to the implant in order to heat it. This causes the bond between bone and implant to loosen and simplifies the explantation. This study focuses on the corrosion undergone by the implant during this procedure. It was possible to quantify the dissolution of titanium during a simulated explantation procedure via Inductively Coupled Plasma Optical Emission Spectroscopy (ICP-OES). Furthermore, the structural changes of the implant surface have been analysed by Electrochemical Impedance Spectroscopy (EIS).

**Keywords:** implant; electro chemistry, corrosion, titanium

## Introduction

Titanium is the material of choice for modern, dental implantology. Its unique properties qualify it for these applications. Its most important property is the phenomenon of osseointegration [1]. Titanium forms a direct bond with human bone if implanted. This goes along with a high biocompatibility and mechanical strength of the bone-implant interface. This however, poses challenges if explantation is necessary [2]. As previously reported, a novel explantation technique involving heating the implant, has been developed [3]. This study focuses on the surface changes of the implant and titanium dissolution during this procedure.

## Results and Discussion

Four identical dental implants (SICace 3.4 · 11.5 mm) have been prepared and embedded into PMMA, to be investigated using a special electrochemical cell. The sample's surface has then been investigated by EIS. Afterwards the explantation procedure was simulated by heating the implant using an electrotome (electro-surgical device) for 60 s immersed in a 0.9 wt.% NaCl solution. The solution was analysed by ICP-OES and the samples were again investigated by EIS.

The experiments consistently showed a decreased capacitance of the sample surface after the procedure as indicated in Figure 1. This decrease is commonly associated with a thickened passivating oxide layer. The ICP-OES analysis however, indicated increased titanium dissolution during the explantation with values in the range of 300 ng cm<sup>-2</sup> of titanium dissolution. Furthermore, the results suggest a direct correlation of dissolved titanium to the decrease in capacitance.

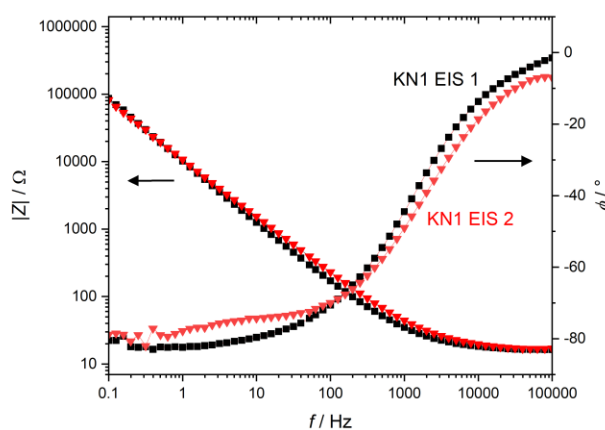


**Figure 1:** Bode plot of one implant before (black) and after (red) the simulated explantation procedure.

## Conclusions

This study successfully quantified the titanium dissolution during this new explantation technique and gave first insights into the structural changes to the implant surface during this procedure. The combined results warrant further research into the corrosion mechanism during this promising, new explantation technique.

## References

- [1] T. Hanawa, *Front. Bioeng. Biotechnol.* **7**, 2019
- [2] R. Delgado-Ruiz.; G. Romanos, *Int J Mol Sci.*, **11**, 2018
- [3] A. Greul, C. Kleber, C. von See, A.W. Hassel, *PSSA (a)* **220**, 2023

## List of Attendants

Last Name	First Name	Affiliation
Achtsnicht	Stefan	University of Applied Science Aachen, Germany
Ahmadi Tabar	Fatemeh	KU Leuven, Belgium
Aliazizi	Fereshteh	KU Leuven, Belgium
Anwar	Muhamad Usman	RPTU Kaiserslautern, Germany
Arreguin Campos	Rocio	Maastricht University, The Netherlands
Atanasova	Elena	Johannes Kepler University Linz, Austria
Bakhshi Sichani	Soroush	KU Leuven, Belgium
Bakker	Erik	University of Geneva, Switzerland
Brunke	Kevin	Hannover Medical School, Germany
Claes	Jean-Marie	Maastricht University, The Netherlands
Cui	Heping	RWTH Aachen, Germany
Di Scala	Flavia	Maastricht University, The Netherlands
Doll	Theodor	Hannover Medical School, Germany
Eyvazi Hesar	Milad	RWTH Aachen, Germany
Frigoli	Margaux	Maastricht University, The Netherlands
Gao	Ziyu	RWTH Aachen, Germany
Ghosh	Eashik	RWTH Aachen, Germany
Greul	Andreas	Johannes Kepler University Linz, Austria
Hassel	Achim Walter	Johannes Kepler University Linz, Austria
He	Tao	RPTU Kaiserslautern, Germany
Heine	Nils	Hannover Medical School, Germany
Hofinger	Manuel	Johannes Kepler University Linz, Austria
Janus	Kevin	University of Applied Science Aachen, Germany
Jiang	Huije	RWTH Aachen, Germany
Karschuck	Tobias	University of Applied Science Aachen, Germany
Kleber	Christoph	Danube Private University Krems, Austria
Knippenberg	Nils	Maastricht University, The Netherlands
Knoll	Maximillian	University of Applied Science Aachen, Germany
Konrad	Martin	Johannes Kepler University Linz, Austria
Krause	Steffi	Queen Mary University of London, UK

Li	Ruixiang	Queen Mary University of London, UK
Link	Anastasija	RPTU Kaiserslautern, Germany
Łuczak	Wiktor	Danube Private University Krems, Austria
Mardare	Andrei Ionut	Johannes Kepler University Linz, Austria
Marroquin Garcia	Ramiro	Maastricht University, The Netherlands
Miyamoto	Ko-ichiro	Tohoku University, Japan
Myndrul	Valerii	Maastricht University, The Netherlands
Nguyen	Minh-Hai	Hannover Medical School, Germany
Onken	Adrian	Hannover Medical School, Germany
Özsoylu	Dua	University of Applied Science Aachen, Germany
Philippaerts	Nathalie	Maastricht University, The Netherlands
Pötscher	Lukas	Johannes Kepler University Linz, Austria
Schmidt	Stefan	University of Applied Science Aachen, Germany
Singh	Animesh Pratap	RWTH Aachen, Germany
Szunerits	Sabine	University of Lille, France
Tsokolakyan	Astghik	A.B. Nalbandyan Institute of Chemical Physics, Armenia
Urban	Csongor Tibor	KU Leuven, Belgium
van Grinsven	Bart	Maastricht University, The Netherlands
van Wissen	Gil	Maastricht University, The Netherlands
Velasco Vélez	Juan Jesús	ALBA Synchrotron, Spain
Vu	Xuan Thang	RWTH Aachen, Germany
Wagner	Torsten	University of Applied Science Aachen, Germany
Welden	Melanie	University of Applied Science Aachen, Germany
Werner	Carl Frederick	Kyoto Institute of Technology, Japan
Zengin	Hüseyin	Johannes Kepler University Linz, Austria
Zhao	Jiazhe	Queen Mary University of London, UK
Zobeley	Clara	RPTU Kaiserslautern, Germany